SECTION 5, 7A and 7B OF CHAMPLAIN BRIDGE

- 2D NON-LINEAR ANALYSES OF EDGE GIRDERS

REPORT SUBMITTED TO:

Ponts Jacques Cartier et Champlain Inc.

Contract Number: 62443

Denis Mitchell, ing., Ph.D.

Denis Mitchell Consulting Inc.

March 18, 2016

1   Contents

1 Introduction

The objective of this study was to gain a better understanding of the performance of edge girders in typical spans of Sections 5, 7A and 7B of the Champlain Bridge. Two-dimensional non-linear analyses were carried out to study the influence of the degree of corrosion of the post-tensioning tendons and the influence of different combinations of strengthening measures on typical edge girders.

Analyses were carried out on spans in Section 5 that contained QP1 or QP2 strengthening measures for determining prioritization for strengthening of these spans with steel trusses.

Girder P7 of span 28W-29W was reanalyzed, accounting for the redistribution of forces due to the loss of tendons due to corrosion that had not been considered previously. This analysis was carried out to determine predicted crack widths and the predicted strength before the girder was strengthened with a truss.

The critical edge girders in the 6 spans of Section 7A and in the 4 spans of Section 7B were analyzed to assess their performance and to prioritize possible future strengthening.

The computer program VecTor2 was used to carry out the study. This analysis package can account for the non-linear stress-strain relationships of the concrete, reinforcing steel and prestressing tendons. Because of the features of this program, various behavioural aspects such as concrete cracking, flexural yielding, concrete crushing and shear distress can be determined. In addition, the program enables an assessment of long-term effects, including concrete shrinkage as well the effects of creep on the concrete stress-strain relationship.

The following scenarios were investigated:

- The 2D non-linear model was adjusted to account for the estimated number of tendons that were lost due to corrosion.
- The redistribution of forces due to the estimated loss of tendons was approximated in the 3D analyses.
- The influence of external longitudinal post-tensioning, PTE1 and PTE2
- The influence of Queen Post 1 (QP1)
- The influence of Queen Post 2 (QP2 and QP2.1)

A separate 3D linear elastic study was carried out by others (Massicotte, 2016) to determine the sharing of the loads among the seven girders in a typical span for both dead loads and different truck loading cases as well as for different strengthening methods. This 3D analysis enabled the determination of forces to be applied to the 2D finite element model of a typical edge girder.

The study concentrated on the behavior of edge girders in Section 5 and Sections 7A and 7B of the Champlain Bridge for a degree of corrosion that simulated the observations and assessments made in 2014 and 2015.

2 Material Properties

2.1 Concrete

The data on the strength of the concrete cores was obtained from a report by TECHNISOL INC. (2006).

2.1.1 Section 5

1. Figure 2.1 shows the concrete compressive strengths obtained from 94 core samples taken from girders in Section 5.
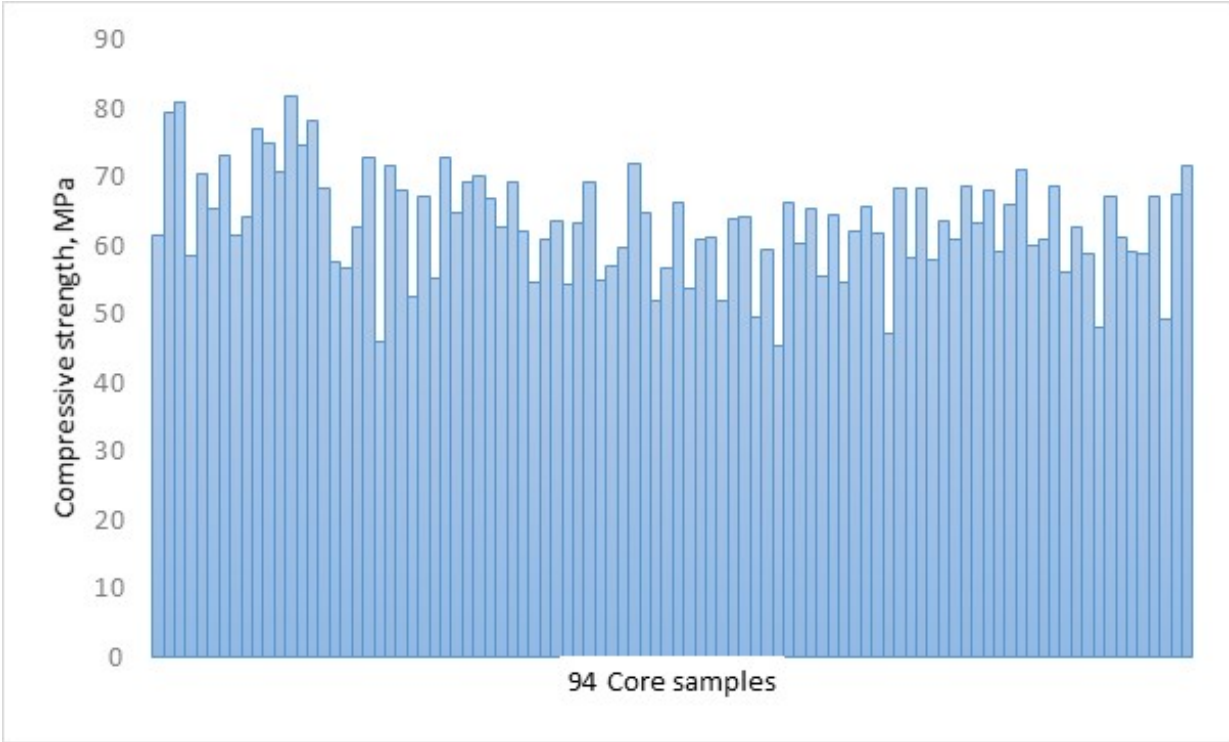
Fig. 2.1: Concrete compressive strengths obtained from core samples in Section 5 of bridge.

2.1.2 Section 7A

Figure 2.2 shows the concrete compressive strengths obtained from 6 core samples taken from girders in Section 7A.
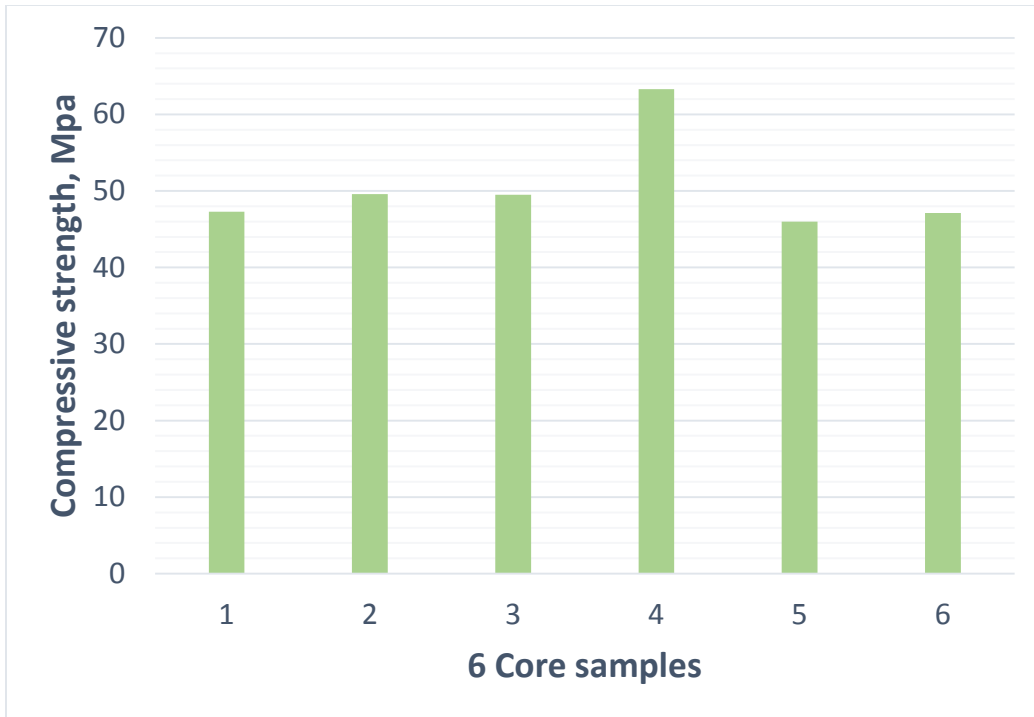
Fig. 2.2: Concrete compressive strengths obtained from core samples in Section 7A of bridge.

2.1.3 Section 7B

Figure 2.3 shows the concrete compressive strengths obtained from 8 core samples taken from girders in Section 7A.
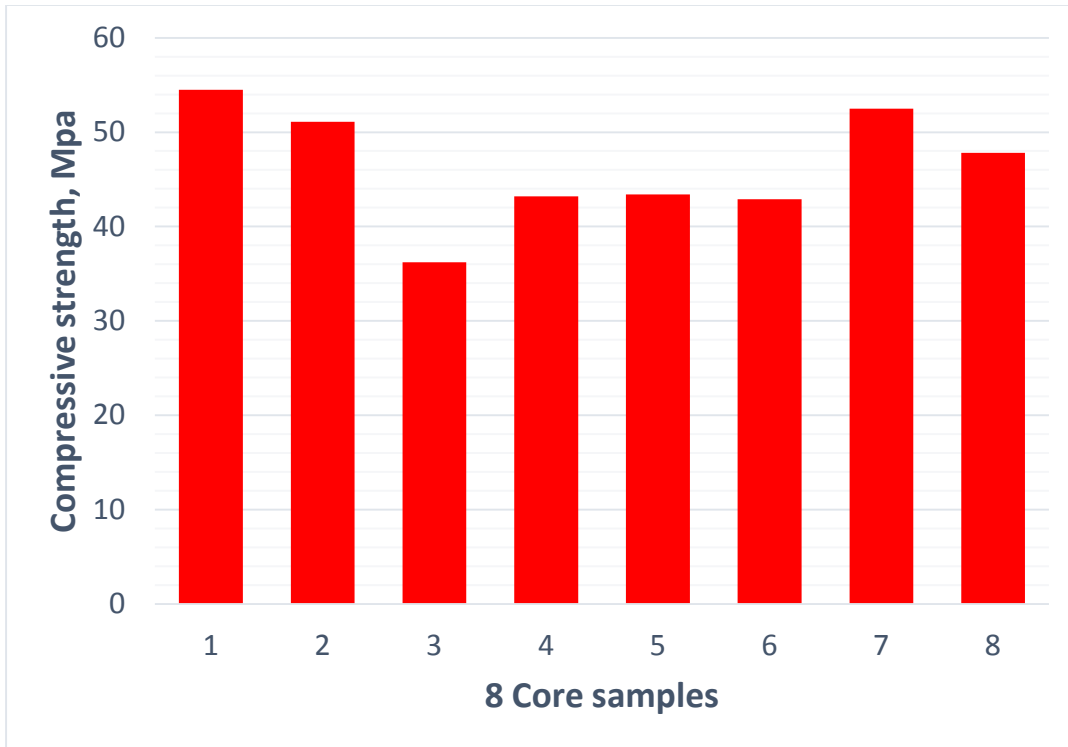
Fig. 2.3: Concrete compressive strengths obtained from core samples in Section 7B of bridge.

2.2 Assessment of Concrete Compressive strengths

2.2.1 Evaluation of Core Samples

Table 2.1 compares the variability of the measured core strengths for Sections 5, 7A and 7B. This table also gives the equivalent specified compressive strength, f_c', to be used for evaluation that was determined using the procedure given in Clause A14.1.2 of CSA S6-14.

Table 2.1: Evaluation of concrete compressive strengths from core samples

Section	Minimum Strength MPa	Maximum Strength MPa	Average Strength MPa	Equivalent f_c' CSA S6 MPa
5	45.5	81.7	63.2	53.9
7A	46.0	63.3	50.5	41.6
7B	36.2	54.5	46.5	38.5

2.3 Concrete Properties Assumed in Analyses

For all of the analyses a concrete tensile strength of $0.33\sqrt{f_c'}$ (MPa units) was assumed.

For short-term loading the different concretes were modelled with non-linear stress-strain relationships with peak compressive strains of 0.00220, 0.00211 and 0.00209 for the concretes in Sections 5, 7A and 7B, respectively.

For the long-term concrete stress-strain relationship the creep factor was determined using the creep equations given in CSA S6-06, resulting in a creep factor of 2.2 at an age of 51 years. The non-linear stress-strain relationships were adjusted so that the peak compressive strains were 0.00704, 0.00675 and 0.00670 for the concretes in Sections 5, 7A and 7B, respectively.

2.4 Reinforcing Steel and Prestressing Steel

2.4.1 Prestressing Steel

2.4.1.1 Sections 5 and 7A
The girders in Section 5 contain 24 post-tensioned tendons and the girders in Section 7A contain either 22 or 24 post-tensioned tendons depending on the span. Each tendon consists of 12 – 7 mm (0.276 in.) diameter prestressing wires. The area of one tendon containing 12 wires was taken as 462 mm². Clause 14.7.4.4 of CSA S6-06 recommends a value of 1600 MPa for the ultimate strength of the prestressing steel, f_{pu}, to be used for the evaluation of bridges constructed before 1963. However, the original calculations (Warycha and Skotecky) for the design of Section 5 indicate that the ultimate strength, f_{pu}, of the prestressing wires was 228 ksi (1572 MPa) for the design of the girders.

The more conservative value for f_{pu} of 1572 MPa was used in the 2D non-linear model and in the sectional analysis. The initial stress in the tendons was assumed to be 0.80 f_{pu}. The short-term modulus of elasticity, E_p, of the prestressing wires was assumed to be 200,000 MPa and the long-term modulus was taken as 171,800 MPa in accordance with the provisions of the CEB-FIP code.

2.4.1.2 Section 7B
The girders in Section 7B are post-tensioned using the GTM system (Grands Travaux de Marseille). The girders in spans 13E-14E, 12E-13E and 10E-11E of Section 7B contain 19 tendons while the girders in span 11E-12E contain 22 tendons. Each tendon consists of 7 strands of 7-wire strands. Hence one tendon has 49 wires. Each wire has a diameter of 3.6 mm, resulting in a tendon area of 500 mm². CSA S6-06 recommends a value of 1600 MPa for the ultimate

strength of the prestressing steel, f_{pu}, to be used for the evaluation of bridges constructed before 1963 and hence this value was assumed in the analyses. The initial stress in the tendons was assumed to be 0.75 f_{pu}. The short-term modulus of elasticity, E_p, of the GTM prestressing strands was assumed to be 195,000 MPa and the long-term modulus was taken as 167,500 MPa in accordance with the provisions of the CEB-FIP code.

2.5 Tendon layouts at midspan

Figure 2.4 compares the tendon locations at midspan for Sections 5, 7A and 7B.
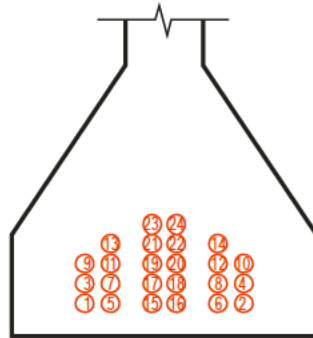
(a) Section 5 & 7A – 176'-4" spans – 24 Freyssinet tendons, 12 wires per tendon
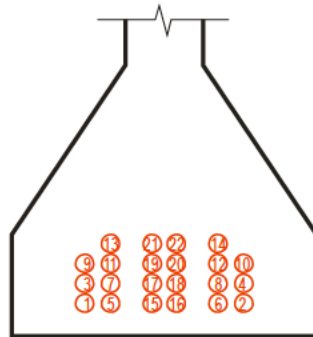
(b) Section 7A – 168'-8" spans – 22 Freyssinet tendons, 12 wires per tendon

12
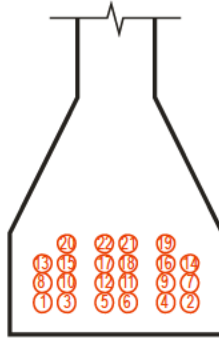
(c) Section 7B – 172'-4" spans – 22 GTM tendons, 7-7 wire strands per tendon (span 11E-12E)
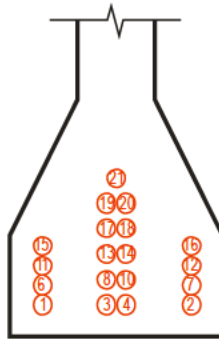
(d) Section 7B – 172'-4" spans – 19 GTM tendons (spans 10E-11E, 12E-13E, 13E-14E)

Fig. 2.4: Tendon layouts at midspan

It is noted that the layout of tendons and the bottom flange geometry for the girders in Sections 5 and 7A provide greater space for the placement of concrete than those of Sections 7A and 7B. The width of the bottom flange in Sections 5 and 7A is 27 in. (686 mm) while the width in Section 7B is 19 in. (483 mm).

2.6 Non-Prestressed Reinforcing steel

The original calculations (Warycha and Skotecky) for the design of Section 5 indicate that they had used an allowable stress in the reinforcing steel of 20,100 psi, indicating that the yield stress was likely 40,000 psi (275 MPa). This yield stress is consistent with the typical reinforcement used during the period of construction and is within the range of yield strengths recommended by CSA S6-06 for evaluation.

It was assumed that the yield strength of the normal reinforcing bars was 275 MPa.

The short-term modulus of elasticity for the reinforcing steel was taken as 200,000 MPa.

3 Estimation of Degrees of Corrosion of Tendons

For the critical span 28W-29W, observations on site indicated that severe corrosion was taking place mainly in the midspan region, at the level of the bottom tendons, in Girder P7. Figure 3.1 gives the data on the extent of corrosion, concluded by the consultants, based on observations on site at midspan of girder P7 in span 28W-29W.

Tendon Numbers	Estimated loss due to corrosion
3, 6, 11, 12, 13, 21, 22, 23, 24	100%
15, 16, 17, 18	50%
7	25%
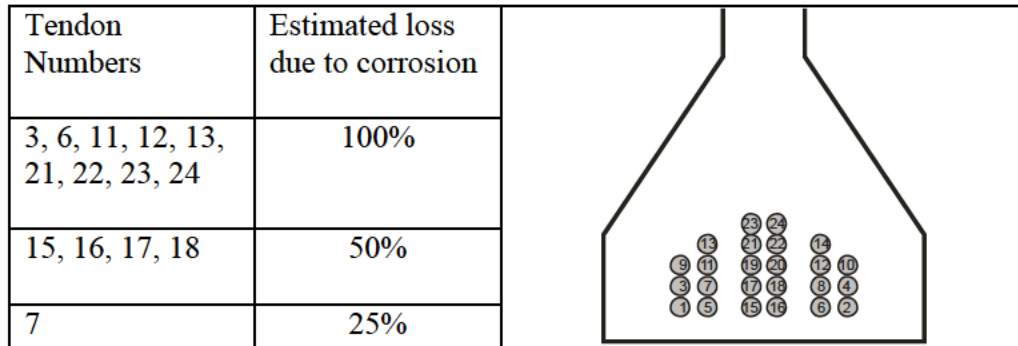
Fig. 3.1: Assumed Degree of corrosion at midspan in girder P7 of span 28W-29W
(December 2014)

Observations for this girder on site and access holes in the web of P7 indicate that the corrosion of the tendons outside of the midspan region had somewhat less corrosion than the tendons in the midspan region. This inspection also revealed that there was some corrosion of the stirrups.

This information provided some guidance on how to treat the degree of corrosion in other girders, that is, with more corrosion in the midspan region and less corrosion in the rest of the girder.

The degrees of corrosion in girders of other spans have been estimated from site inspections and these values are given in the MasterData Table updated on November 10, 2015.

4 Loads, Load Factors and Material Resistance factors

4.1 Loads and Load Factors

The dead load was determined and checked with the analysis obtained from CSI Bridge (3D study).

The live loading due to trucks and vehicular traffic conformed to the requirements of S6-06 for CL-625 truck loading and specified lane loadings. For example, for maximum moment in girder P7 at midspan the following cases were studied:

- CL-625 loading on the exterior southbound lane
- CL-625 loading on two lanes (exterior and adjacent southbound lanes)
- CL-625 loading on all three southbound lanes
- CL-625 lane loading on the exterior southbound lane
- CL-625 lane loading on two lanes (exterior and adjacent southbound lanes)
- CL-625 lane loading on all three southbound lanes

For these cases the trucks were positioned to cause maximum moment near midspan.

A value of 0.25 was assumed for the dynamic load allowance for cases with the CL-625 loading (first 3 cases listed above). Modification factors for multi-lane loading were 1.0, 0.9 and 0.8 for one lane, 2 lanes and 3 lanes loaded, respectively. From the 3D structural analysis it was determined that the most critical case for maximum moment at midspan was for the CL-625 lane loading on all three southbound lanes.

The following load factors were obtained from Section 14 – "Evaluation" of CSA S6-06, considering the estimated target reliability indices and the type of loading:

- Dead load factor for girders: 1.09 (category D1)
- Dead load factor for diaphragms, deck, asphalt and barriers: 1.18 (category D2)
- Live load factor: 1.63 (truck loading)

4.2 Material Resistance Factors

The material resistance factors used to determine the factored resistances of girder P7 conformed to the requirements in Section 8.4.6 of CSA S6-06. These material resistance factors are as follows:

- Material resistance factor for concrete, ϕ_c 0.75

- Material resistance factor for reinforcing bars, ϕ_s 0.90
- Material resistance factor for prestressing steel, ϕ_p 0.95

4.3 Maximum Moments in Midspan Regions

The maximum moments in the midspan regions for typical edge girders in Sections 5, 7A and 7B are given in Table 4.1.

Table 4.1: Maximum moments in midspan regions for Sections 5 and 7

Load	Section 5 and 7A 176'- 4'' spans kNm	Section 7A 168'- 8'' spans kNm	Section 7B 172'- 4'' spans kNm
D1	10,069	9290	9615
D2	4360	4004	4341
L	6098	5759	6080
Service D1 + D2 +L	20,526	19,053	20,035
Factored 1.09D1 + 1.18D2 + 1.63L	26,059	24,238	25,513

5   2D Non-Linear Finite Element Model

5.1   Description of Finite Element Model for Section 5

The finite element modelling was carried out with the program "VecTor2" (Vecchio 2015), version 3.8.

Fig. 5.1 shows the finite element mesh used to model an exterior girder in Section 5. The model includes the precast girder, one-half of the slab and one-half of the diaphragms between girders. The total length of the beam is 176 feet (53.64 m) and the distance between the centres of the bearings is 172 feet (52.42 m). The different coloured rectangular elements represent different concrete thicknesses and amounts of horizontal and vertical reinforcement. The post-tensioning tendons are also shown. The light blue elements represent groupings of 3 tendons while the dark blue elements are single tendons (12-7 mm diameter wires per tendon). There are 24 tendons in the girder.
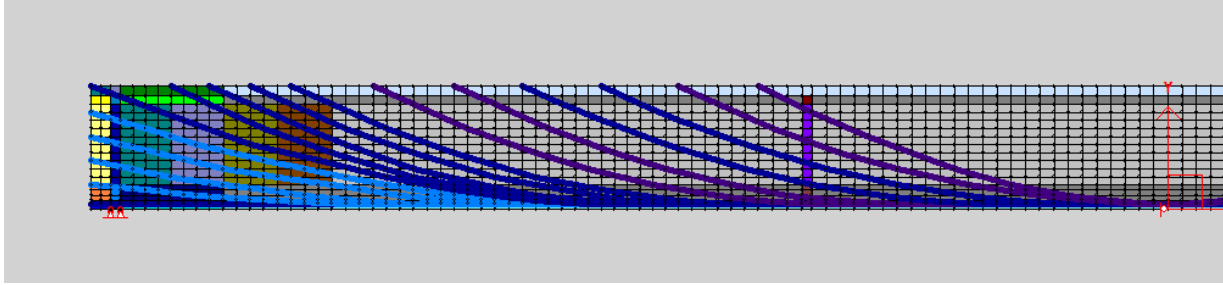
Fig. 5.1: Finite element model for P7 (symmetrical about midspan)

5.2 Determining Forces Applied to Typical Exterior Girder

A 3D linear elastic model of all of the structural elements in a typical span enabled the determination of forces in the superstructure. This analysis was carried out using CSI Bridge. This analysis was used to determine the forces applied to the exterior girders due to the interaction of an exterior girder with the other structural components in a span for different loading cases. Forces due to this interaction were applied to the 2D non-linear finite element model of a typical exterior girder to be able to study the performance of the girder for different conditions.

The 2D non-linear analyses performed did not consider the redistribution of forces between an exterior girder and the rest of the superstructure that may occur due to inelastic behavior of the exterior girder.

5.3 Loads Applied to the Finite Element Model for Maximum Moment at Midspan

The dead load was applied in two different load cases: one with just the girder self-weight (D1) and the other with the additional dead loads (D2), considering the slab, diaphragms, barrier, asphalt and an allowance for utilities, acting on the exterior girder. The midspan moment due to service dead loading is 14,430 kNm in an exterior girder in Section 5.

Figure 5.2 shows the shear force diagram that matches the shears from the 3-D model on the edge girder due to the critical live loading case for maximum moment at midspan for Section 5. This controlling load case has 3 traffic lanes loaded with lane loads. The lane load consists of 80% of the CL-625 truck plus a uniformly distributed load of ▋ kN/m. Due to the fact that 3 lanes are loaded a modification factor for multiple lane loading equal to 0.80 was applied.

17
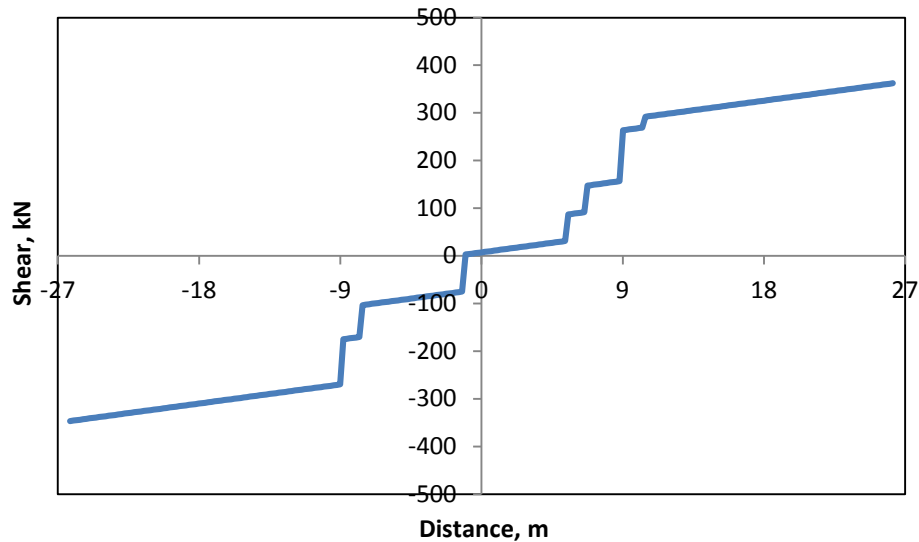
Fig. 5.2: Shear force diagram for determining the loading of the edge girder in Section 5 due to the critical live loading case for maximum moment at midspan.

The loading from the 3D model was simulated in the 2D model of the exterior girder with a combination of uniform loading on the top, point loads applied at the top to simulate the axle loads and vertical shears applied to the diaphragms. Figure 5.3 shows the live load applied to the model for the controlling load case for maximum moment at midspan. This critical service live loading case results in a moment near midspan of 6,200 kNm.

A shrinkage strain of 0.347 x 10^{-3}, obtained from the 3D analysis, was applied to the concrete.
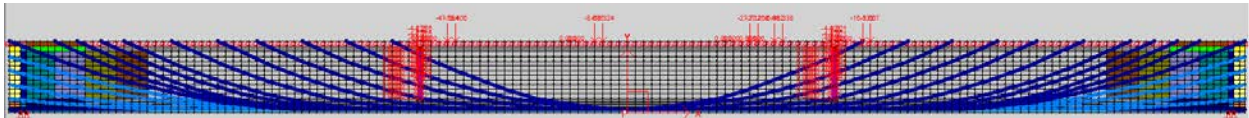
Fig. 5.3: Controlling load case for midspan moment under service live load.

5.4 Accounting for Loss of Tendons and Stirrups due to Corrosion

This section describes the manner in which the effects of tendon losses due to corrosion were accounted for in the 2D analyses. The procedure is illustrated for the case of the exterior girder P7 in span 28W-29W. First it was necessary to make assumptions concerning the degree of corrosion of the tendons as well as the stirrups. From the conclusions made by the consultants, based on observations on site (see Section 3), it was assumed that 11.25 tendons were lost at

midspan due to corrosion leaving 12.75 tendons. This represents a loss of 46.9% of the tendons at midspan. A uniform degree of corrosion of 40% of the tendons was assumed for the tendons outside of the midspan region. In addition, a uniform degree of corrosion of 40% was assumed for the stirrups.

Figure 5.4 shows the modelling of the loss of tendons due to corrosion, with the tendons in the midspan region (orange colour) indicating the concentrated corrosion assumed at midspan. In addition the cross-sectional areas of the stirrup reinforcement were reduced by 40%.
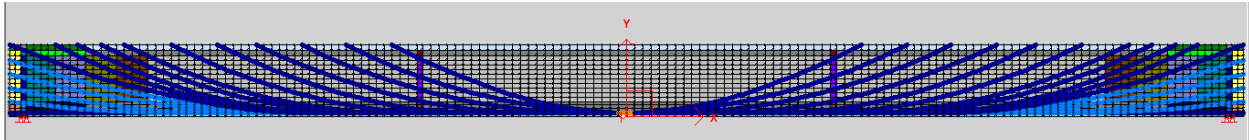
(a) Overall view
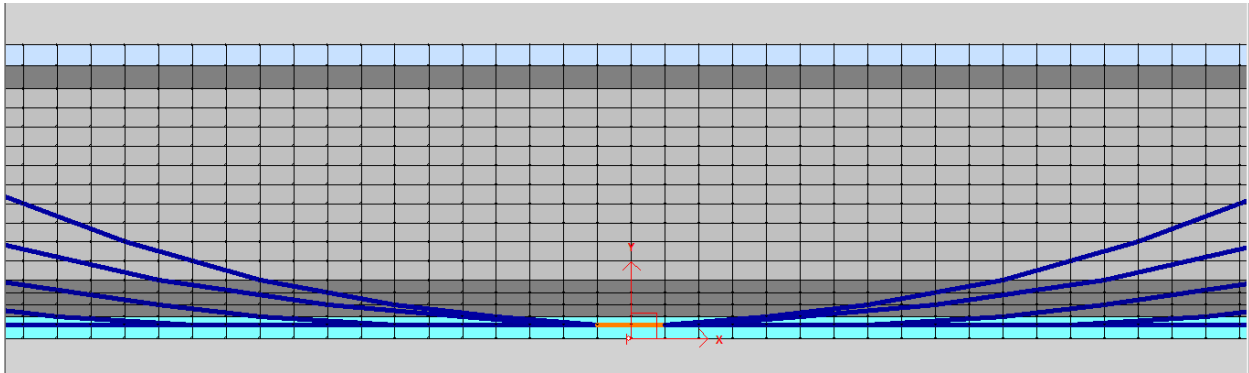
(a) Close-up of midspan region

Fig. 5.4: Modelling of corroded tendons

It is noted that the loss of tendons due to corrosion in an exterior girder will cause restraint effects from the remaining six girders that are connected to the edge girder by the diaphragms and the deck. To account for this effect in the 3D model a 1000 kN unit tensile force was applied to the girder at the centre of gravity of the prestressing at locations 4 m on either side of midspan of the girder. This unit tensile force of 1000 kN was applied in the 3D model to girder P1 to study the effects of restraint from the other girders. In addition, a separate force of 1000 kN was applied to girder P7 to represent tendon losses in this girder. This technique was used to determine the restraint effects in girder P7 due to tendon losses in girders P1 and P7. Figures 5.5 and 5.6 show the resulting restraint actions on P7 due to the 1000 kN force on P7 and P1 from the 3D analyses.
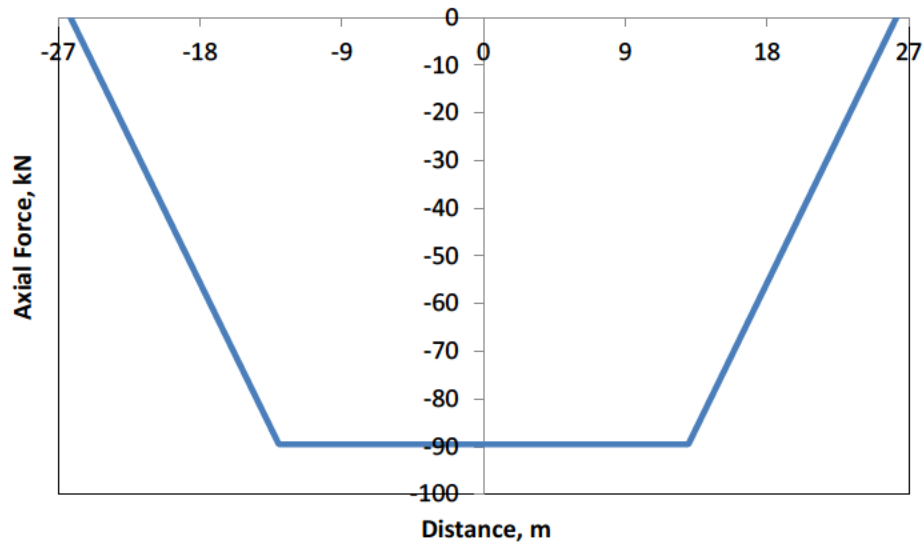
(a) Axial load
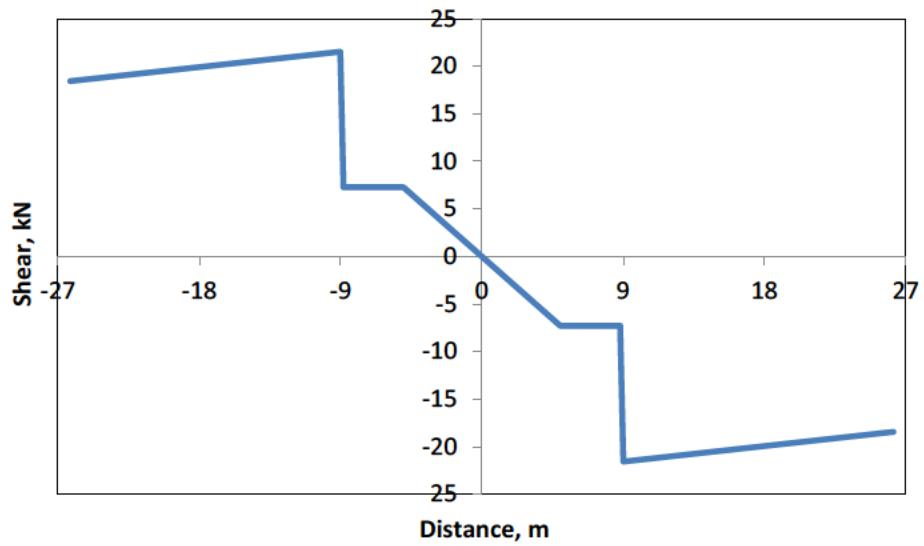
(b) Shear

Fig. 5.5: Restraint actions on P7 due to a unit tensile force of 1000 kN on P7.
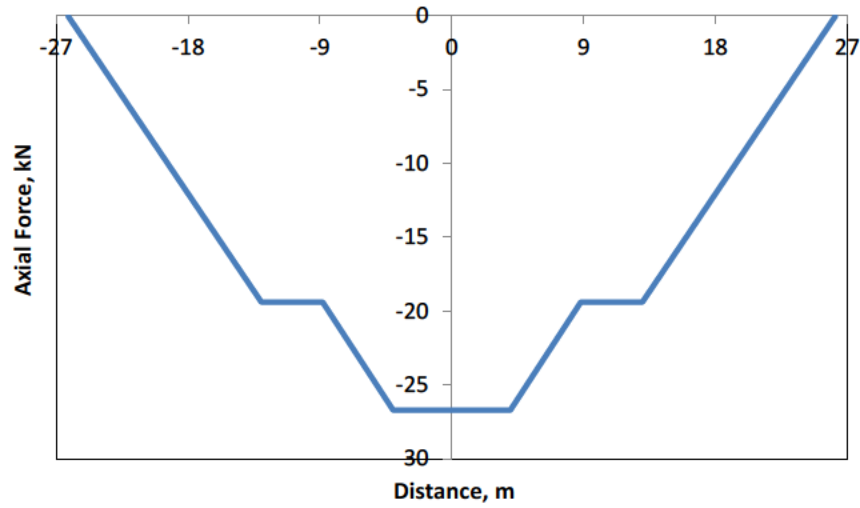
(a) Axial Load
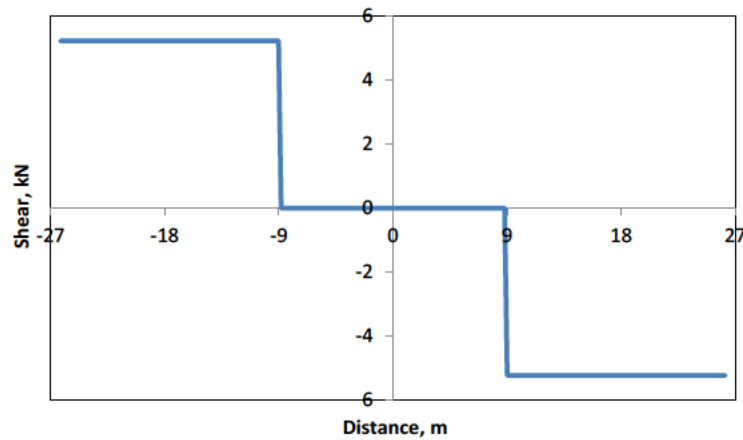
(b) Shear

Fig. 5.6: Restraint actions on P7 due to a unit tensile force of 1000 kN on P1.

In order to determine the force associated with the loss of one tendon in Section 5 and 7A it was assumed that the tendon force after all losses is:

$$P_f = A_p f_p = 462 \times 0.49 \times 1572 = 355.9 \text{ kN}$$

Hence, for example, if there were 11.25 tendons lost, as assumed in P7 of span 28W-29W then the unit load case results shown in Fig. 5.5 would be multiplied by a factor of:

$$\frac{11.25 \times 355.9}{1000} = 4.00 \text{ to determine the restraint effects on P7.}$$

21

In addition, for this same span, if there were 2 tendons lost, as assumed in P1 of span 28W-29W then the unit load case results shown in Fig. 5.6 would be multiplied by a factor of:

$$\frac{2 \times 355.9}{1000} = 0.712 \text{ for the additional restraint effects on P7.}$$

To determine the combined restraint effects of the loss of 11.25 strands in P7 and the loss of 2 strands in P1 these two effects are added together to determine the restraint effects in P7 and these forces were applied to the 2D nonlinear model.

This approach was used to determine the elastic restraint effects in different spans with varying degrees of corrosion.

5.5 Accounting for Strengthening Measures

The effects of different strengthening measures, including external horizontal post-tensioning (PTE and PTE2), Queen Post 1 (QP1) and Queen Post 2 (QP2 and QP2.1), were first analysed using the 3D model. The forces from the 3D model, acting on the edge girder being analysed, were then applied to the 2D non-linear model to simulate the effects of strengthening.

The effects of the strengthening have been simulated in the 2D non-linear model by the application of loads on the edge girder to correspond to the linear elastic forces obtained from the 3D analysis of the entire bridge span with seven girders. Because the effects of the strengthening measures were modelled using applied forces, the stiffness of the added post-tensioning was neglected.

6 Evaluation of Girder P7 in Span 28W-29W (Section 5)

6.1 Introduction

To obtain more accurate predictions, including the redistribution of forces due to loss of tendons due to corrosion, the response of Girder P7 in span 28W-29W was determined using the approaches described in Section 5. It is noted that before the Superbeam and Truss were used to strengthen this girder, Girders P1 and P7 had very unsymmetrical PTE forces of 2109 kN and 1226 kN, respectively when significant cracking developed in the midspan region.

6.2 Predicted Response of As-Designed Girder with no Corrosion and no Strengthening – Service Load

This analysis represents the original condition of the girder, except a concrete compressive strength of 53.9 MPa was assumed to account for the increase in strength with time. No strengthening was considered.

No cracking was predicted under service loading (D + L), with first flexural cracking is predicted to occur at a load level of D + 2.5L if the long-term material properties are assumed.

6.3 Predicted Response of As-Designed Girder with no Corrosion and no Strengthening – Factored Load

An analysis under factored loading was carried out using material resistance factors for the concrete, reinforcing steel and prestressing steel (see Section 4.2). This analysis uses the conditions of the girder as originally designed but with a concrete compressive strength of 53.9 MPa. It is noted that no cracking is predicted, even under factored loading, for the critical live loading condition for maximum moment at midspan. The factored loading was equal to:

$$1.09 \times D1 + 1.18 \times D2 + 1.63 \times L$$

In order to assess the maximum factored resistance of girder P7, the live loading was increased incrementally until failure was predicted. Figure 6.1 shows the conditions of the girder at predicted failure, assuming that there is no corrosion of the reinforcing bars or tendons. It is noted that the girder is predicted to fail in flexure. The predicted flexural cracks extend over the full depth of the web and there is only minor inclined cracking due to shear. This analysis was carried out by first loading the girder with factored dead loads and then increasing the live load to cause failure. The resulting factored loading to cause failure is given by:

$$1.09 \times D1 + 1.18 \times D2 + X \times L$$

Where X is the load factor on the live load, L, to cause failure. From the non-linear analysis this factor was determined to be 4.40. This is greater than the required live load factor of 1.63 for the evaluation of the girder. Another way of expressing the margin of safety is by using the demand/capacity ratio, D/C, which for this case is 0.62.
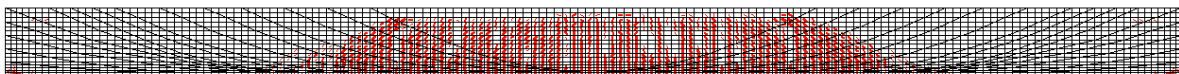
28W P7 Fac Fl 0 cr   PAN MODE   Displace/Cracks: Crack Dir'ns   Displacement Factor = 4.40

(a) Overall view
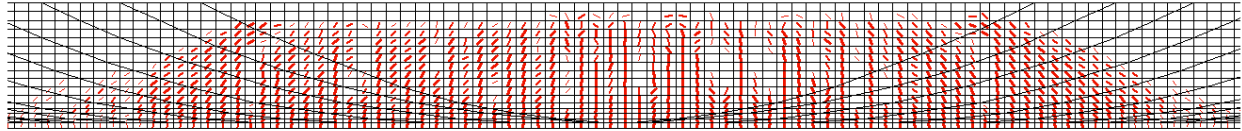
28W P7 Fac Fl 0 cr   PAN MODE   Displace/Cracks: Crack Dir'ns   Displacement Factor = 4.40

(b) Close-up of midspan region

Fig. 6.1: Conditions of as-designed girder at flexural ultimate under 4.40 times live load (without corrosion).

6.4 Predicted Behaviour of Girder P7, with Corrosion and External Post-Tensioning (PTE)

In 1998 only girder P7 of span 28W-29W was strengthened using external post-tensioning applied at the level of the bottom flange (see Fig. 6.2). A total of 8 - 15mm diameter strands (4 on each side of girder P7) were installed. These strands, with an ultimate strength, f_{pu}, of 1860 MPa, were initially stressed to $0.6f_{pu}$. From the analysis carried out using CSI Bridge it was determined that after all losses this stress would reduce to $0.54f_{pu}$. This gives a total prestressing force after all losses of:

$$P_{final} = 8 \times 140 \times 0.54 \times 1860 = 1125 \text{ kN}$$

The MasterData Table (November 10, 2015) reports an initial PTE force of 1226 kN. Hence the value used for analysis, after all prestress losses was taken as:

$$P_{final} = 0.9 \times 1226 = 1103 \text{ kN}$$

It is noted that at this time (1998) the PTE was applied only to P7 and not to P1 in span 28W-29W.
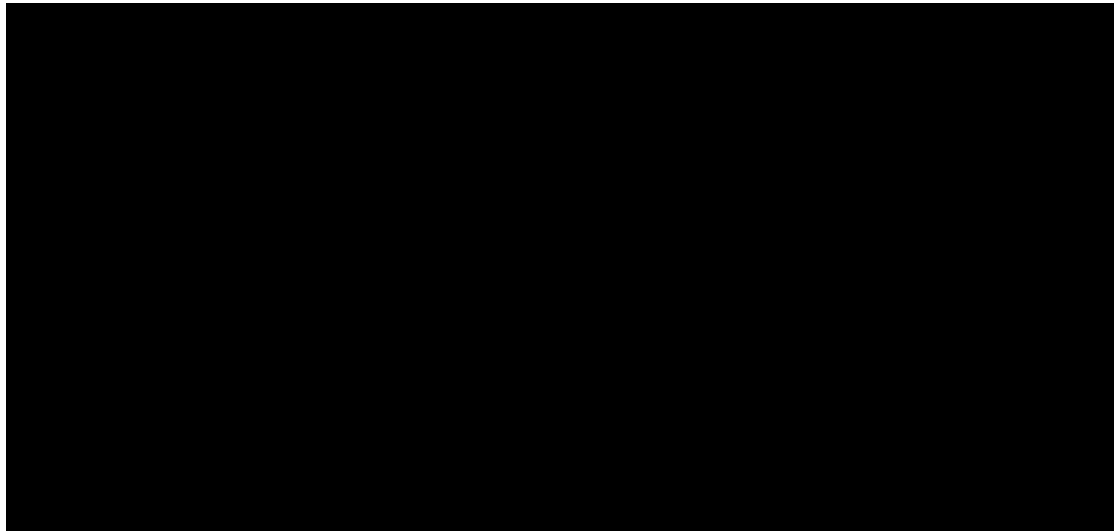
Fig. 6.2: Details of PTE for girder P7 in span 28W-29W added in 1998 (PJCCI drawing 125101-06, 1998).

It is noted that the 3D analysis that was carried out indicates that with this tendon force applied to P7 only, the effective axial force in girder P7 at midspan was 554 kN. This means that only about 50% of the applied PTE is active at midspan of girder P7. This loss of PTE in girder P7 is due to the significant spreading of compression that occurs in the superstructure.

From the structural drawings of AECOM (2011) it was determined that a different level of PTE was added to girder P1 of span 28W-29W in the period 2012-2013. The drawings show that a total of 18 - 15mm diameter strands (9 on each side of girder) were installed on girder P1 (see Fig. 6.3). From the MasterData Table, the initial force was 2109 kN and hence the total assumed prestressing force after all losses was:

$P_{final} = 0.9 \times 2109 = 1898$ kN
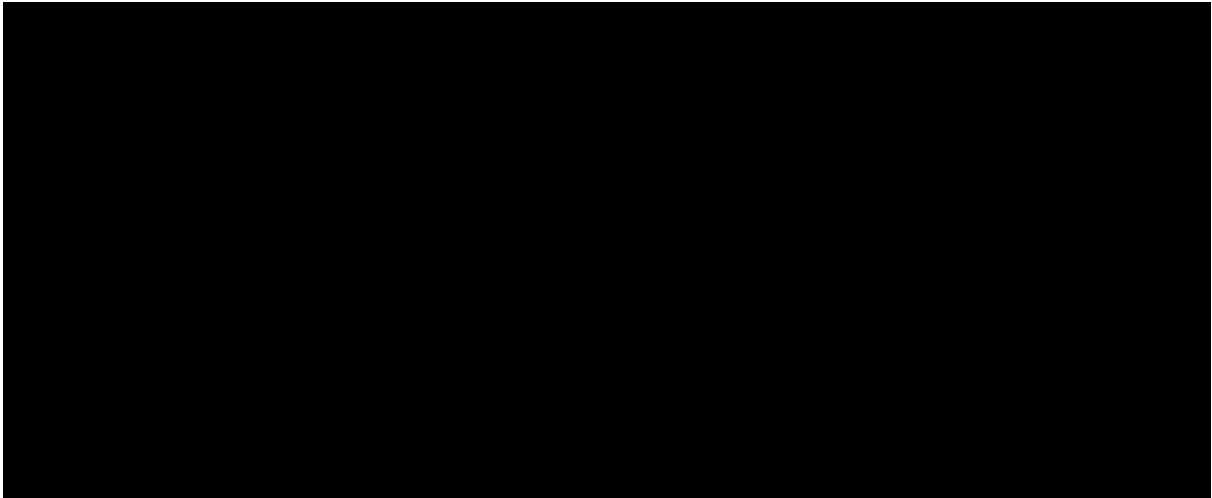
Fig. 6.3: Details of PTE for girder P1 in span 28W-29W added in 2012 (AECOM, drawing 125570 -32, 2012).

The 3D analysis indicates that the effect of adding PTE to girder P1 is to induce tension in girder P7. If the combined effect of the PTE on girder P7 and P1, as described above, is considered then, from the 3D analysis, the effective axial compression on P7 is reduced to 302 kN. It is assumed that both of these PTE levels were applied to span 28W-29W and were present when the severe cracking was observed in 2013.

Figure 6.4 shows the axial force and shear force diagrams corresponding to the forces applied to the 2D model of girder P7 to simulate the external horizontal post-tensioning. Figure 6.5 shows the forces applied to the 2D model to simulate the effects of PTE on P7.
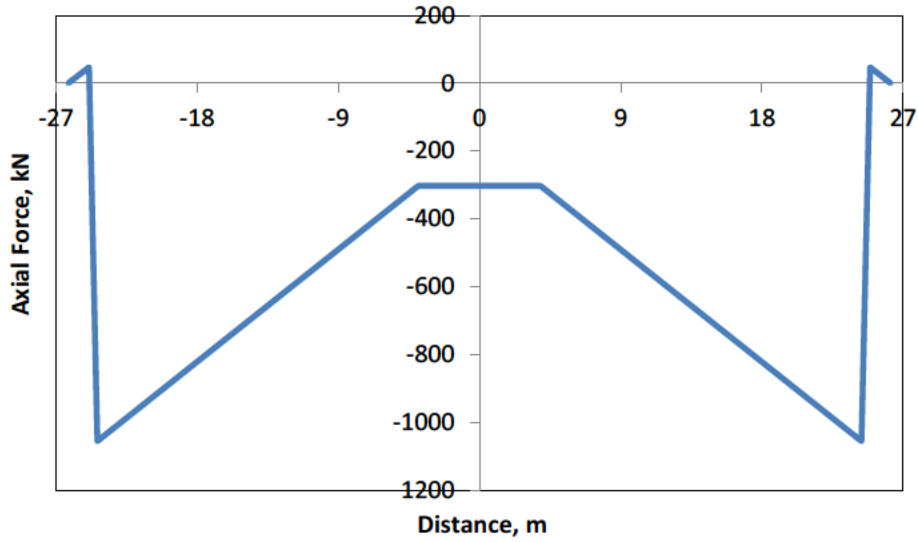
(a) Axial force
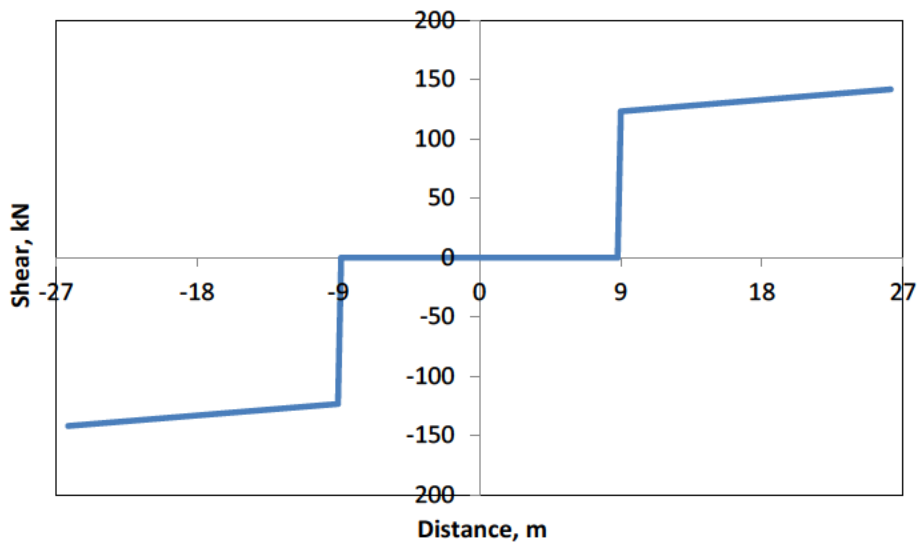
(b) Shear force

Fig. 6.4: Axial force and shear force diagrams corresponding to the forces applied to the 2D model of girder P7 to simulate the external horizontal post-tensioning.
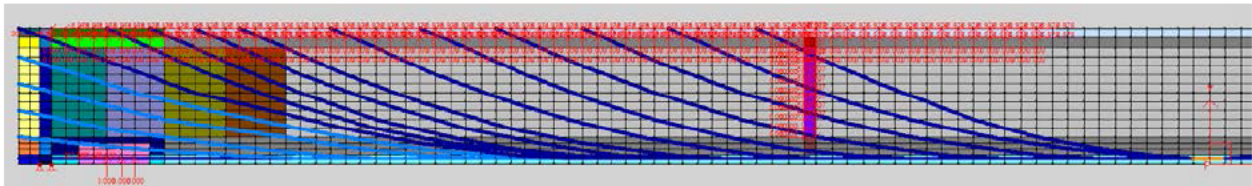
Fig. 6.5 Forces applied to girder P7 to simulate the PTE on Girders P7 and P1.

26

6.5 Behaviour of Girder P7 due to Service Loading, with Corrosion and PTE

Figure 6.6 shows the predicted cracking in the midspan region for girder P7 with corroded tendons and corroded stirrups after the external post-tensioning has been applied. The prestressing steel area has been reduced in the midspan region to simulate the loss of 11.25 tendons (46.9% corrosion) and the stirrups and prestressing steel areas have been reduced by 40% in other regions of the girder. Short-term material properties were used in making this prediction. It is noted that the application of these two different levels of PTE in P1 and P7 did not prevent cracking. The predicted maximum crack widths are 0.16 mm in both the bottom of the flange and in the flange taper, respectively. First cracking is predicted to occur at a load corresponding to D + 0.9L.

28W PTE Nom Fl 11.25 cr · · · PAN MODE · · · Displace/Cracks: Crack Dir'ns · Displacement Factor = 1.00

(a) Overall view

28W PTE Nom Fl 11.25 cr · · · PAN MODE · · · Displace/Cracks: Crack Dir'ns · Displacement Factor = 1.00
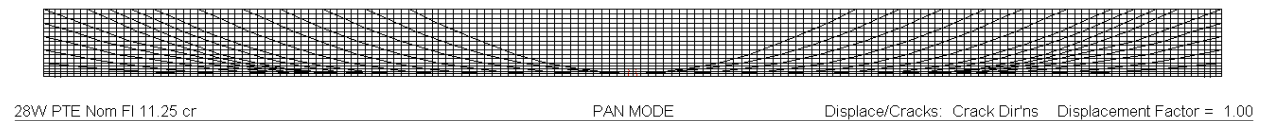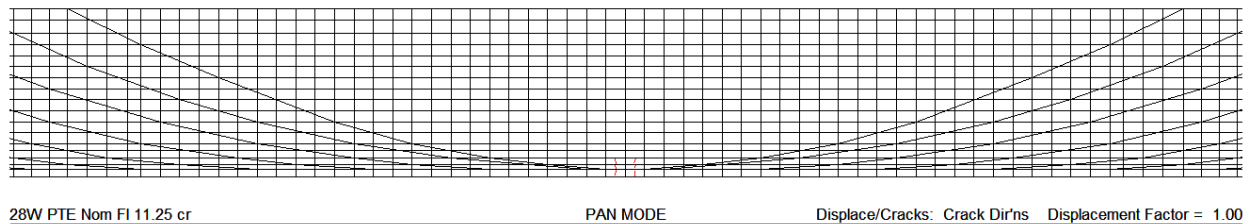
(b) Close-up of midspan region

Fig. 6.6: Cracking predictions for maximum moment at midspan for short-term service loads with corroded tendons and corroded stirrups, strengthened with PTE.

Figure 6.7 shows a similar prediction, but with long-term material properties. The predicted maximum crack widths are 0.66, 0.91, and 0.39 mm in the bottom of the flange, in the flange taper and in the bottom of the web, respectively. First cracking is predicted to occur at a load corresponding to D + 0.7L.

28W PTE LT Nom Fl 11.25 cr · · · PAN MODE · · · Displace/Cracks: Crack Dir'ns · Displacement Factor = 1.00

(a) Overall view

28W PTE LT Nom Fl 11.25 cr   PAN MODE   Displace/Cracks: Crack Dir'ns   Displacement Factor = 1.00
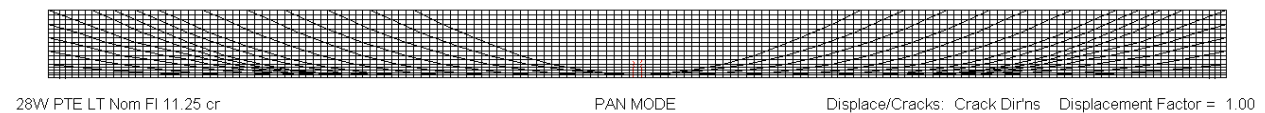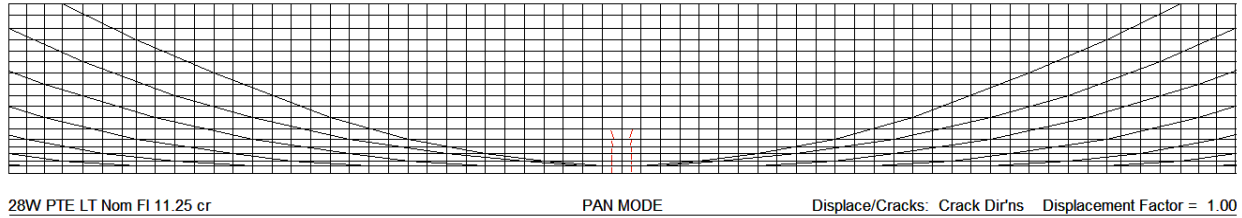
(b) Close-up of midspan region

Fig. 6.7: Cracking predictions for maximum moment at midspan for long-term service loads with corroded tendons and corroded stirrups, strengthened with PTE.

6.6 Behaviour of Girder P7 due to Factored Loading, with Corrosion and PTE

Figure 6.8 shows the condition of girder P7 at maximum predicted factored resistance for the live loading case causing maximum moment at midspan with corroded tendons and corroded stirrups, strengthened with PTE.

The girder is predicted to fail in flexure with very large cracks near midspan and flexural cracks occurring over a length of about one-third of the span. Inclined cracking was also predicted near the diaphragms. Failure is predicted at a live load corresponding to a live load factor of 1.96, somewhat above the 1.63 required. The D/C ratio is 0.94.

28W PTE Fac Fl 11.25 cr   PAN MODE   Displace/Cracks: Crack Dir'ns   Displacement Factor = 1.96

(a) Overall view

28W PTE Fac Fl 11.25 cr   PAN MODE   Displace/Cracks: Crack Dir'ns   Displacement Factor = 1.96
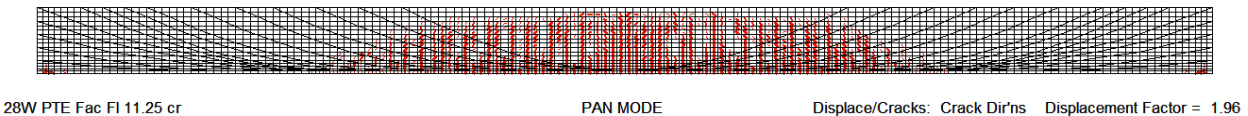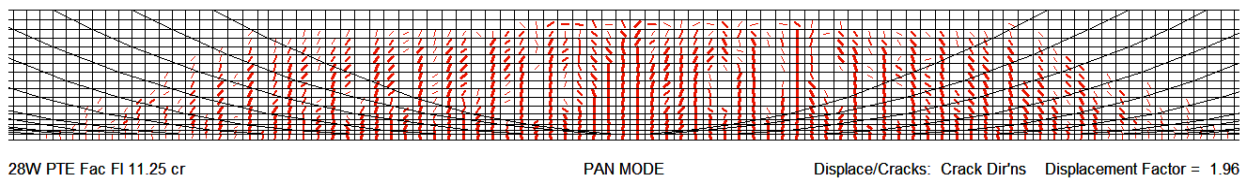
(b) Close-up of midspan region

Fig. 6.8: Predicted factored resistance for maximum moment at midspan with corroded tendons and corroded stirrups, strengthened with PTE.

6.7 Conclusions on the Performance of Girder P7 in Span 28W-29W

The 2D nonlinear analysis indicates that significant flexural cracking (maximum crack width of 0.91 mm) in the midspan region is predicted to occur when 11.25 tendons have been lost due to corrosion under a live loading equal to the service live loading specified in CSA S6-06. This significant cracking is unacceptable. It is noted that following the observation of significant cracking in the midspan region of girder P7 in November 2013, the Superbeam was used to help support the girder until a truss was positioned under the girder and jacked against the bottom flange.

It is noted that the D/C ratio is predicted to be extremely close to 1.0. Although this D/C ratio of 1.0 would be satisfactory in a new bridge without corrosion, the uncertainty associated with the degree of corrosion and the risk of further corrosion renders this unacceptable. The predicted cracking under service loading is also unacceptable.

7 Evaluation of Combined Effects of PTE and QP1 on Section 5 Girders

7.1 Introduction

This section examines the influence of the PTE and QP1 strengthening measures on the expected performance of the exterior girders in spans of Section 5 that had been strengthened with QP1.

7.2 QP1 Strengthening Measures

The overall length of the girders in Section 5 is 176'-0", resulting in a centre-to-centre span of 172'-0". Figure 7.1 shows the general aspects of the strengthening using QP1 (AECOM 2011). The post-tensioning consisted of 4 - 36 mm diameter high-strength bars (1035 MPa ultimate strength) on each external girder, P1 and P7.
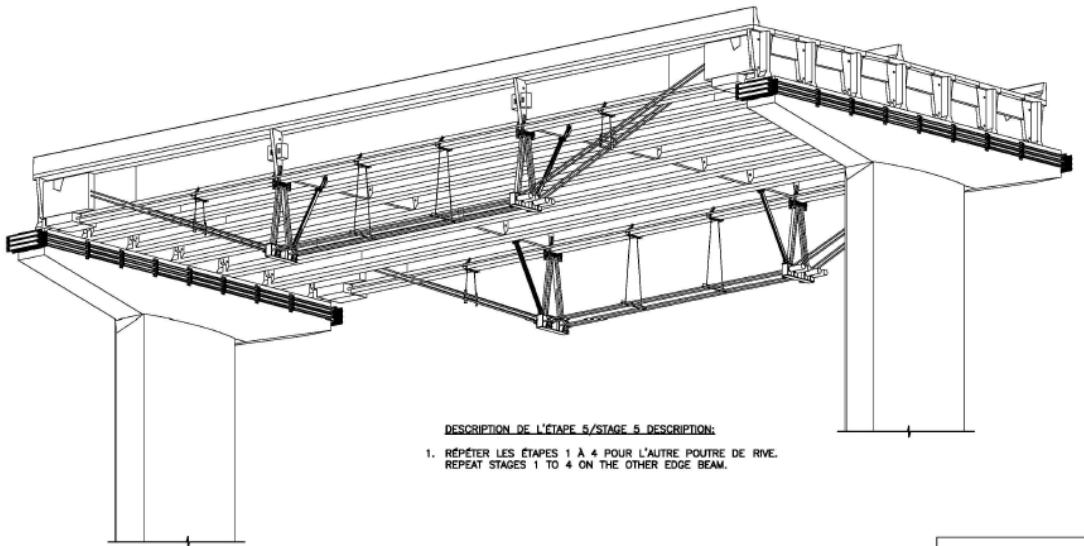
Fig. 7.1: Queen Post 1 Strengthening (AECOM 2011)

As an example of the QP1 strengthening measures, the force levels used in QP1 for span 34W-35W will be discussed. In 2009 the exterior girders of span 34W-35W was strengthened using QP1 and the stressing records (Construction Euler Inc. 2009) indicated that the desired force per high-strength bar was 475 kN. It is noted that the stressing sequence involved stressing two of the four bars to 1.25 x 475 kN or about 600 kN and then the remaining two bars were stressed to 475 kN. In order to study the effects of QP1 that had been used in 2009 the total force in the 4 horizontal high-strength bars, including allowance for sequential post-tensioning and long-term losses was assumed to be 4 x 475 kN = 1900 kN. This approach was taken for all of the spans with QP1 strengthening.

A typical span was modelled using the 3D model and the resulting forces applied to the exterior girders were used to apply forces in the 2D non-linear model. Due to the large forces anchored in the web of the girder near its end, the designers thickened the web over its full height and over a length of about 3.5m. This anchorage block region was simulated in the 2D non-linear model by thickening the web in this region.

It is noted that the structural drawings for strengthening using QP1 show a variety of stressing levels depending on the level of PTE, the assumed degree of corrosion and the concrete strength of the diaphragms (see Fig. 7.2). The level of post-tensioning for the QP1 strengthening was set equal to the values in the November 10, 2015 MasterData Table.

ÉTAT DE LA POUTRE DE RIVE EDGE BEAM CONDITION		RÉSISTANCE EN COMPRESSION f'c DU BÉTON DES DIAPHRAGMES DIAPHRAGM CONCRETE COMPRESSIVE STRENGTH f'c (MPa)				
TENSION DE PRÉCONTRAINTE EXTÉRIEURE LONGITUDINALE EXISTANTE EXISTING EXTERIOR LONGITUDINAL PRESTRESSING LOAD	QUANTITÉ DE CÂBLES INTERNES PERDUS* QUANTITY OF INTERNAL CABLES LOST*	30	35	40	45	>50
1874kN	0	275	350	375	400	425
1874kN	2	300	350	375	400	425
1874kN	4	335	375	375	415	425
2344kN	4	300	335	350	375	400
2344kN	6	325	335	360	375	400
2812kN	6	285	310	325	340	350
2812kN	8	300	325	335	350	360
3281kN	8	260	275	315	315	335
3281kN	10	275	285	315	325	335

TENSION FINALE (T) (kN) PAR BARRE DE PRÉCONTRAINTE HORIZONTALE
(APRÉS PERTES INSTANTANÉES)

FINAL JACKING FORCE (T) (kN) PER HORIZONTAL PRESTRESSING BAR
(AFTER INSTANTANEOUS LOSSES)

Fig. 7.2: Jacking forces used in 2012-2013 for spans strengthened with QP1 AECOM drawing 1255570-47, 2011).

7.3 Key parameters of Spans with PTE and QP1

Table 7.1 summarizes some of the main factors in judging which spans and which girders that were strengthened with PTE and QP1 in Section 5 are the most critical.

Table 7.1 Key parameters for Section 5 spans with PTE and QP1 from the November 10, 2015 MasterData Table

Span	Girder	# tendons Lost/original # (Nov 10, 2015 MDT)	PTE kN	QP1 kN	CEC (2014 inspection)
34W-35W	P1	2/24	1876	1900	3
	P7	4/24	1876	1900	3
33W-34W	P1	5/24	2161	1900	1
	P7	3/24	1902	1900	2
32W-33W	P1	3/24	1875	1660	3
	P7	8/24	3515	1660	1
31W-32W	P1	2/24	1879	1900	3
	P7	5/24	1879	1900	1
29W-30W	P1	5/24	1873	1900	3
	P7	4/24	1750	1900	1
27W-28W	P1	3/24	1875	1700	2
	P7	11/24	2850	1700	1
26W-27W	P1	1/24	1923	1500	3
	P7	9/24	1695	1500	1
23W-24W	P1	1/24	1969	1900	3
	P7	3/24	1430	1900	2
21W-22W	P1	7/24	2918	1440	1

	P7	4/24	2691	1440	1
12W-13W	P1	8/24	3052	1360	1
	P7	7/24	3038	1360	1
6W-7W	P1	8/24	1872	1160	3*
	P7	4/24	3435	1160	3

*- note that the CEC was 1 in the winter of 2013

The issues concerning those girders that were considered to be most critical are discussed below.

7.4 Span 31W-32W

This span has been chosen for retrofit with modular trusses in 2015. The reason for giving this span significant priority is the condition of the girder with fibre wrapping of the bottom flange resulting in significant water retention in the flange and an uncertain degree of corrosion.

7.5 Span 27W-28W

This span has been chosen for retrofit with modular trusses in 2015. Girder P7 of this span has the largest estimated number of strands lost (11) due to corrosion of all of the girders with QP1 strengthening in Section 5. However it does have a reasonably high level of PTE that has similar force values on P1 and P7 and reasonably high level of force in the QP1 strengthening.

7.5.1 Modelling of Girder P7

Non-linear analysis was carried out on Girder P7 of span 27W-28W. In order to account for losses in the PTE, the forces were reduced by 10% resulting in a force of 1688 kN PTE on P1 and 2565 kN PTE on P7. Symmetrical QP1 forces of 1700 kN were assumed on each of P1 and P7.

Figure 7.3 shows the non-linear finite element model and the forces applied to simulate a unit horizontal load of 1000 kN in QP1. Figure 7.4 shows the axial load and shear force diagram due to a QP1 force of 1700 kN.
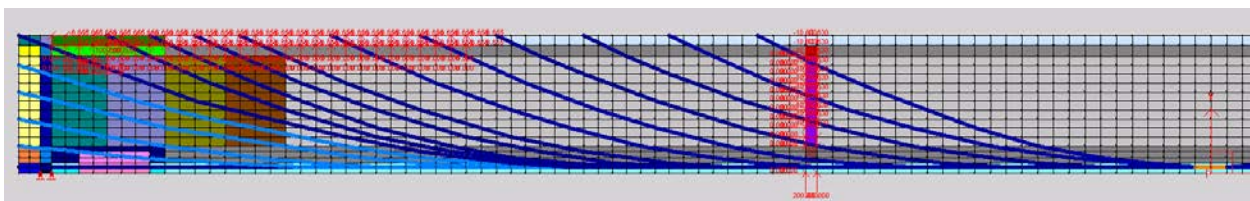
Fig. 7.3: Unit loading case used to simulate the effects of QP1 on girder P7.
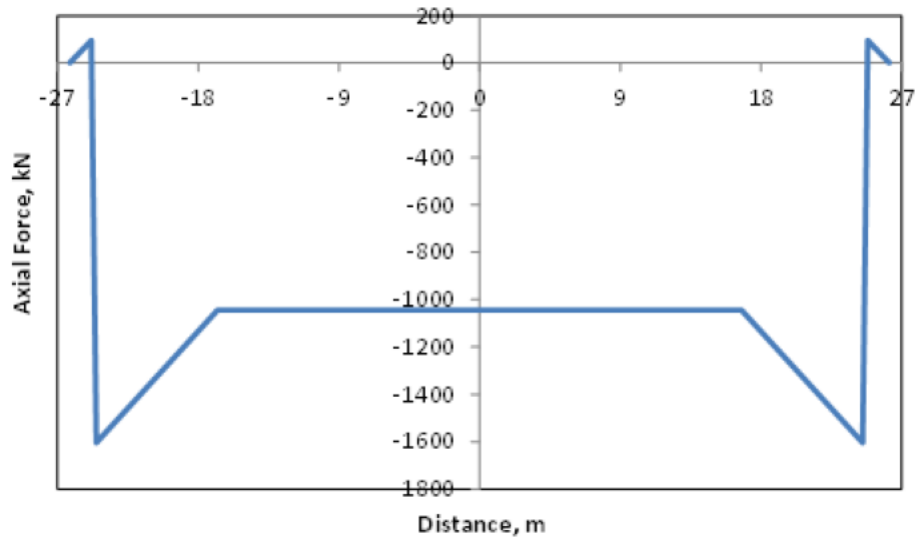
(a) Axial Force
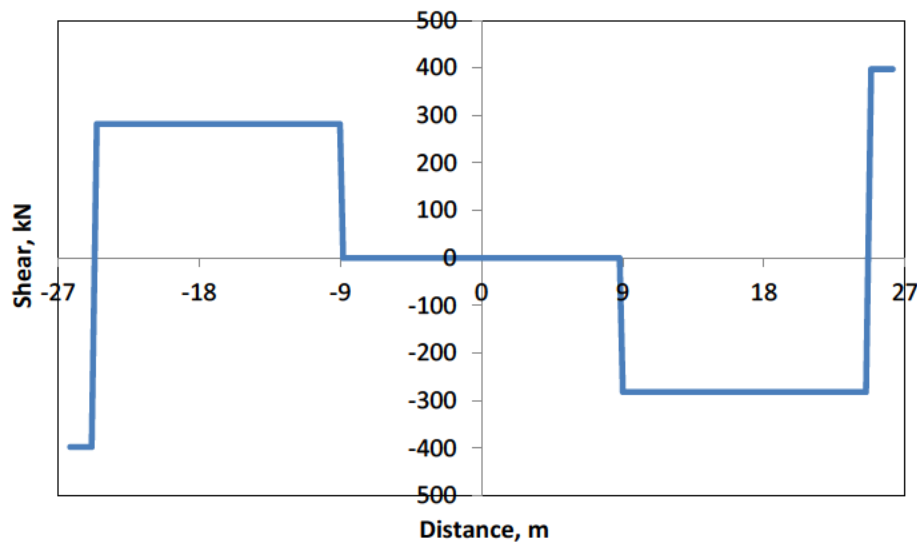
(b) Shear force

Fig. 7.4: Axial force and shear force diagrams corresponding to the forces applied to the 2D model of girder P7 to simulate 1700 kN in QP1 (Span 27W-28W)

Figure 7.5 shows the axial load and shear force diagrams corresponding to the loads applied to the girder to simulate the loading case for the PTE on P7.

(a) Axial force

(b) Shear force

Fig. 7.5: Axial force and shear force diagrams corresponding to the forces applied to the 2D model of girder P7 to simulate PTE forces of 1688 kN PTE on P1 and 2565 kN PTE on P7 (span 27W-28W)).

7.5.2 Results for Critical Loading at Midspan under Service Loading for Combined Case of QP1 and PTE (Girder P7 – Span 27W-28W)

A general level of corrosion for the girder of 39% was assumed for all reinforcement in the span except that in the midspan region it was assumed that 11 tendons were lost due to corrosion (45.8% corrosion) as indicated in the MasterData Table.

The results from the analysis indicate that under short-term and long-term conditions flexural cracking would occur at midspan when the girder is subjected to dead load plus 2.0 and 1.8 times the service live load, respectively.

Figure 7.6 shows the crack patterns at the maximum factored loading that girder P7 can carry. The girder reached a factored load corresponding to factored dead loading plus 3.18 times the live load. The D/C ratio is 0.70.

27W PTE+ QP1 Fac Fl 11 cr   PAN MODE   Displace/Cracks: Crack Dir'ns   Displacement Factor = 3.18

27W PTE+ QP1 Fac Fl 11 cr   PAN MODE   Displace/Cracks: Crack Dir'ns   Displacement Factor = 3.18
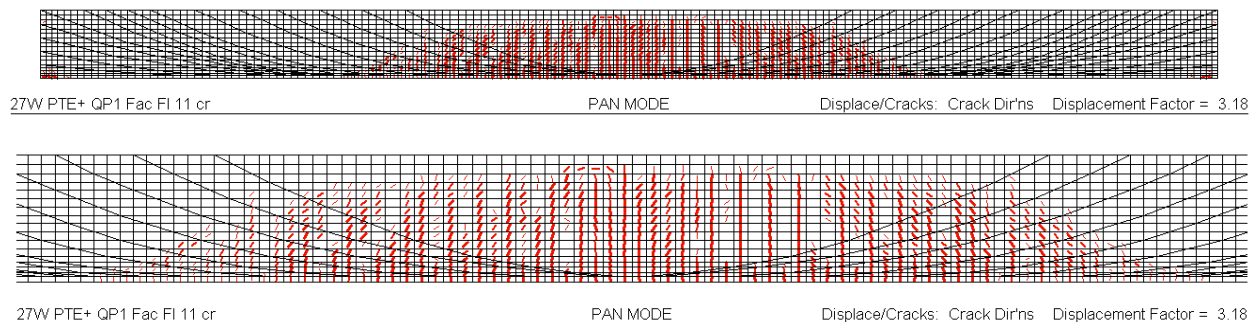
Fig. 7.6: Crack patterns at maximum factored resistance corresponding to factored dead load plus 3.18 times service live load. Corrosion considered (P7 in span 27W-28W).

7.6 Span 12W-13W

This span has an estimated number of strands lost due to corrosion of 8 in P1 and 7 in P7. The PTE is virtually symmetrical but has a somewhat lower level of QP1 force than 9 of the other spans.

7.6.1 Modelling of Girder P1

Non-linear analysis was carried out on Girder P1 (P7 has slightly less estimated corrosion) of span 12W-13W. In order to account for losses in the PTE, the average of the applied forces on P1 nd P7 was reduced by 10% resulting in a force of 2747 kN PTE on P1 and 2734 kN on P7. Symmetrical QP1 forces of 1360 kN were assumed on each of P1 and P7.

Figure 7.7 shows the forces applied to simulate the the 1360 kN QP1.
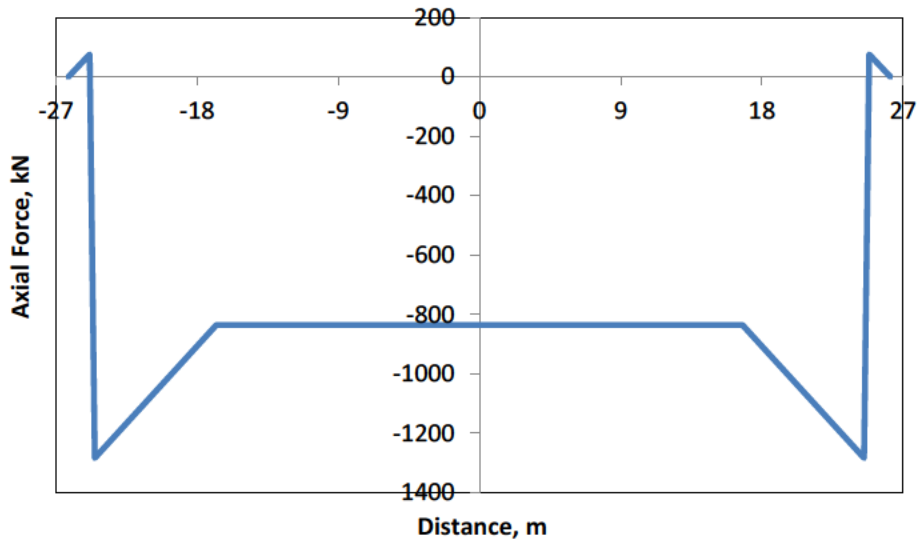
(a) Axial Force
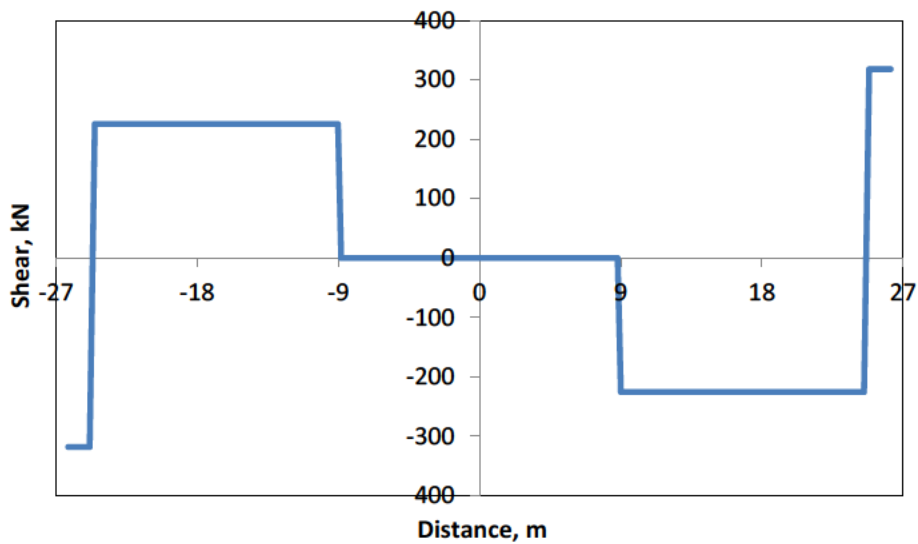
(c) Shear force

Fig. 7.7: Axial force and shear force diagrams corresponding to the forces applied to the 2D model of girder P7 to simulate 1360 kN in QP1 (span 12W-13W).

Figure 7.8 shows the forces applied to P1 to simulate the loading case for the symmetrical PTE forces on P1 and P7.

(c) Axial force

(d) Shear force

Fig. 7.8: Axial force and shear force diagrams corresponding to the forces applied to the 2D model of girder P1 to simulate symmetrical applied PTE forces of 2747 kN PTE on P1 and 2734 kN on P7 (span 12W-13W).

7.6.2 Results for Critical Loading at Midspan under Service Loading for Combined Case of QP1 and PTE (Girder P1)

A general level of corrosion for the girder of 30% for all reinforcement in the span except that in the midspan region it was assumed that 8 tendons were lost due to corrosion (33% corrosion).

The results from the analysis indicate that under short-term and long-term conditions flexural cracking would occur at midspan when the girder is subjected to dead load plus 2.5 and 2.2 times the service live load, respectively.

7.6.3 Results for Critical Loading at Midspan under Factored Loading

Figure 7.9 shows the crack patterns at the maximum factored loading that girder P1 can carry. The girder reached a factored load corresponding to factored dead loading plus 3.67 times the live load. This corresponds to a D/C ratio of 0.65.

12W PTE+ QP1 Fac Fl 8 cr   PAN MODE   Displace/Cracks: Crack Dir'ns   Displacement Factor = 3.67

12W PTE+ QP1 Fac Fl 8 cr   PAN MODE   Displace/Cracks: Crack Dir'ns   Displacement Factor = 3.67

Fig. 7.9: Crack patterns at maximum factored resistance corresponding to factored dead load plus 3.67 times service live load. Corrosion considered (Girder P1 of span 12W-13W)..

7.7 Span 6W-7W

This span has an estimated number of strands lost due to corrosion of 8 in P1 and 4 in P7. The PTE is very unsymmetrical with 1872 kN on P1 and 3435 kN on P7, with the lower value on the critical girder, P1. In addition, this span has the lowest level of QP1 force, 1160 kN, than the other spans.

7.7.1 Modelling of Girder P1

Non-linear analysis was carried out on Girder P1 (P7 has a lower estimated loss of tendons) of span 6W-7W. In order to account for losses in the PTE, the average of the applied forces on P1 and P7 was reduced by 10% resulting in a force of 1685 kN PTE on P1 and 3092 kN on P7. Symmetrical QP1 forces of 1160 kN were assumed on each of P1 and P7.

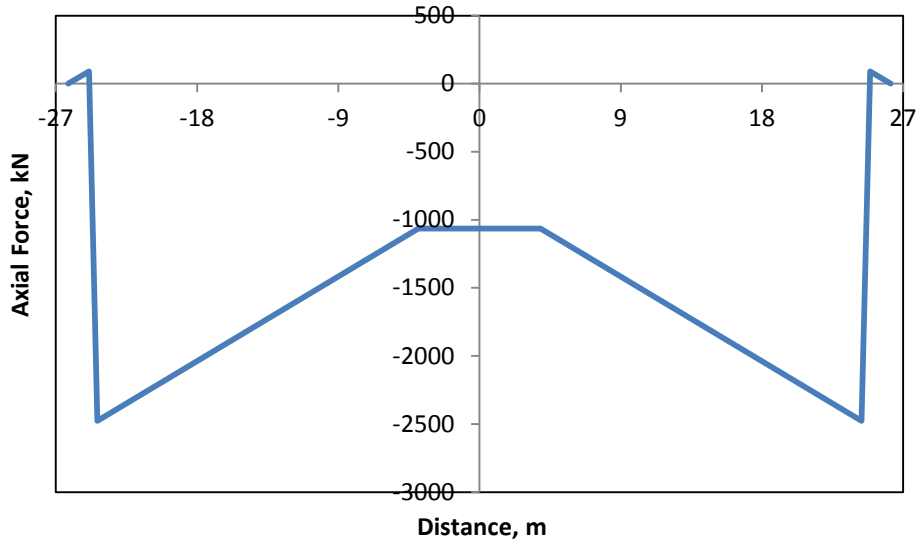Figure 7.10 shows the resulting forces applied to simulate the the 1160 kN force in QP1.
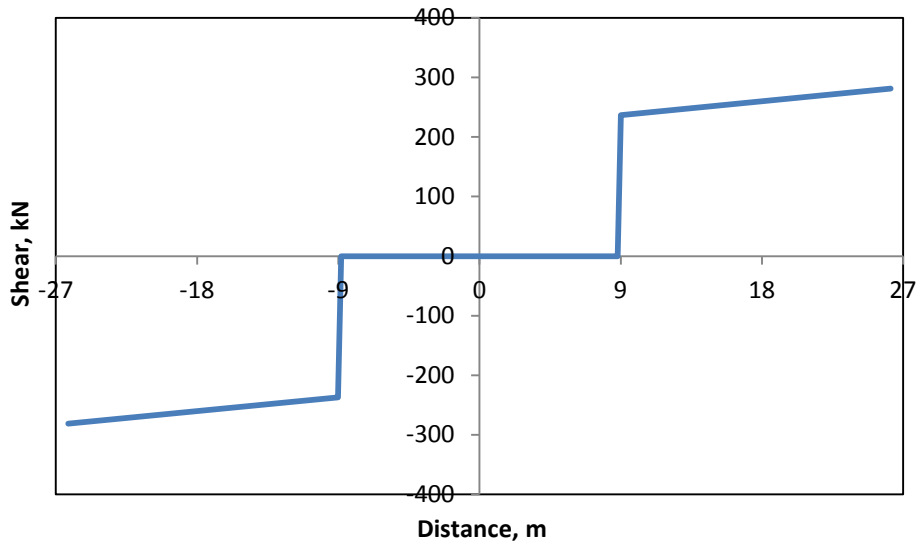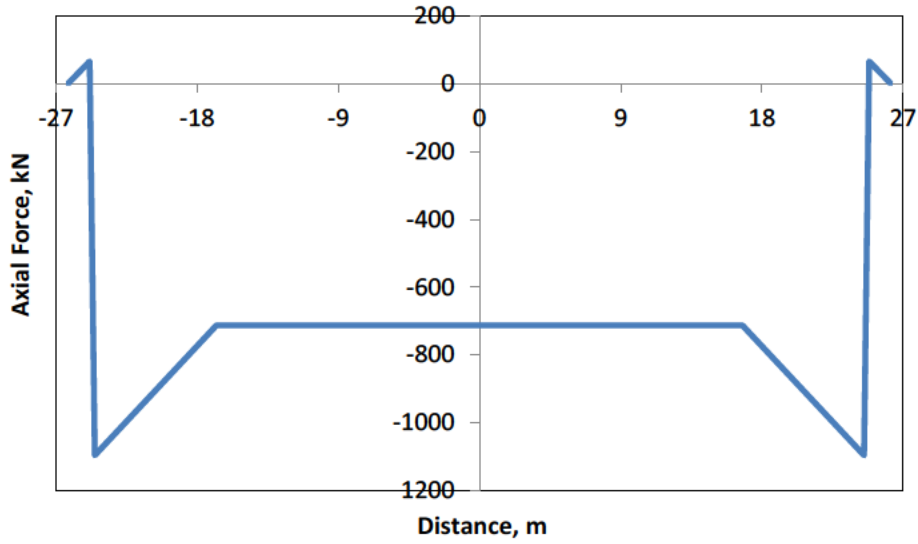
(a) Axial Force
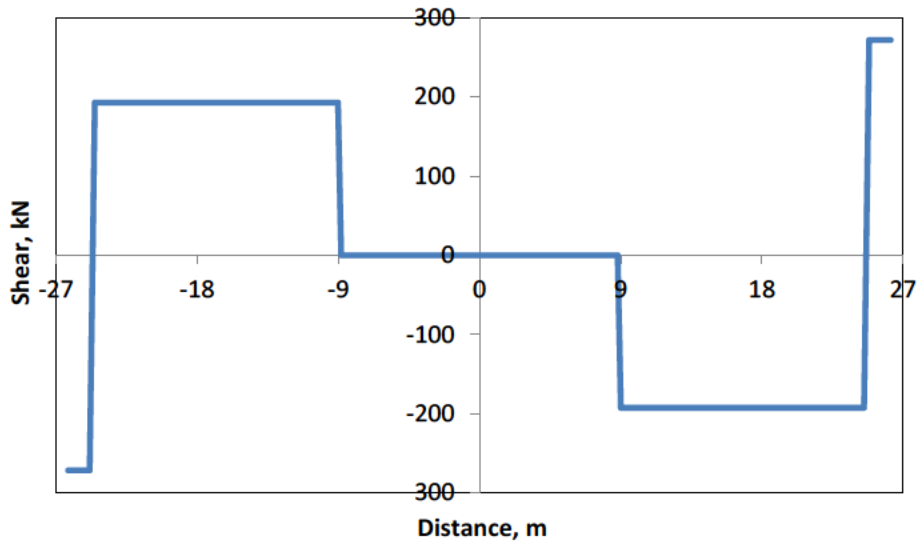
(b) Shear force

Fig. 7.10: Axial force and shear force diagrams corresponding to the forces applied to the 2D model of girder P1 to simulate 1160 kN in QP1 (span 6W-7W).

Figure 7.11 shows the forces applied to P1 to simulate the loading case for the very unsymmetrical PTE forces on P1 and P7.

39
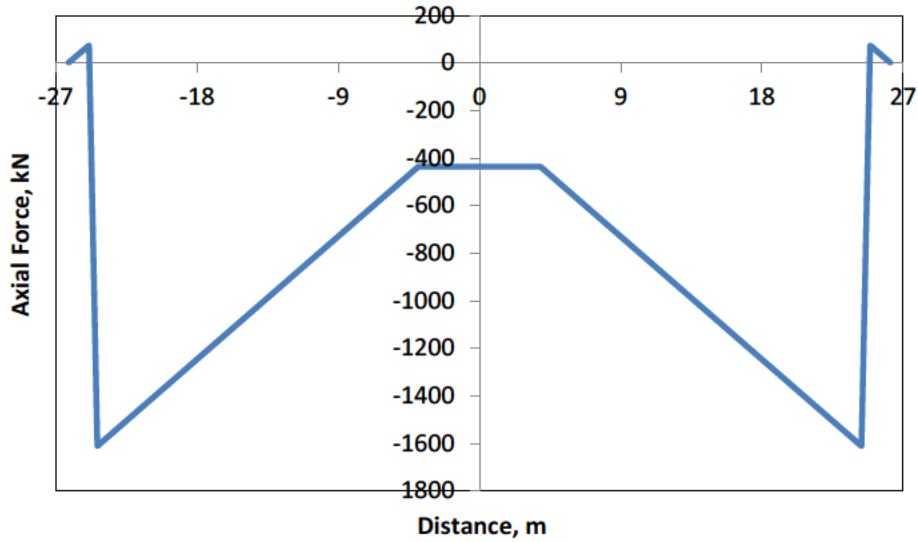
(a) Axial force

(b) Shear force

Fig. 7.11: Axial force and shear force diagrams corresponding to the forces applied to the 2D model of girder P1 to simulate unsymmetrical PTE forces of 1685 kN PTE on P1 and 3092 kN on P7 (span 6W-7W).

7.7.2 Results for Critical Loading at Midspan under Service Loading for Combined Case of QP1 and PTE (Girder P1)

For this analysis a general level of corrosion for the girder of 30% for all reinforcement in the span except that in the midspan region it was assumed that 8 tendons were lost due to corrosion (33% corrosion).

The results from the analysis indicate that under short-term and long-term conditions flexural cracking would occur at midspan when the girder is subjected to dead load plus 1.9 and 1.6 times the service live load, respectively.

7.7.3 Results for Critical Loading at Midspan under Factored Loading in P1

Figure 7.12 shows the crack patterns at the maximum factored loading that girder P1 can carry. The girder reached a factored load corresponding to factored dead loading plus 2.93 times the service live load. This represents the state of girder P1 of span 6W-7W with 8 strands corroded at midspan, giving a flexural D/C raio of 0.76.

6W PTE+QP1 Fac Fl 8 cr   PAN MODE   Displace/Cracks: Crack Dir'ns   Displacement Factor = 2.93

6W PTE+QP1 Fac Fl 8 cr   PAN MODE   Displace/Cracks: Crack Dir'ns   Displacement Factor = 2.93
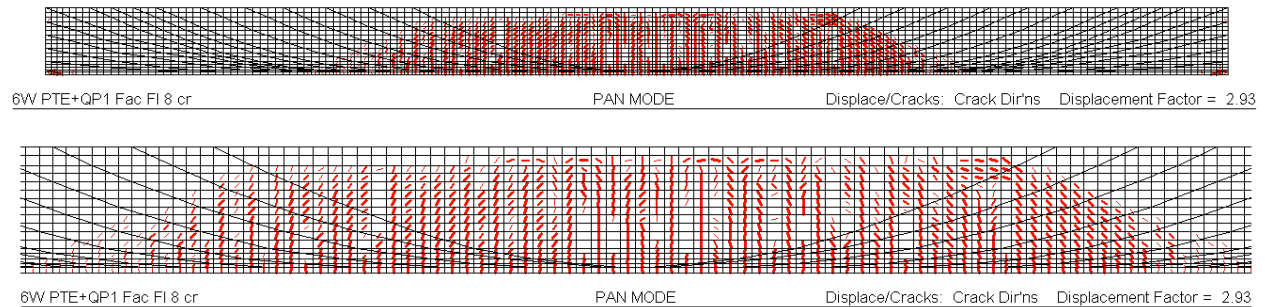
Fig. 7.12: Crack patterns at maximum factored resistance corresponding to factored dead load plus 2.93 times service live load. Corrosion of 8 strands at midspan considered (Girder P1 of span 6W-7W).

7.8 Span 32W-33W

The critical girder in span 32W-33W is girder P7 with an estimated tendon loss at midspan of 8 tendons. The force in the QP1 tendons are 1660 kN on both P1 and P7. The PTE forces are unsymmetrical with tendon forces equal to 1875 kN on P1 and 3515 kN on P7.

7.8.1 Modelling of Girder P7

Non-linear analysis was carried out on Girder P7 (P1 has a lower estimated loss of tendons) in span 32W-33W. In order to account for losses in the PTE, the average of the applied forces on P1 and P7 was reduced by 10% resulting in a force of 1688 kN PTE on P1 and 3164 kN on P7. Symmetrical QP1 forces of 1660 kN were assumed on each of P1 and P7.

Figure 7.13 shows the resulting forces applied to simulate the the 1660 kN force in QP1.
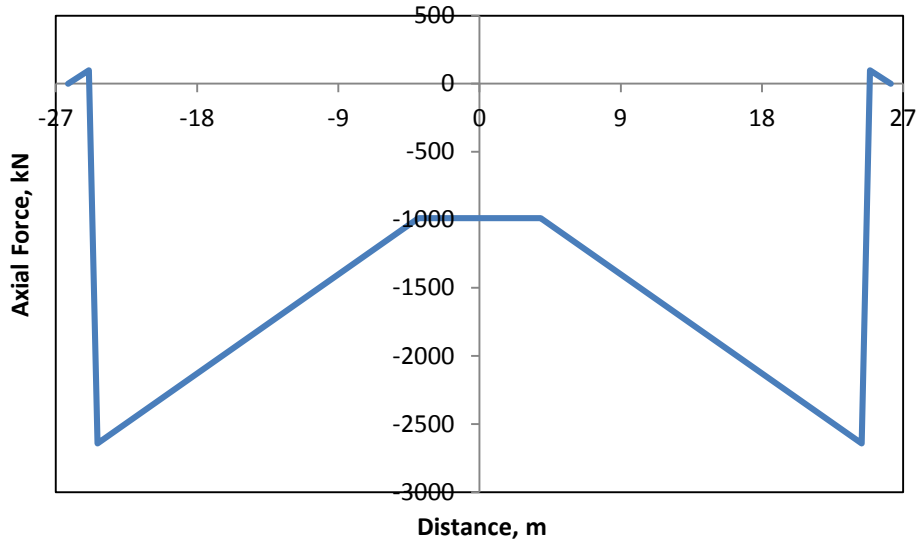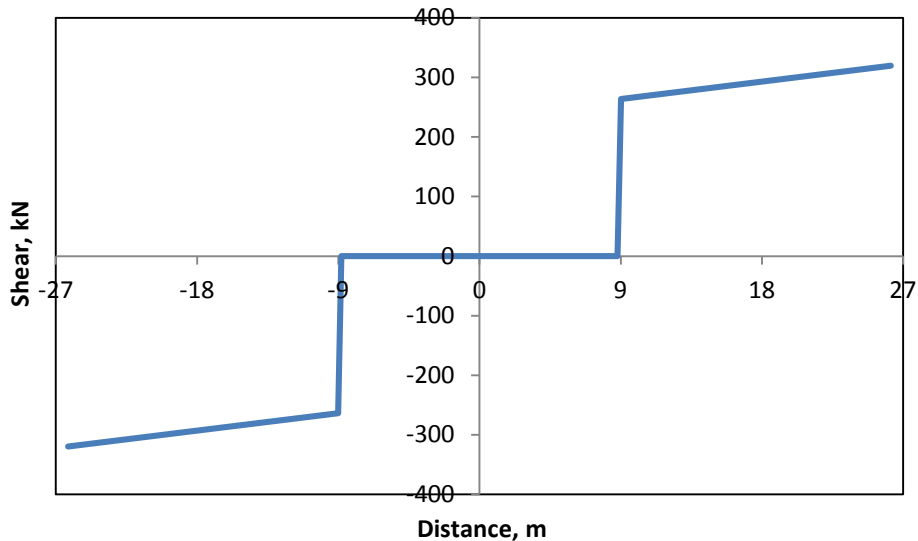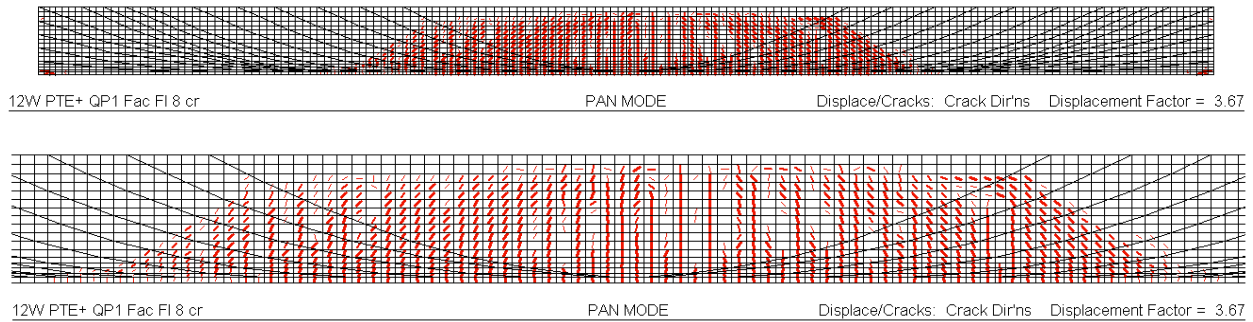
41
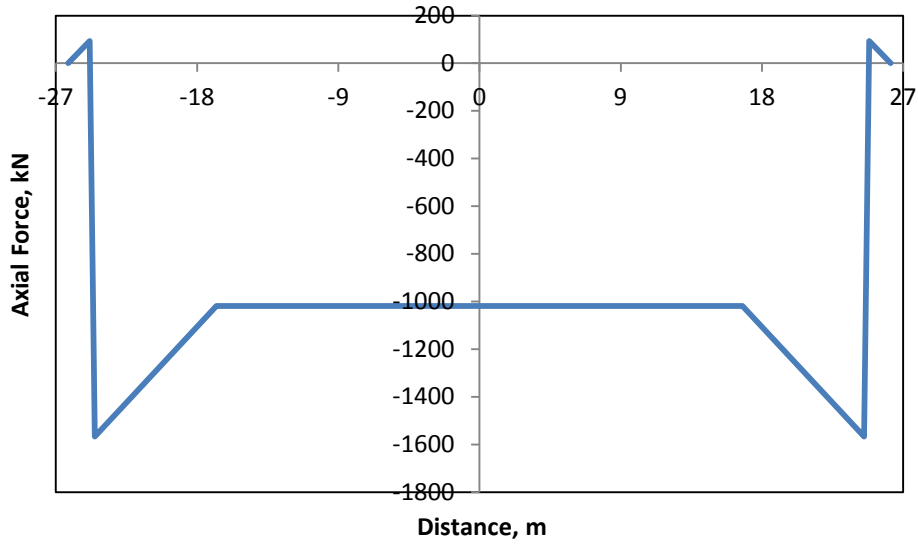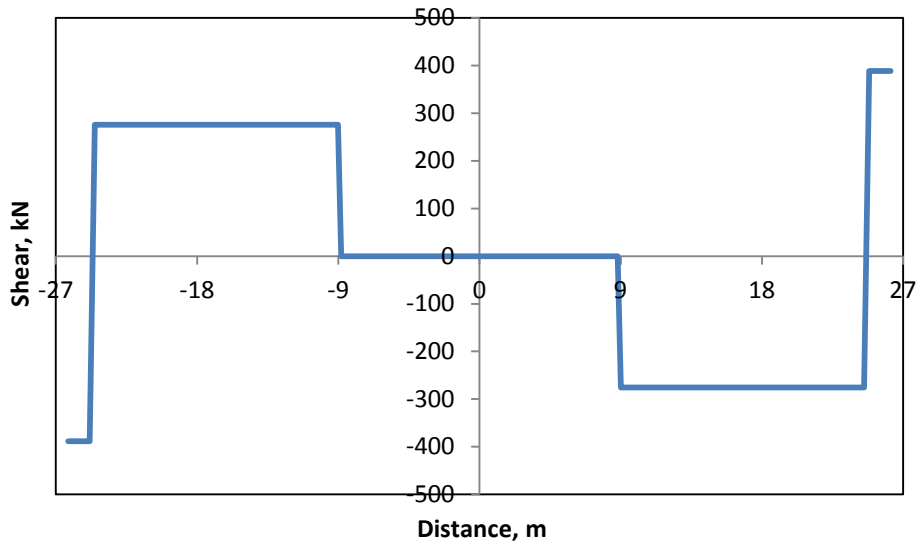
(a) Axial force

(b) Shear force

Fig. 7.13: Axial force and shear force diagrams corresponding to the forces applied to the 2D model of girder P7 to simulate 1660 kN in QP1 (span 32W-33W).

Figure 7.14 shows the resulting axial force and shear forces acting on girder P7 in span 32W-33W due to the unsymmetrically applied PTE forces in P1 and P7.

(a) Axial force

(b) Shear force

Fig. 7.14: Axial force and shear force diagrams corresponding to the forces applied to the 2D model of girder P7 to simulate unsymmetrical PTE forces of 1688 kN PTE on P1 and 3164 kN on P7 (span 32W-33W).

7.8.2 Results for Critical Loading at Midspan under Service Loading for Combined Case of QP1 and PTE (Girder P7)

For this analysis a general level of corrosion for the girder of 30% for all reinforcement in the span except that in the midspan region it was assumed that 8 tendons were lost due to corrosion (33% corrosion).

The results from the analysis indicate that under short-term and long-term conditions flexural cracking would occur at midspan when the girder is subjected to dead load plus 2.4 and 2.1 times the service live load, respectively.

7.8.3 Results for Critical Loading at Midspan under Factored Loading in P1

Figure 7.15 shows the crack patterns at the maximum factored loading that girder P7 can carry. The girder reached a factored load corresponding to factored dead loading plus 3.59 times the live load. This represents the state of girder P7 of span 32W-33W with 8 strands corroded at midspan, giving a flexural D/C raio of 0.65.

32W PTE+QP1 Fac Fl 8 cr   PAN MODE   Displace/Cracks: Crack Dir'ns   Displacement Factor = 3.59

32W PTE+QP1 Fac Fl 8 cr   PAN MODE   Displace/Cracks: Crack Dir'ns   Displacement Factor = 3.59

Fig. 7.15: Crack patterns at maximum factored resistance corresponding to factored dead load plus 3.59 times service live load. Corrosion of 8 strands at midspan considered (Girder P7 of span 32W-33W).

7.9 Span 26W-27W

The critical girder in span 26W-27W is girder P7 with an estimated tendon loss at midspan of 9 tendons. The force in the QP1 tendons is 1500 kN on both P1 and P7. The PTE forces are unsymmetrical with tendon forces equal to 1923 kN on P1 and 1695 kN on P7.

7.9.1 Modelling of Girder P7

Non-linear analysis was carried out on Girder P7 (P1 has a lower estimated loss of tendons) in span 26W-27W. In order to account for losses in the PTE, the average of the applied forces on P1 and P7 was reduced by 10% resulting in a force of 1731 kN PTE on P1 and 1526 kN on P7. Symmetrical QP1 forces of 1500 kN were assumed on each of P1 and P7.

Figures 7.16 shows the resulting forces applied to simulate the the 1500 kN force in QP1.
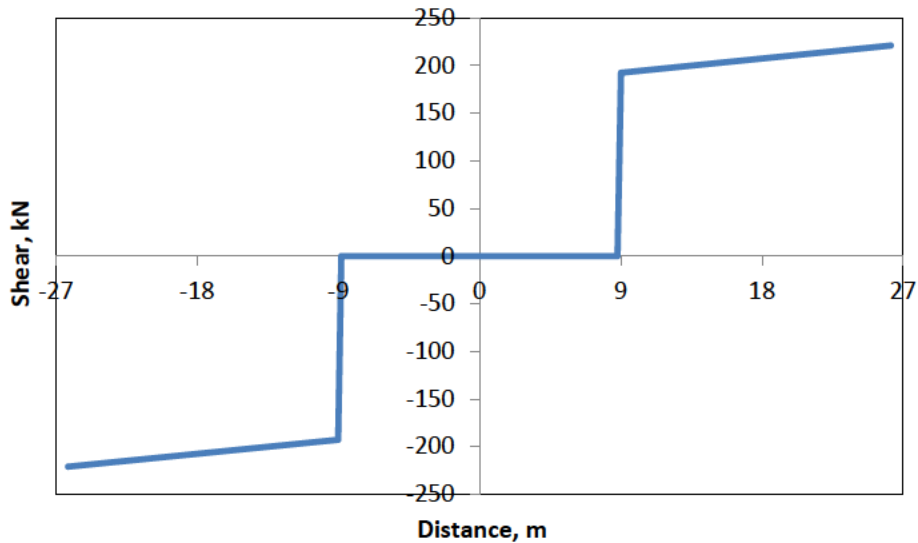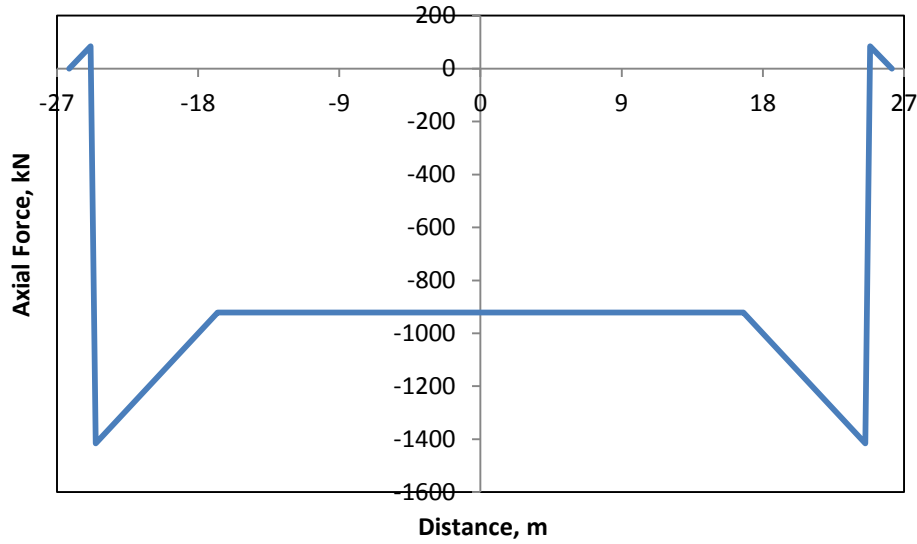

(a) Axial force
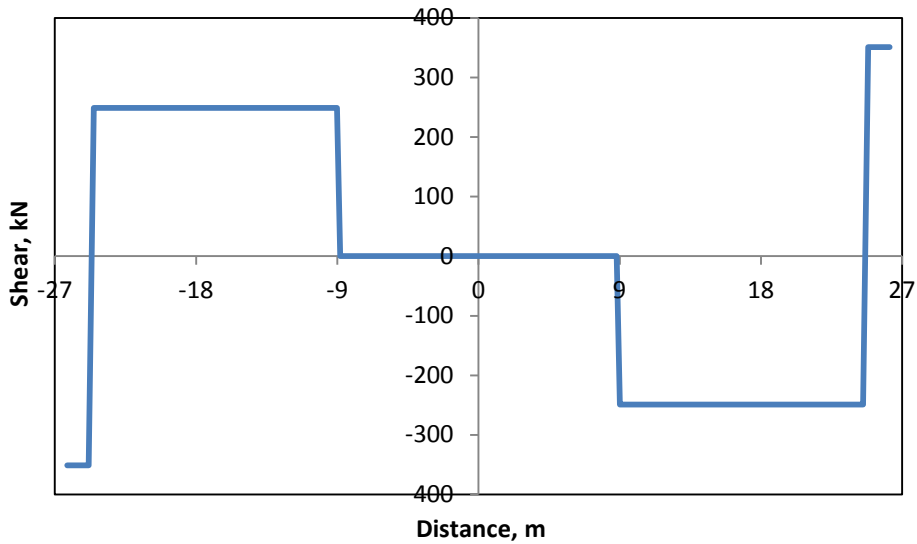
(b) Shear force

Fig. 7.16: Axial force and shear force diagrams corresponding to the forces applied to the 2D model of girder P7 to simulate 1500 kN in QP1 (span 26W-27W).

Figure 7.17 shows the resulting axial force and shear forces acting on girder P7 in span 26W-27W due to the unsymmetrically applied PTE forces in P1 and P7.
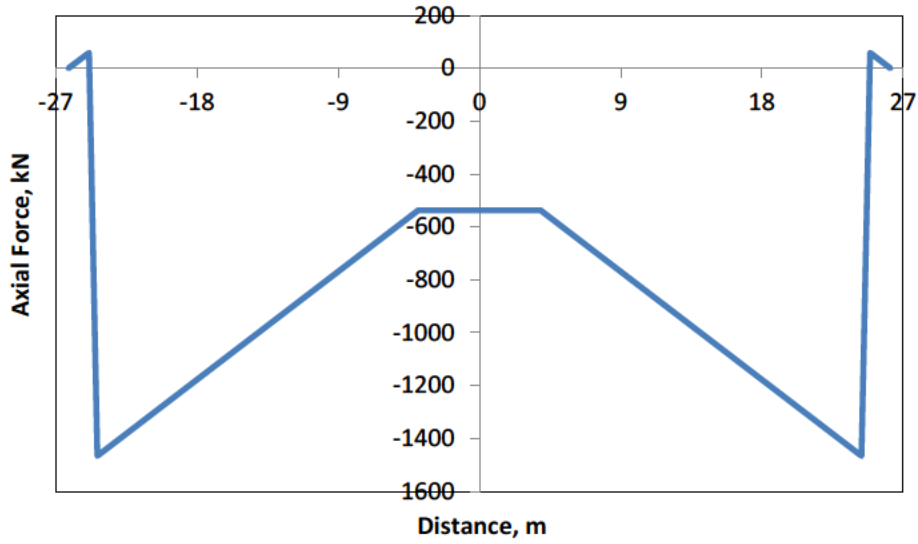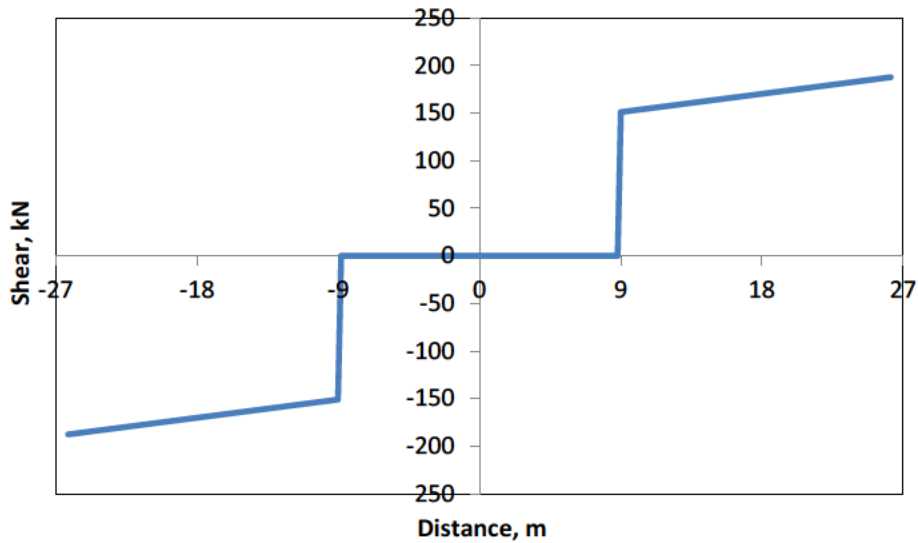
(a) Axial force

(b) Shear force

Fig. 7.17: Axial force and shear force diagrams corresponding to the forces applied to the 2D model of girder P7 to simulate unsymmetrical PTE forces of 1731 kN PTE on P1 and 1526 kN on P7 (span 26W-27W).

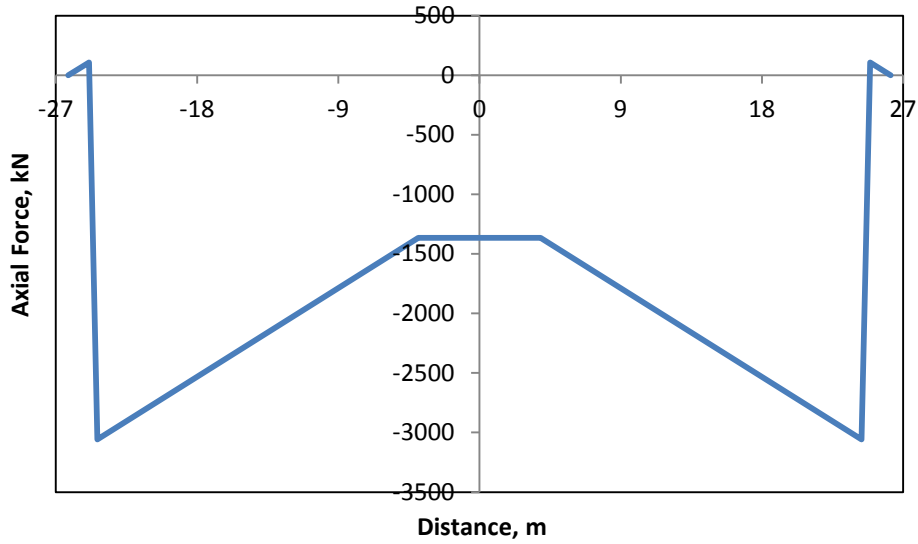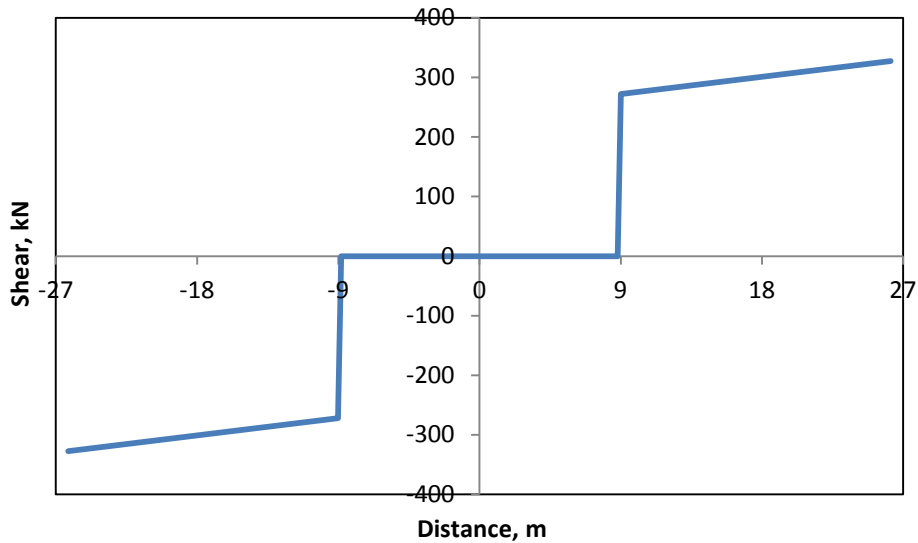## 7.9.2 Results for Critical Loading at Midspan under Service Loading for Combined Case of QP1 and PTE (Girder P7)

For this analysis a general level of corrosion for the girder of 32% for all reinforcement in the span except that in the midspan region it was assumed that 9 tendons were lost due to corrosion (37.5% corrosion).

The results from the analysis indicate that under short-term and long-term conditions flexural cracking would occur at midspan when the girder is subjected to dead load plus 2.1 and 1.8 times the service live load, respectively.

7.9.3 Results for Critical Loading at Midspan under Factored Loading in P1

Figure 7.18 shows the crack patterns at the maximum factored loading that girder P7 can carry. The girder reached a factored load corresponding to factored dead loading plus 3.42 times the live load. This represents the state of girder P7 of span 32W-33W with 9 strands corroded at midspan, giving a flexural D/C raio of 0.69.

26Wr PTE+QP1 Fac Fl 9 cr   PAN MODE   Displace/Cracks: Crack Dir'ns   Displacement Factor = 3.42

26Wr PTE+QP1 Fac Fl 9 cr   PAN MODE   Displace/Cracks: Crack Dir'ns   Displacement Factor = 3.42
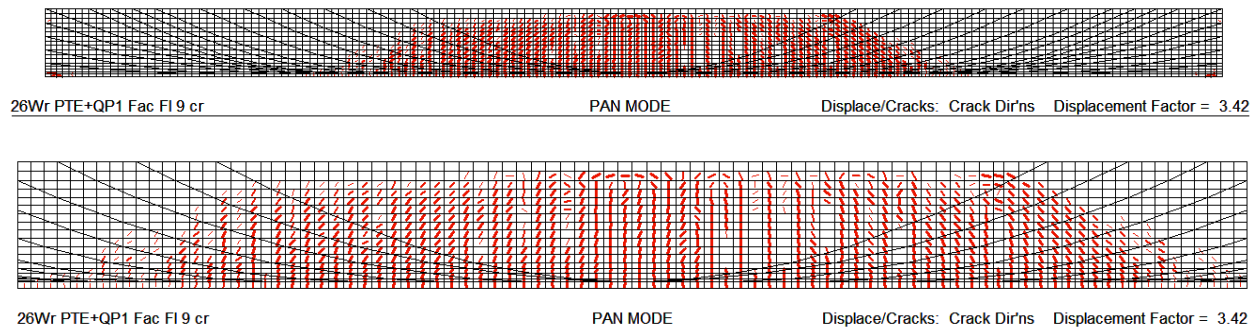
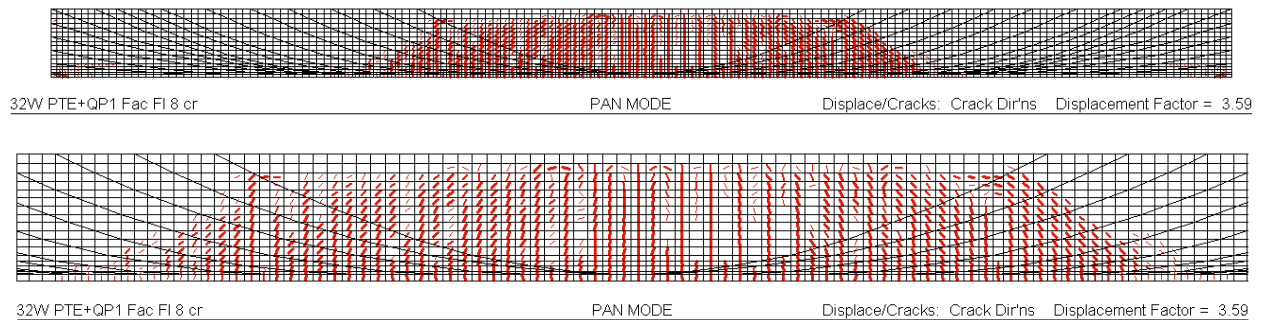Fig. 7.18: Crack patterns at maximum factored resistance corresponding to factored dead load plus 3.42 times service live load. Corrosion of 9 strands at midspan considered (Girder P7 of span 26W-27W).

7.10 Non-Linear Analysis results for Other Spans in Section 5 with QP1

Similar analyses were carried for other spans in Section 5 that were strengthened with QP1. The results are summarized in Section 9.

8 Evaluation of Combined Effects of PTE and QP2 on Section 5 Girders

8.1 QP2 Strengthening Measures

Figure 8.1 shows the general aspects of the strengthening using QP2 (AECOM 2011). The post-tensioning consisted of 16 pairs of 15.2 mm diameter strands (area of 140 mm^2) having an ultimate strength of 1860 MPa (ASTM A416) on each edge girder, P1 and P7.
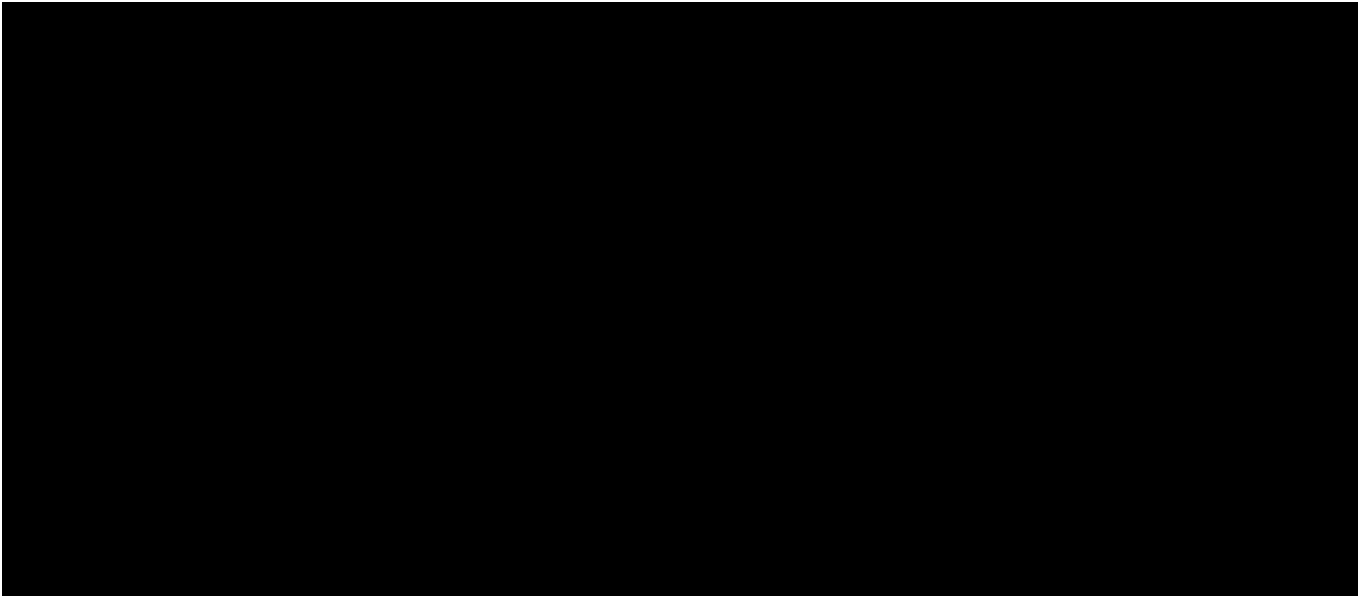
Fig. 8.1: Strengthening details for QP2 (AECOM drawing 1255570-49, 2011).

The 2011 AECOM drawings give jacking force levels in each strand as a function of the degree of corrosion assumed, the level of PTE and the concrete strength of the interior diaphragms (see Fig. 8.2). The values of the jacking forces at the ends of the tendons were taken from the November 10, 2015 MasterData Table. For example, span 39W-40W has 32 strands at 120 kN per strand giving a total initial prestressing force of 32 x 120 = 3840 kN.

ÉTAT DE LA POUTRE DE RIVE EDGE BEAM CONDITION		# DE NOUVEAU MONOTORON NEW SINGLE STRAND	RÉSISTANCE EN COMPRESSION f'c DU BÉTON DES DIAPHRAGMES DIAPHRAGM CONCRETE COMPRESSIVE STRENGTH f'c (MPa)				
TENSION DE PRÉCONTRAINTE EXTÉRIEURE LONGITUDINALE EXISTANTE EXISTING EXTERIOR LONGITUDINAL PRESTRESSING LOAD	QUANTITÉ DE CÂBLES INTERNES PERDUS* QUANTITY OF INTERNAL CABLES LOST*		30	35	40	45	> 50
1874 kN	0	1 ● 4 / 5 ● 8 / 9 ● 12 / 13 ● 16	80 kN	95 kN	105 kN	120 kN	130 kN
1874 kN	2	1 ● 4 / 5 ● 8 / 9 ● 12 / 13 ● 16	80 kN	95 kN	105 kN	120 kN	130 kN
1874 kN	4	1 ● 4 / 5 ● 8 / 9 ● 12 / 13 ● 16	80 kN	95 kN	105 kN	120 kN	130 kN
2344 kN	4	1 ● 4 / 5 ● 8 / 9 ● 12 / 13 ● 16	80 kN	95 kN	105 kN	120 kN	130 kN
2344 kN	6	1 ● 4 / 5 ● 8 / 9 ● 12 / 13 ● 16	80 kN	95 kN / 105 kN	105 kN	120 kN	130 kN

TENSION FINALE (T) PAR MONOTORON
(APRÉS PERTES INSTANTANÉES)

ÉTAT DE LA POUTRE DE RIVE EDGE BEAM CONDITION		# DE NOUVEAU MONOTORON NEW SINGLE STRAND	RÉSISTANCE EN COMPRESSION f'c DU BÉTON DES DIAPHRAGMES DIAPHRAGM CONCRETE COMPRESSIVE STRENGTH f'c (MPa)				
TENSION DE PRÉCONTRAINTE EXTÉRIEURE LONGITUDINALE EXISTANTE EXISTING EXTERIOR LONGITUDINAL PRESTRESSING LOAD	QUANTITÉ DE CÂBLES INTERNES PERDUS* QUANTITY OF INTERNAL CABLES LOST*		30	35	40	45	> 50
2812 kN	6	1 ● 4 / 5 ● 8	80 kN	95 kN	105 kN	105 kN	105 kN
		9 ● 12 / 13 ● 16	105 kN	105 kN		130 kN	130 kN
2812 kN	8	1 ● 4 / 5 ● 8	80 kN	95 kN	105 kN	105 kN	105 kN
		9 ● 12 / 13 ● 16	105 kN	105 kN		130 kN	130 kN
3281 kN	8	1 ● 4 / 5 ● 8	80 kN	95 kN	105 kN	105 kN	105 kN
		9 ● 12 / 13 ● 16	105 kN	105 kN		130 kN	130 kN
3281 kN	10	1 ● 4 / 5 ● 8	80 kN	95 kN	105 kN	105 kN	105 kN
		9 ● 12 / 13 ● 16	105 kN	105 kN		130 kN	130 kN

* CETTE QUANTITÉ NE POURRA ÊTRE CONFIRMÉE QU'AU MOMENT DE LA RÉFECTION DE LA POUTRE (PHASE DE DÉMOLITION). IL SERA ALORS DÉTERMINÉ PAR L'INGÉNIEUR SI UN RENFORCEMENT EN CISAILLEMENT DE LA POUTRE EST REQUIS (VOIR DESSIN 125570-30).

* THIS QUANTITY SHALL ONLY BE CONFIRMED AT THE MOMENT OF THE BEAM REPAIRS (DEMOLITION PHASE). AT THAT MOMENT THE ENGINEER SHALL DETERMINE IF A BEAM SHEAR REINFORCEMENT IS REQUIRED (SEE DRAWING 125570-30)

Fig. 8.2: Jacking forces used in 2012-2013 for spans strengthened with QP2 (AECOM drawing 1255570-53, 2011).

A typical span was modelled using the 3D model and the resulting forces applied to the exterior girders were used to apply forces in the 2D model. Due to the large forces anchored in the web of the girder near its end, the designers thickened the web as shown by the shaded areas in Fig. 8.1. This anchorage block region was simulated in the 2D non-linear model by thickening the web in this region.

8.2 Key Parameters for PTE and QP2 Strengthening

To study the combined effects of the external post-tensioning and QP2 the critical girder in span 39W-40W and the critical girder in span 42W-43W were investigated. Table 8.1 summarizes some of the main factors in judging which girders are the most critical.

Table 8.1: Key parameters for Section 5 spans with PTE and QP2 from November 10, 2015 MasterData Table

Span	Girder	# tendons Lost/original # (Nov 10, 2015 MDT)	PTE kN	QP2 kN	CEC (2014 inspection)
42W-43W	P1	5/24	1600	4160	1
	P7	6/24	1580	4160	3
39W-40W	P1	10/24	1874	3840	1
	P7	3/24	1875	3840	1

The issues concerning those girders that were considered to be most critical are discussed below.

8.3 Span 39W-40W

Girder P1 of this span has the largest estimated number of tendons lost (10) due to corrosion, considering the girders in the two spans with QP2 strengthening. Span 39W-40W has a slightly smaller QP2 force than span 42W-43W and has symmetrically applied PTE forces on P1 and P7.

8.3.1 Modelling of Girder P1

Non-linear analysis was carried out on Girder P1 of span 39W-40W. In order to account for losses in the PTE, the forces were reduced by 10% resulting in a applied PTE force of 1687 kN on P1 and on P7. Symmetrical QP2 forces of 3456 kN (reduced by 10% to account for sequential post-tensioning and losses) were applied to the model on each of P1 and P7.

Figure 8.3 shows the non-linear finite element model and the forces applied to simulate the unit loading of 1000 kN QP2 force at the ends of each exterior girder.
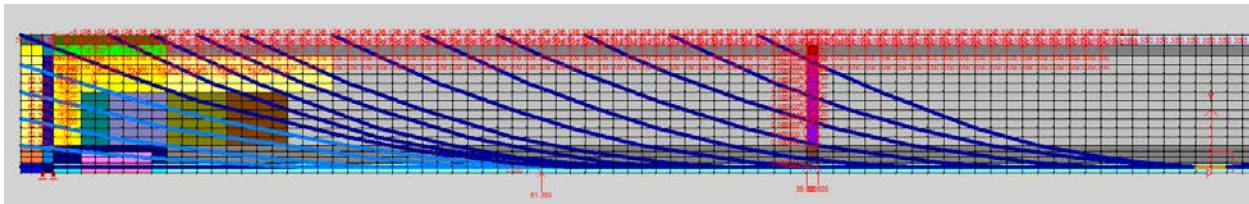
Fig. 8.3: Unit loading (1000 kN) case used to simulate the effects of QP2 on girders P1 and P7.

Figure 8.4 shows the resulting axial and shear force diagrams for the applied QP2 force of 3456 kN applied at the ends of each exterior girder.
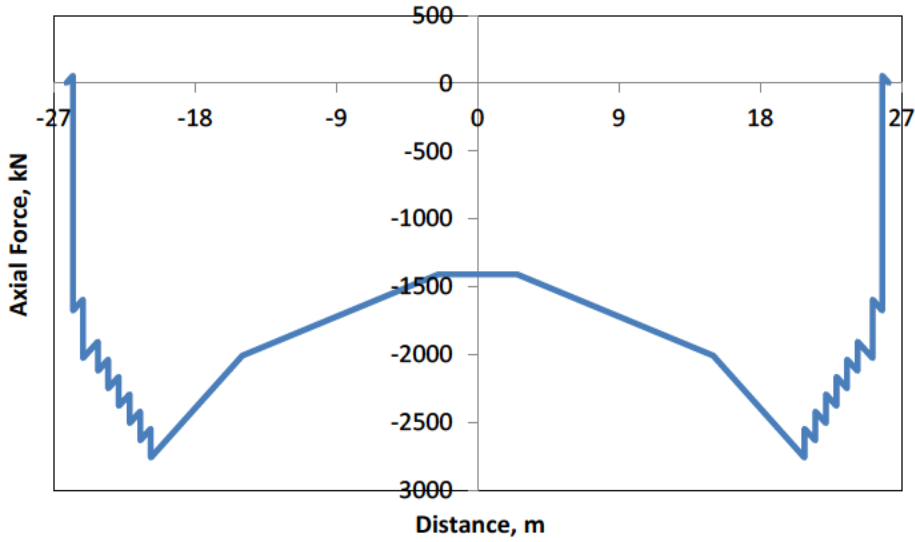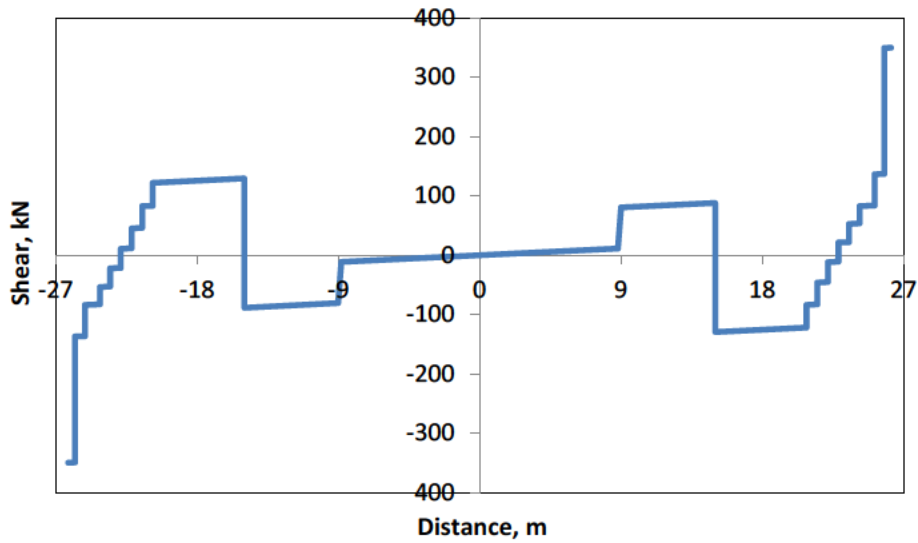
(a) Axial force

(b) Shear force

Fig. 8.4: Axial forces and shears in Girder P1 of span 39W-40W due to symmetrically applied QP2 forces of 3456 kN on P1 and P7

Figure 8.5 shows the resulting axial and shear force diagrams for the applied PTE force of 1687 kN applied at the ends of each exterior girder.
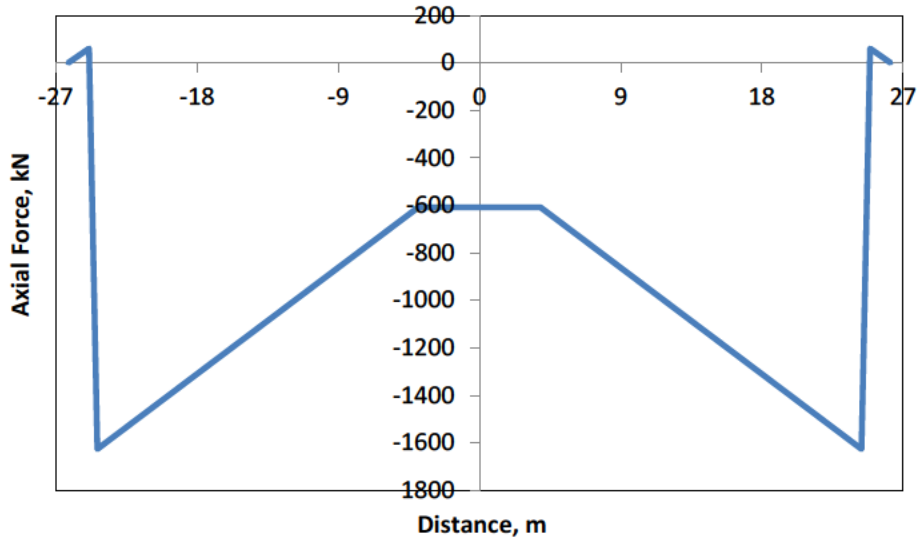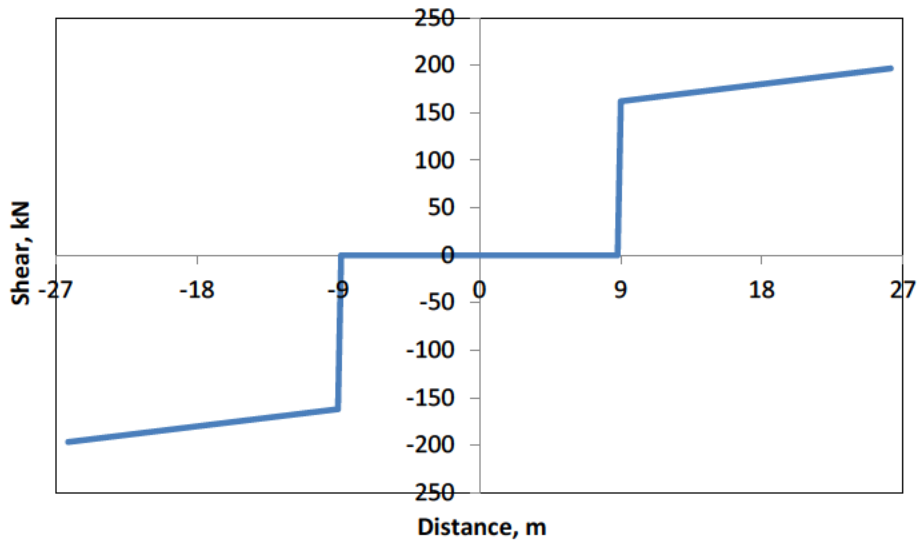
(a) Axial force

(b) Shear force

Fig. 8.5: Axial forces and shears due to symmetrically applied PTE forces of 1687 kN on P1 and P7 in span 39W-40W.

8.3.2 Results for Critical Loading at Midspan under Service Loading for Combined Case of QP2 and PTE - Girder P1

For the analysis it was assumed that 10 out of the 24 tendons were lost due to corrosion at midspan, as reported in the November 10 , 2015 MasterData Table. This resulted in a loss of

tendons of 41.7% in the midspan region. It was assumed that outside of this midspan region the post-tensioned tendons and the stirrups had a uniform loss due to corrosion of 35% of their areas.

Predicted first flexural cracking in the midspan region occurred at service dead load plus 1.8 and 1.6 times the service live load for short-term and long-term loading, respectively.

8.3.3 Results for Critical Loading at Midspan under Factored Loading in P1 of Span 39W-40W

Figure 8.6 shows the cracking predicted in girder P1 of span 39W-40W due to factored loading. The live load was increased until failure was predicted.

Failure was predicted when the live load factor reached 3.02, compared with a factor of 1.63 required by the CHBDC (CSA S6-14). This resulted in a D/C ratio of 0.75.
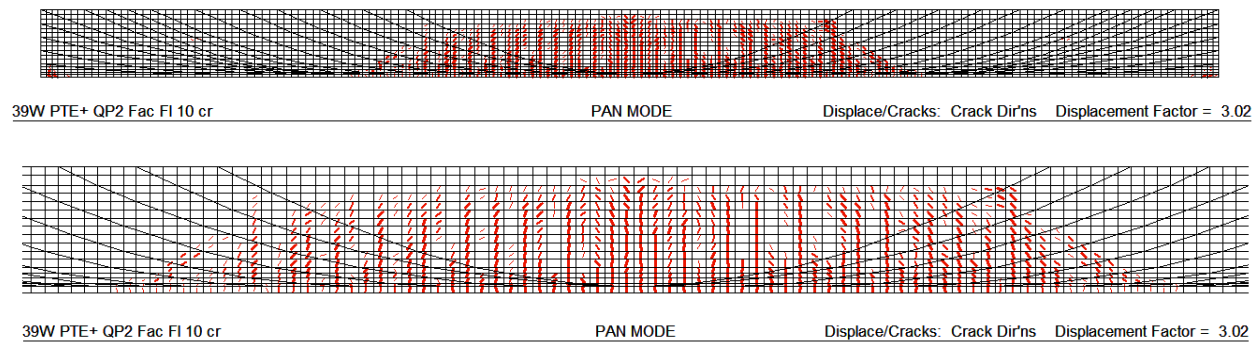
Fig. 8.6: Predicted failure at a live load factor of 3.02 of girder P1 in span 39W-40W assuming 10 tendons lost at midspan.

8.4 Span 42W-43W

Girder P7 of this span has an estimated 6 tendons lost due to corrosion. This span is not as critical as span 39W-40W due to the fewer number of tendons lost and the slightly higher QP2 force of 4160 kN. Span 42W-43W has fairly symmetrical PTE forces, with 1580 kN applied to P7 and 1600 kN applied to P1.

8.4.1 Modelling of Girder P7

Non-linear analysis was carried out on Girder P7 of span 42W-43W. To account for losses in the PTE, the forces were reduced by 10% resulting in a applied PTE force of 1440 kN on P1 and 1422 kN on P7. Symmetrical QP2 forces of 3744 kN (reduced by 10% to account for losses) were applied to the model on each of P1 and P7.

Figure 8.7 shows the resulting axial and shear force diagrams for the applied QP2 force of 3744 kN applied at the ends of each exterior girder.
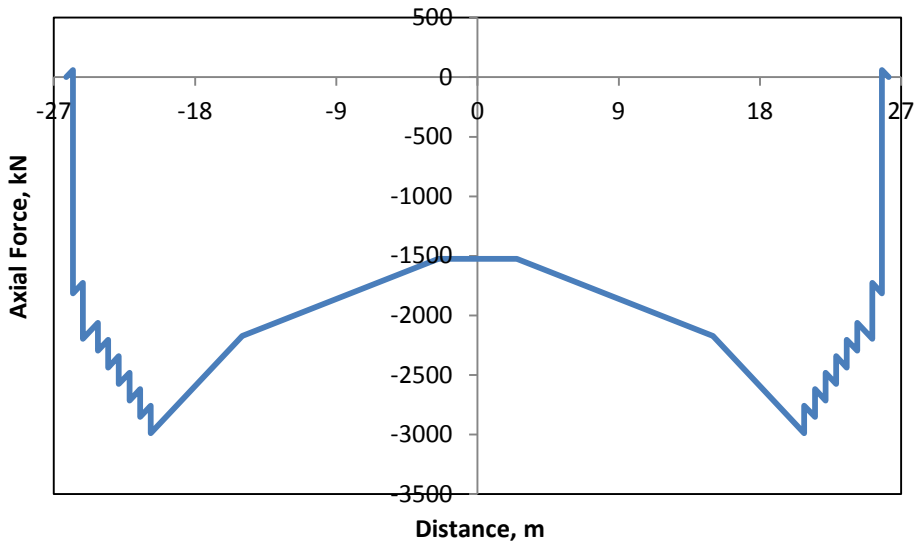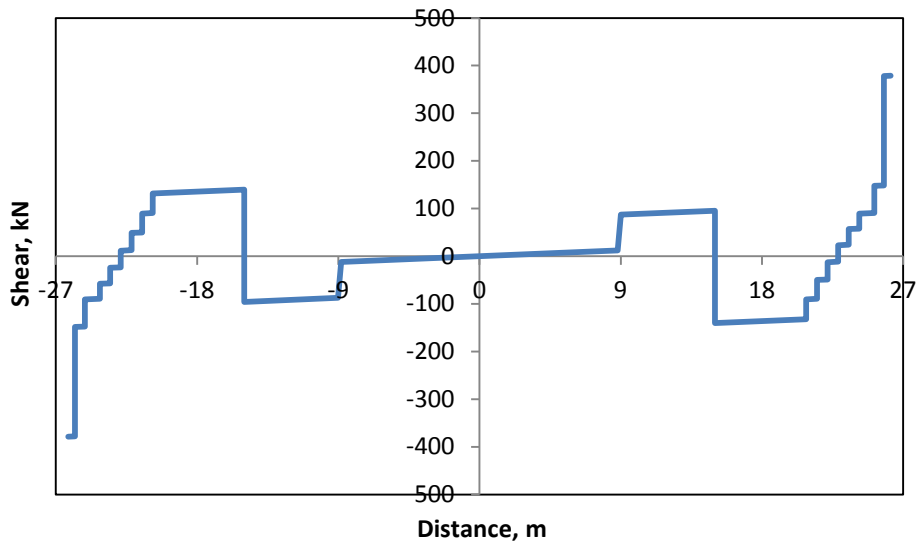
(a) Axial force

(b) Shear force

Fig. 8.7: Axial forces and shears in Girder P7 of span 42W-43W due to symmetrically applied QP2 forces of 3744 kN on P1 and P7

Figure 8.8 shows the resulting axial and shear force diagrams on girder P7 due to the applied PTE forces on P1 and P7.
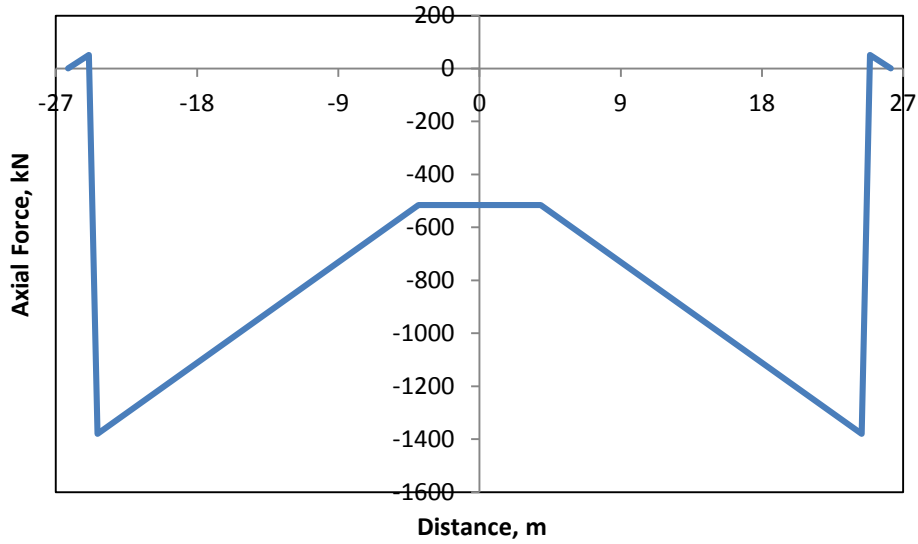
(a) Axial force
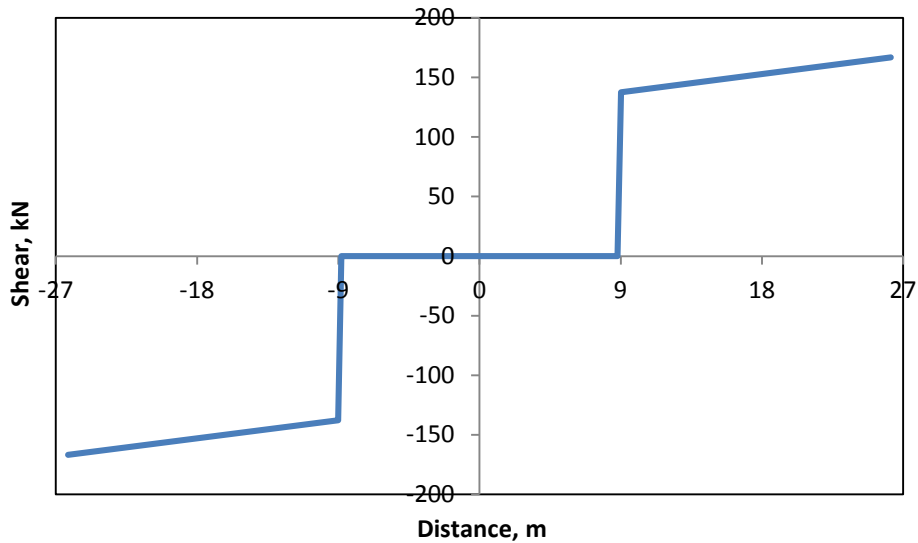
(b) Shear force

Fig. 8.8: Axial forces and shears due to applied PTE forces of 1440 kN on P1 and 1422 kN on P7 in span 42W-43W.

8.4.2 Results for Critical Loading at Midspan under Service Loading for Combined Case of QP2 and PTE - Girder P7

For the analysis it was assumed that 6 out of the 24 tendons were lost due to corrosion at midspan, as reported in the November 10 , 2015 MasterData Table. This resulted in a loss of

tendons of 25% in the midspan region. It was assumed that outside of this midspan region the post-tensioned tendons and the stirrups had a uniform loss due to corrosion of 22% of their areas.

Predicted first flexural cracking in the midspan region occurred at service dead load plus 2.7 and 2.3 times the service live load for short-term and long-term loading, respectively.

8.4.3 Results for Critical Loading at Midspan under Factored Loading in P7 of Span 42W-43W

Figure 8.9 shows the cracking predicted in girder P7 of span 42W-43W due to factored loading. The live load was increased until failure was predicted.

Failure was predicted when the live load factor reached 3.83, compared with a factor of 1.63 required by the CHBDC (CSA S6-14). This resulted in a D/C ratio of 0.64.

42W PTE+ QP2 Fac Fl 6 cr   PAN MODE   Displace/Cracks: Crack Dir'ns   Displacement Factor = 3.83

42W PTE+ QP2 Fac Fl 6 cr   PAN MODE   Displace/Cracks: Crack Dir'ns   Displacement Factor = 3.83
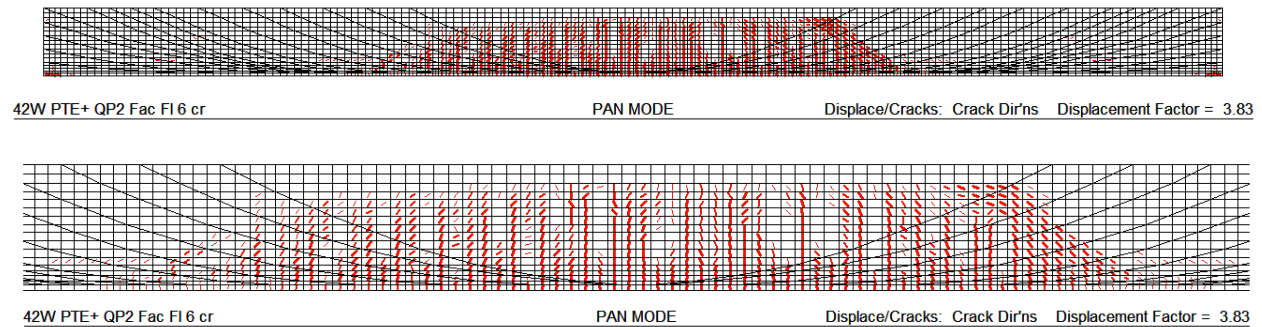
Fig. 8.9: Predicted failure at a live load factor of 3.83 of girder P7 in span 42W-43W assuming 6 tendons lost at midspan.

9   Prioritization of Section 5 Spans strengthened with QP1 or QP2

Figure 9.1 shows the factor, X, applied to the service live load that results in predicted flexural cracking. The 11 spans containing QP1 strengthening measures are shown in dark blue and the 2 spans with QP2 strengthening measures are shown in light blue (on the right in Fig. 9.1). These factors are all above 1.5 for the spans considered.
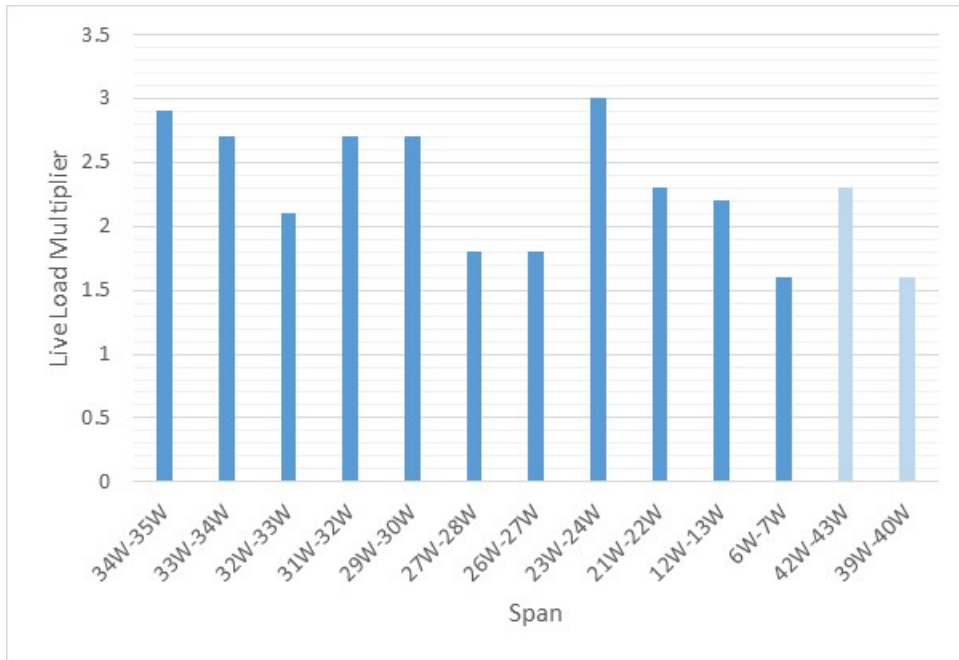
Fig. 9.1: Factor, X, on service live load to cause flexural cracking at midspan.

Figure 9.2 shows the factor, X, applied to the service live load that results in predicted flexural ultimate at midspan. These factors are all above the CSA S6 required live load factor of 1.63.
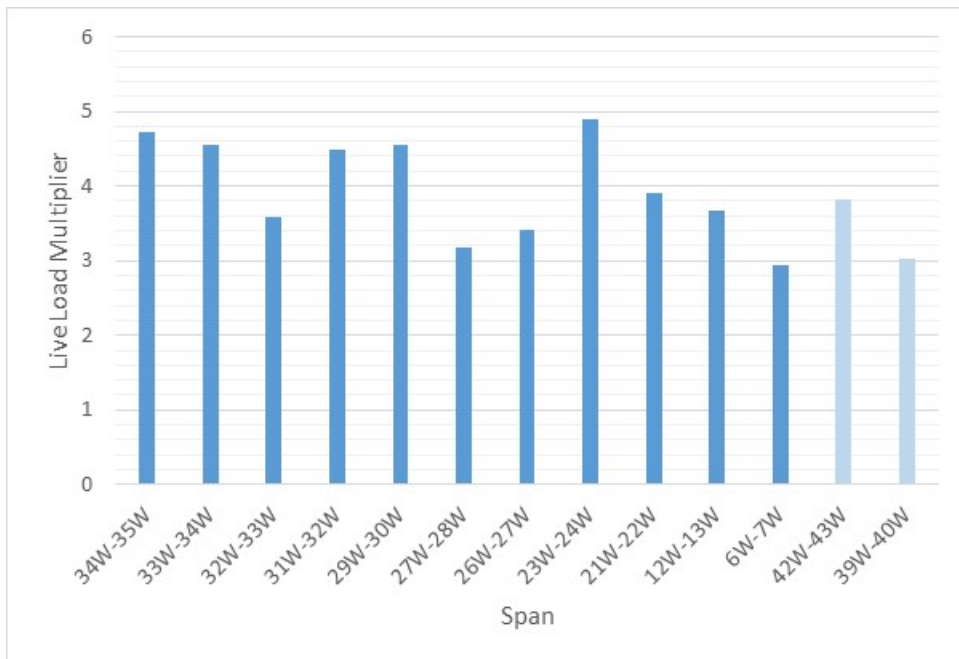
Fig. 9.2: Factor, X, on service live load to cause flexural failure at midspan.

Figure 9.3 shows the variation in the predicted values of demand-to-capacity (D/C) ratios for the spans in Section 5 with either QP1 or QP2. There are 3 spans having predicted D/C ratios equal to or above 0.70.
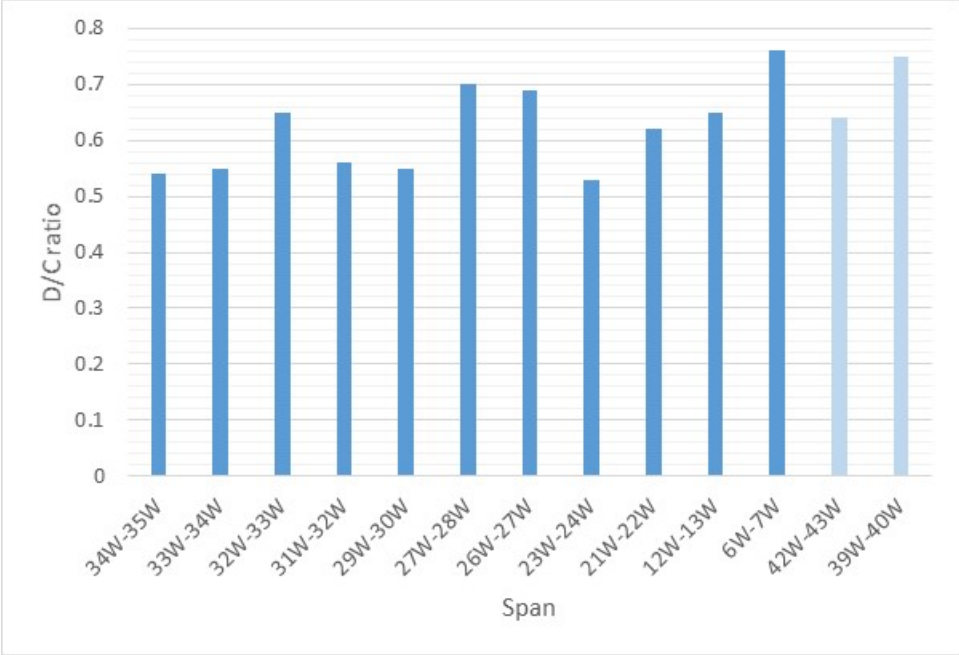
Fig. 9.3: Predicted D/C ratios for flexure at midspan.

Table 9.1 shows the key parameters used to judge the priority for strengthening measures for the Section 5 spans with either QP1 or QP2. Also indicated are those spans with trusses placed in 2015.

Table 9.1: Determining priority for strengthening with trusses

Span	Critical Girder	# tendons Lost/original # (Nov 10, 2015 MDT)	░░░	Priority	Comments
Spans with QP1					
34W-35W	P7	4/24		12	
33W-34W	P1	5/24		10	
32W-33W	P7	8/24		5	
31W-32W	P7	5/24		9	Truss applied in 2015
29W-30W	P1	5/24		11	
27W-28W	P7	11/24		3	Truss applied in 2015
26W-27W	P7	9/24		4	
23W-24W	P7	3/24		13	
21W-22W	P1	7/24		8	
12W-13W	P1	8/24		6	Note: P7 has 7 lost tendons
6W-7W	P1	8/24		1	
Spans with QP2					
42W-43W	P7	6/24		7	
39W-40W	P1	10/24		2	

10 Evaluation of Section 7A Spans

10.1 Introduction

There are six spans in section 7A. Spans 4E-5E, 5E-6E, 6E-7E and 7E-8E all have girders with a total length of 176'-0" and a centre-to-centre span of 172'-0" and contain 24 post-tensioned tendons. Spans 8E-9E and 9E-10 have girders with a total length of 168'-4" and a centre-to-centre span of 164'-4" and contain 22 tendons. The cross-sectional geometry of the girders are

the same as those in Section 5. The prestressing tendons consist of 12 - 7 mm diameter wires (see Section 2.4 for properties assumed).

Table 10.1: Key parameters for the 6 spans in Section 7A

Span	Girder	# tendons Lost/original # (Nov 10, 2015 MDT)	PTE kN	QP1 kN	QP2 kN	PTE2 kN
9E-10E*	P1	6/22	3435			5022
	P7	1/22	2205			5022
						2678 (P3)
						2678 (P5)
8E-9E*	P1	1/22	2205		3784	
	P7	7/22	2850		3784	
7E-8E	P1	3/24	780		3360	
	P7	8/24	1372		3360	
6E-7E	P1	4/24	949	1900		
	P7	8/24	1252	1900		
5E-6E	P1	5/24	2273	960		
	P7	5/24	840	960		
4E-5E	P1	7/24	1388			5022
	P7	5/24	1200			5022

* Shorter spans

10.2 PTE2 Strengthening Measures

Figure 10.1 shows the details of the PTE2 strengthening measures. This additional external post-tensioning is applied to the girder above the level of existing PTE. The steel anchorage block is bolted to the web of the girder
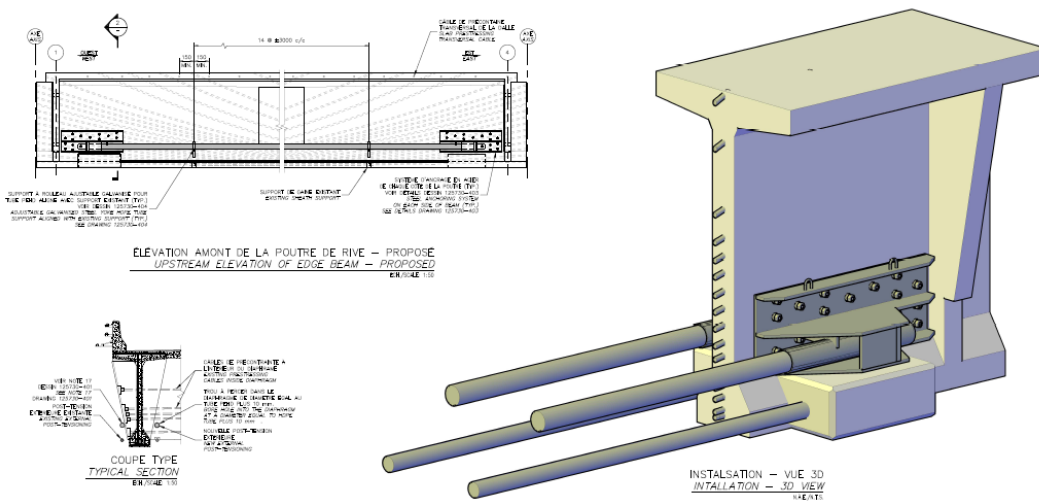
Fig. 10.1: Details of PTE2 strengthening (DESSAU drawing number 125730-402, 2013)

10.3 Section 7A - Shorter Span 8E-9E

Girders P1 and P7 of this span have 1 tendon lost and 7 tendons lost, respectively due to corrosion. This resulted in a loss of tendons of 32% in the midspan region. It was assumed that outside of this midspan region the post-tensioned tendons and the stirrups had a uniform loss due to corrosion of 29% of their areas. The applied PTE was 2205 kN on P1 and 2850 kN on P7. In addition QP2 forces of 3784 kN and 3744 kN were applied to Girders P1 and P7. This span is 164'-4" center-to-center of bearings and contained 22 tendons. For the 2D non-linear analyses the PTE forces were reduced by 10% giving 1985 kN and 2656 kN in P1 and P7, respectively. The QP2 forces were also reduced by 10% in the analyses giving 3406 kN and 3370 kN for P1 and P7, respectively.

10.3.1   Results for Critical Loading at Midspan under Service Loading for Combined Case of QP2 and PTE - Girder P7

Flexural cracking is predicted to occur at a load corresponding to 2.6 and 2.2 times the live loading for short term and long-term predictions, respectively.

10.3.2   Results for Critical Loading at Midspan under Factored Loading for Combined Case of QP2 and PTE - Girder P7

Figure 10.2 shows the cracking at the predicted maximum load carrying capacity of Girder P7. Failure is predicted to occur under factored dead load plus 3.59 times the live load. The girder is predicted to fail by flexural yielding in the midspan region. At this maximum load inclined shear cracks are also predicted to occur. The predicted D/C ratio is 0.66.

8E PTE+QP2 Fac Fl 7 cr   PAN MODE   Displace/Cracks: Crack Dir'ns   Displacement Factor = 3.59

8E PTE+QP2 Fac Fl 7 cr   PAN MODE   Displace/Cracks: Crack Dir'ns   Displacement Factor = 3.59

Fig. 10.2: Predicted failure of girder P7 in span 8E-9E at a live load factor of 3.59 assuming 7 tendons lost at midspan.

10.4 Section 7A - Shorter Span 9E-10E

Girders P1 and P7 of this span has 6 tendons lost and 1 tendon lost, respectively due to corrosion. This resulted in a loss of tendons of 27% in the midspan region for girder P1. It was assumed that outside of this midspan region the post-tensioned tendons and the stirrups had a uniform loss due to corrosion of 24% of their areas. This span is 164'-4" center-to-center of bearings and contained 22 tendons. The applied PTE was 3435 kN on P1 and 2205 kN on P7. PTE2 forces of 5022 kN were applied to Girder P1 and to Girder P7. In addition, PTE2 forces of 2678 kN were applied to Girder P3 and to Girder P5. For the 2D non-linear analyses the PTE forces were reduced by 10% giving 3092 kN and 2087 kN on P1 and P7, respectively. The PTE2 forces were taken as 4520 kN on P1 and P7 and as 2410 kN on P3 and P5.

10.4.1   Results for Critical Loading at Midspan under Service Loading with PTE2 - Girder P1

Flexural cracking is predicted to occur at a load corresponding to 2.9 and 2.5 times the live loading for short term and long-term predictions, respectively. Figure 10.3 shows the modelling of the steel plate anchorage of the PTE2 (bright yellow rectangles) with the PTE2 forces applied along the length of the steel plate. Figure 10.3 also shows the predicted cracking in Girder P1 at service load. The cracks radiating out from the anchor plate are due to the spreading of the compressive stresses into the web of the girder producing "bursting" tensile stresses. The maximum predicted crack with is 1 mm just above the plate.

9E PTE+PTE2 LT Nom Fl 6 cr   PAN MODE   Displace/Cracks: Crack Dir'ns   Displacement Factor = 1.00
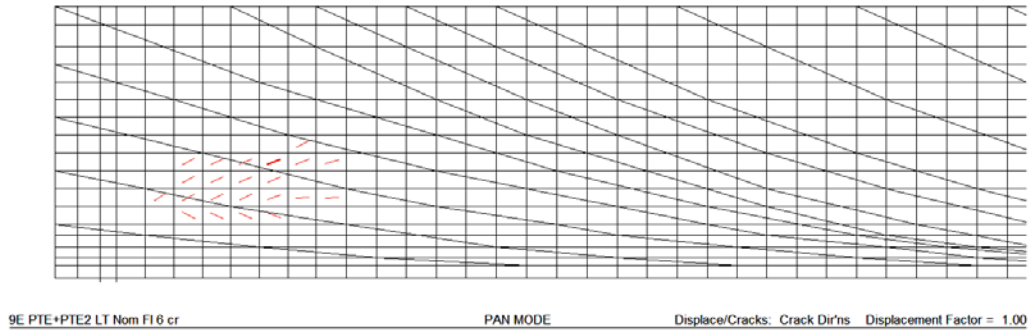
Fig. 10.3 Modelling of anchorage of PTE2 in Girder P1 of Span 9E-10E and predicted cracks in anchorage region of PTE2 at service load.

10.4.2 Results for Critical Loading at Midspan under Factored Loading with PTE2 - Girder P1

Figure 10.4 shows the cracking at the predicted maximum load carrying capacity of Girder P1. Failure is predicted to occur under factored dead load plus 3.75 times the live load. The girder is predicted to fail by flexural yielding in the midspan region. At this maximum load significant inclined shear cracks are also predicted to occur as well as longitudinal splitting cracks. It is noted that the FRP shear strengthening strips were not included in this analysis and hence the shear cracking at flexural ultimate would be better controlled. The predicted D/C ratio is 0.62.

9E PTE+PTE2 Fac Fl 6 cr   PAN MODE   Displace/Cracks: Crack Dir'ns   Displacement Factor = 3.75

9E PTE+PTE2 Fac Fl 6 cr   PAN MODE   Displace/Cracks: Crack Dir'ns   Displacement Factor = 3.75

9E PTE+PTE2 Fac Fl 6 cr   PAN MODE   Displace/Cracks: Crack Dir'ns   Displacement Factor = 3.75
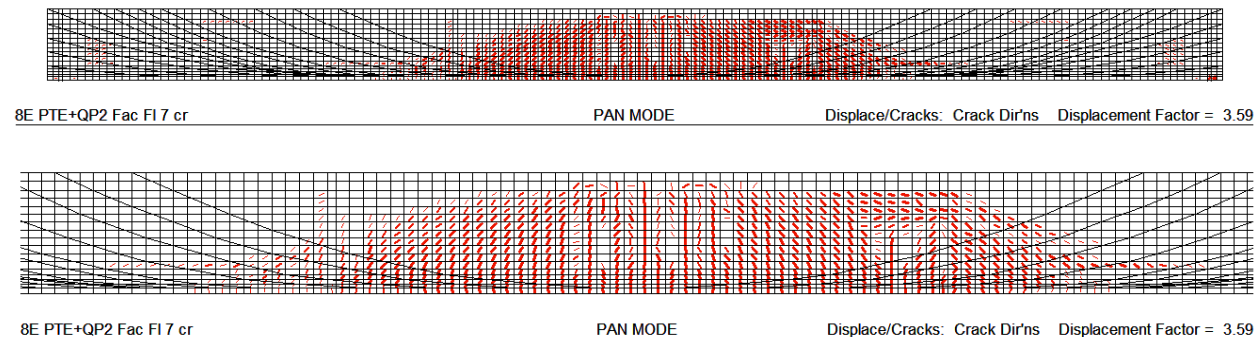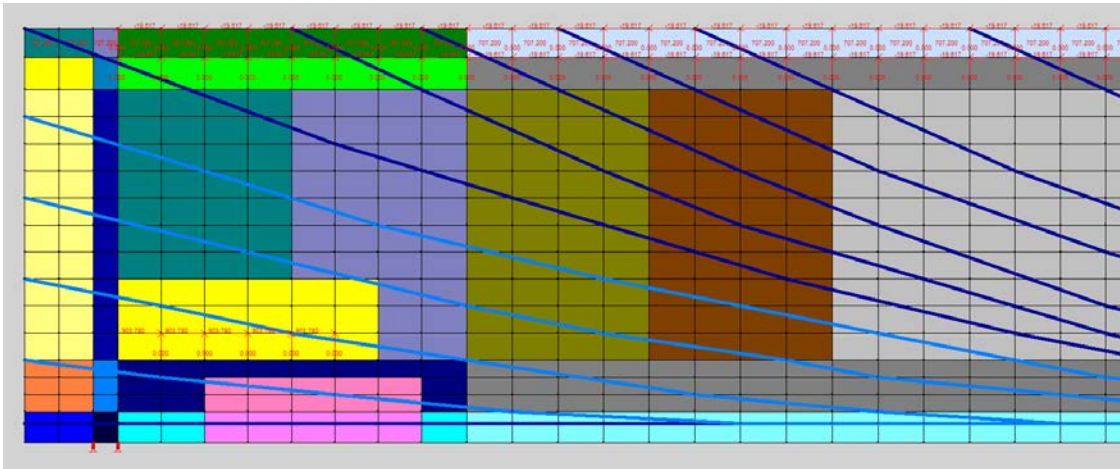
Fig. 10.4: Predicted failure of girder P7 in span 9E-10E at a live load factor of 3.75 assuming 6 tendons lost at midspan.

10.5 Section 7A - Longer Span 7E-8E

Girders P1 and P7 of this span has 3 tendons lost and 8 tendons lost, respectively due to corrosion. This resulted in a loss of tendons of 33% in the midspan region in girder P7. It was assumed that outside of this midspan region the post-tensioned tendons and the stirrups had a uniform loss due to corrosion of 30% of their areas. This span is 172'-0" center-to-center of bearings and each girder contains 24 tendons. The applied PTE was 780 kN on P1 and 1372 kN on P7. The span was strengthened with QP2 forces of 3360 kN on P1 and on P7. For the 2D non-linear analyses the PTE forces were reduced by 10% resulting in forces of 702 kN and 1235 kN in P1 and P7, respectively. The QP2 forces were also reduced by 10% in the analyses giving an average value of 3024 kN on P1 and on P7.

10.5.1   Results for Critical Loading at Midspan under Service Loading for Combined Case of QP2 and PTE - Girder P7

Flexural cracking is predicted to occur at a load corresponding to 1.7 and 1.4 times the live loading for short term and long-term predictions, respectively.

10.5.2   Results for Critical Loading at Midspan under Factored Loading for Combined Case of QP2 and PTE - Girder P7

Figure 10.5 shows the cracking at the predicted maximum load carrying capacity of Girder P7. Failure is predicted to occur under factored dead load plus 2.85 times the live load. The girder is predicted to fail by flexural yielding in the midspan region. At this maximum load inclined shear cracks are also predicted to occur. The predicted D/C ratio is 0.77.
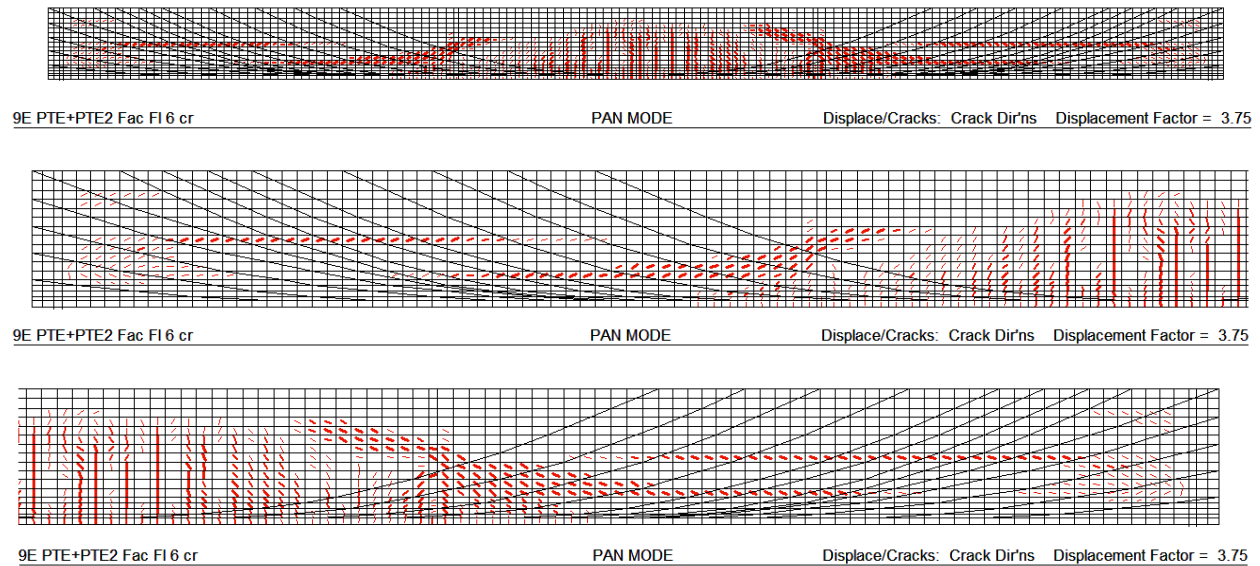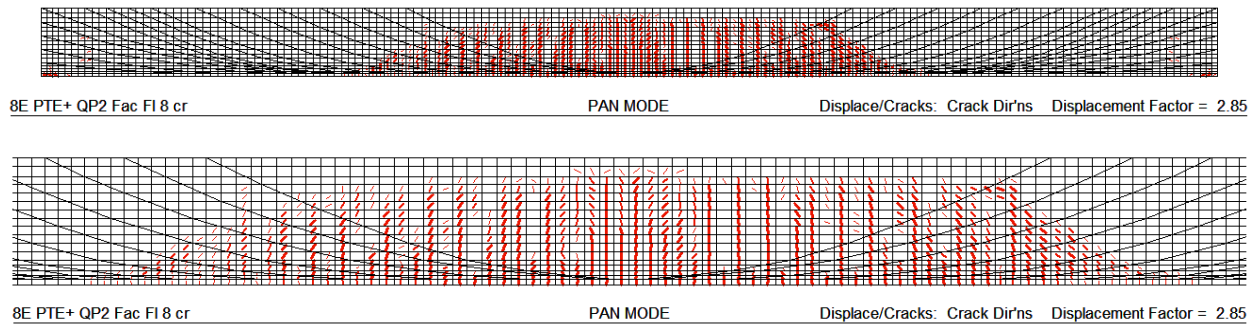

Fig. 10.5: Predicted failure of girder P7 in span 7E-8E at a live load factor of 2.85 assuming 8 tendons lost at midspan.

10.6 Section 7A - Longer Span 6E-7E with PTE and QP1

Girders P1 and P7 of this span has 4 tendons lost and 8 tendons lost, respectively due to corrosion. This span is 172'-0" center-to-center of bearings and each girder contains 24 tendons.

This resulted in a loss of tendons of 33% in the midspan region in girder P7. It was assumed that outside of this midspan region the post-tensioned tendons and the stirrups had a uniform loss due to corrosion of 30% of their areas. The applied PTE was 949 kN on P1 and 1252 kN on P7. The span was strengthened with QP1 forces of 1900 kN on P1 and on P7. For the 2D non-linear analyses the PTE forces were reduced by 10% resulting in forces of 854 kN and 1127 kN in P1 and P7, respectively.

10.6.1 Results for Critical Loading at Midspan under Service Loading for Combined Case of QP1 and PTE - Girder P7

Flexural cracking is predicted to occur at a load corresponding to 3.0 and 2.6 times the live loading for short term and long-term predictions, respectively.

10.6.2 Results for Critical Loading at Midspan under Factored Loading for Combined Case of QP1 and PTE - Girder P7

Figure 10.6 shows the cracking at the predicted maximum load carrying capacity of Girder P7. Failure is predicted to occur under factored dead load plus 4.40 times the live load. The girder is predicted to fail by flexural yielding in the midspan region. At this maximum load inclined shear cracks are also predicted to occur. The predicted D/C ratio is 0.61.


6E PTE+QP1 Fac Fl 8 cr   PAN MODE   Displace/Cracks: Crack Dir'ns   Displacement Factor = 4.40

6E PTE+QP1 Fac Fl 8 cr   PAN MODE   Displace/Cracks: Crack Dir'ns   Displacement Factor = 4.40

Fig. 10.6: Predicted failure of girder P7 in span 6E-7E at a live load factor of 4.40 assuming 8 tendons lost at midspan.

10.7 Section 7A - Longer Span 5E-6E with PTE and QP1

Girders P1 and P7 of this span has 4 tendons lost and 5 tendons lost, respectively due to corrosion. This resulted in a loss of tendons of 21% in the midspan region in girder P7. It was assumed that outside of this midspan region the post-tensioned tendons and the stirrups had a uniform loss due to corrosion of 18% of their areas. This span is 172'-0" center-to-center of bearings and each girder contains 24 tendons. The applied PTE was 2273 kN on P1 and 840 kN on P7. The span was strengthened with QP1 forces of 960 kN on P1 and on P7. For the 2D non-linear analyses the PTE forces were reduced by 10% resulting in forces of 2046 kN and 756 kN in P1 and P7, respectively.

10.7.1 Results for Critical Loading at Midspan under Service Loading for Combined Case of QP1 and PTE - Girder P7

Flexural cracking is predicted to occur at a load corresponding to 2.6 and 2.1 times the live loading for short term and long-term predictions, respectively.

10.7.2 Results for Critical Loading at Midspan under Factored Loading for Combined Case of QP1 and PTE - Girder P7

Figure 10.7 shows the cracking at the predicted maximum load carrying capacity of Girder P7. Failure is predicted to occur under factored dead load plus 3.75 times the live load. The girder is predicted to fail by flexural yielding in the midspan region. At this maximum load inclined shear cracks are also predicted to occur. The predicted D/C ratio is 0.66.
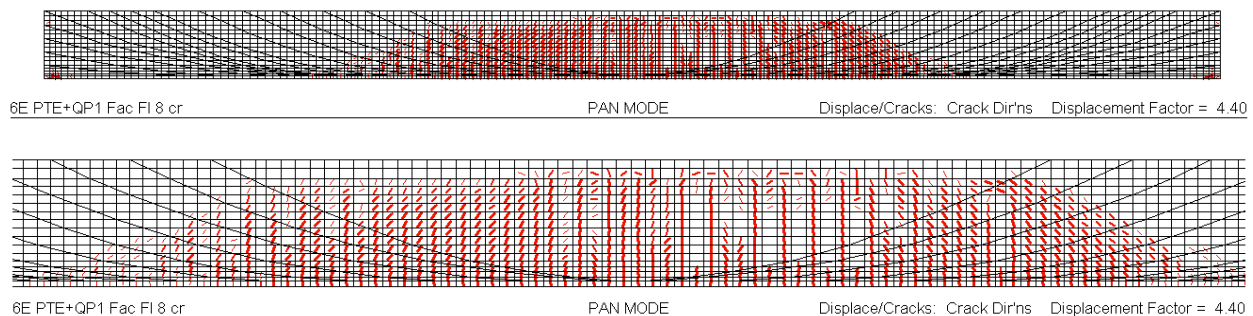

5E PTE+QP1 Fac Fl 5 cr   PAN MODE   Displace/Cracks: Crack Dir'ns   Displacement Factor = 3.75

5E PTE+QP1 Fac Fl 5 cr   PAN MODE   Displace/Cracks: Crack Dir'ns   Displacement Factor = 3.75

Fig. 10.7: Predicted failure of girder P7 in span 5E-6E at a live load factor of 3.75 assuming 5 tendons lost at midspan.

10.8 Section 7A - Longer Span 4E-5E with PTE and PTE2

Girders P1 and P7 of this span have 7 tendons lost and 5 tendons lost, respectively due to corrosion. This resulted in a loss of tendons of 29% in the midspan region in girder P7. It was assumed that outside of this midspan region the post-tensioned tendons and the stirrups had a uniform loss due to corrosion of 26% of their areas. This span is 172'-0" center-to-center of bearings and each girder contains 24 tendons. The applied PTE was 1388 kN on P1 and 1200 kN on P7. The span was additionally strengthened with PTE2 forces of 5022 kN on P1 and on P7. For the 2D non-linear analyses the PTE forces were reduced by 10% resulting in forces of 1249 kN and 1080 kN in P1 and P7, respectively. Similarly, the PTE2 forces applied were reduced to 4520 kN.

10.8.1 Results for Critical Loading at Midspan under Service Loading with PTE and PTE2 - Girder P1

Flexural cracking is predicted to occur at a load corresponding to 2.4 and 2.0 times the live loading for short term and long-term predictions, respectively. Figure 10.8 shows the predicted cracking in Girder P1 at service load at one end of girder P1. The cracks radiating out from the anchor plate are due to the spreading of the compressive stresses into the web of the girder producing "bursting" tensile stresses. The maxim predicted crack with is 1 mm just above the plate.

4E PTE+PTE2 LT Nom Fl 7 cr   PAN MODE   Displace/Cracks: Crack Dir'ns   Displacement Factor = 1.00
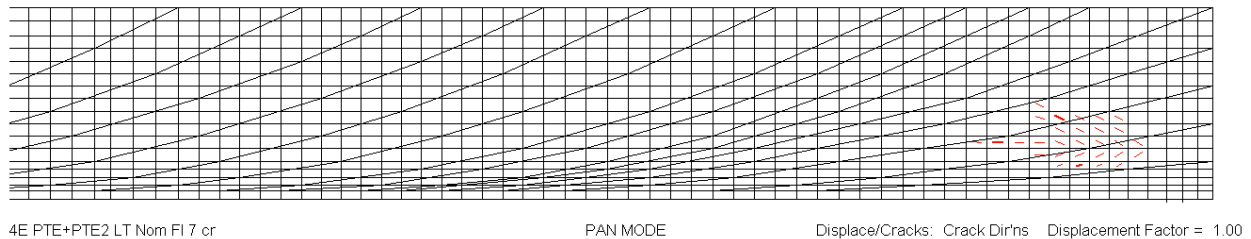
Fig. 10.8: Predicted cracks in anchorage region of girder P1 due to PTE2 at service load.

10.8.2 Results for Critical Loading at Midspan under Factored Loading with PTE and PTE2 - Girder P1

Figure 10.9 shows the cracking at the predicted maximum load carrying capacity of Girder P1. Failure is predicted to occur under factored dead load plus 3.34 times the live load. The girder is predicted to fail by flexural yielding in the midspan region. At this maximum load significant inclined shear cracks are also predicted to occur as well as longitudinal splitting cracks. It is noted that the FRP shear strengthening strips were not included in this analysis and hence the shear cracking at flexural ultimate would be better controlled. The predicted D/C ratio is 0.70.

4E PTE+PTE2 Fac Fl 7 cr   PAN MODE   Displace/Cracks: Crack Dir'ns   Displacement Factor = 3.34

4E PTE+PTE2 Fac Fl 7 cr   PAN MODE   Displace/Cracks: Crack Dir'ns   Displacement Factor = 3.34

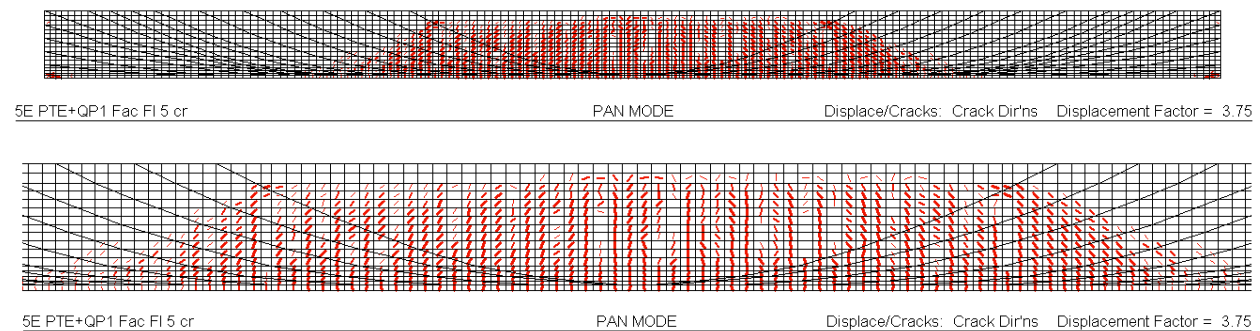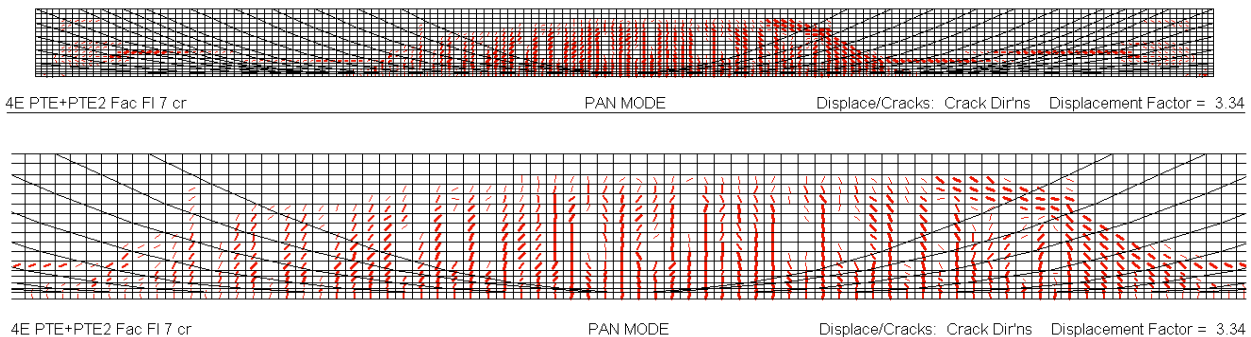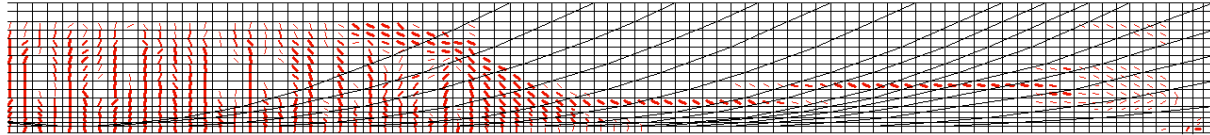4E PTE+PTE2 Fac Fl 7 cr   PAN MODE   Displace/Cracks: Crack Dir'ns   Displacement Factor = 3.34

Fig. 10.9: Predicted failure of girder P1 in span 4E-5E at a live load factor of 3.34 assuming 7 tendons lost at midspan.

11 Evaluation of Section 7B Spans

11.1 Introduction

Table 11.1 gives some of the key parameters for the 4 spans in Section 7B. The overall beam lengths were 172'-1" (52.451 m), with a span, centre-to-centre of bearings, of 168'-0" (51.206 m). Spans 10E-11E13E-14E, 12E-13E and 10E-11E were post-tensioned with 19 GTM strands. Span 11E-12E had 22 GTM strands. The properties of the GTM strands are described in Section 2.4. The girders in the 7B spans all had 7 diaphragms (5 interior and 2 at ends) compared to the 4 diaphragms (2 interior and 2 at ends) between the girders in Sections 5 and 7A.

11.2 QP2.1 Strengthening Measures

Figure 11.1 shows the details of the QP2 strengthening measures applied to girders P1 and P7 in spans 11E-12E, 12E-13E and 13E-14E. This QP2 strengthening measure is sometimes referred to as QP2.1 because it differs from the other QP2 details used in Section 5 and 7A. There are only 16 strands per girder rather than 32 strands as found in Sections 5 and 7A. In addition there are only two deviation points in the span, each being located at the first interior diaphragm as shown in Fig. 11.1.

68
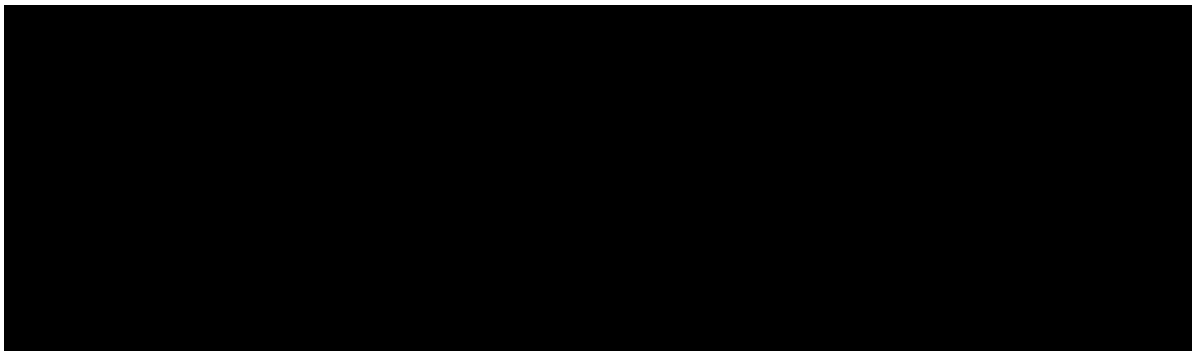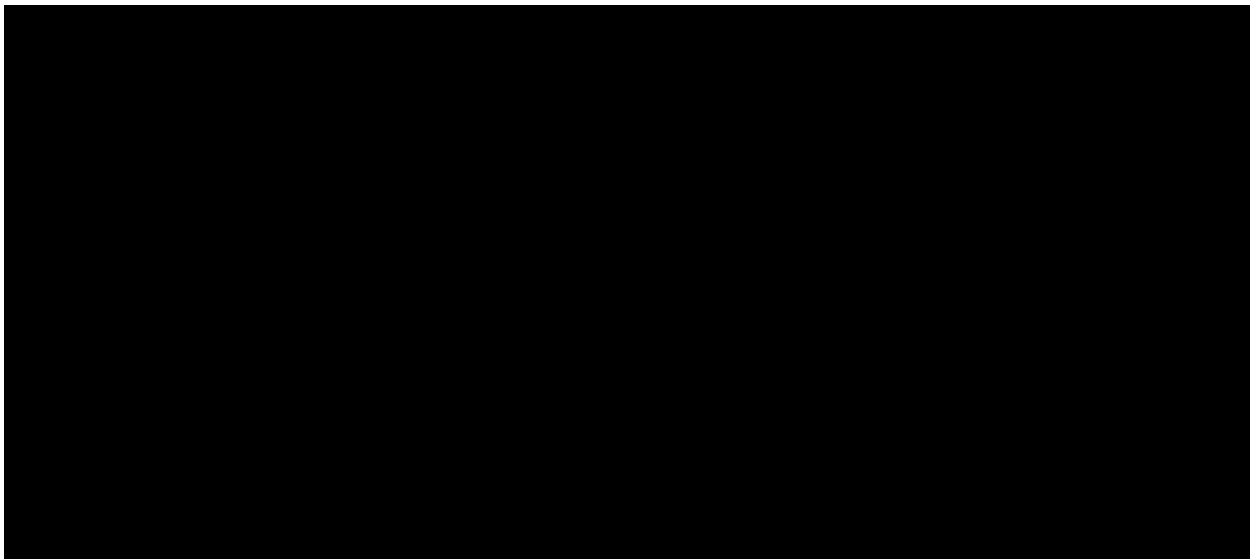
Fig. 11.1: QP2.1 strengthening measures in Section 7B (AECOM drawing numbers 125649-16 & 21, 2012)

Table 11.1: Key parameters for the 4 spans in Section 7B

Span	Girder	# tendons Lost/original # (Nov 10, 2015 MDT)	PTE kN	QP2 kN	PTE2 kN
13E-14E	P1	0/19	1879	1456	
	P7	5/19	1003	1664	
12E-13E	P1	1/19	949	1664	
	P7	4/19	2344	1664	
11E-12E	P1	1/22	2491	1296	
	P7	4/22	2485	1456	
10E-11E*	P1	2/19	2621		2678
	P7	4/19	651		2678
					2678 (P3)
					2678 (P5)

* Span 10E -11E was analysed in its condition before PTE2 was added

11.3 Span 10E-11E

11.3.1   Repairs and Tendon Inspections

The bottom flanges of both P1 and P7 of span 10E-11E were repaired in 2011. Figure 11.2 shows the condition of the bottom flange of P7, just before the repair in August 2011.

Fig. 11.2: Condition of bottom flange of Girder P7 in span 10E-11E in August 2011.

In August 2011 some concrete in the bottom flange was removed and some of the tendons were exposed in girder P7 of span 10E-11E. As shown in Fig. 11.3, the inspection revealed that tendons #6, 11 and 15 were ineffective and that tendon #1 was 50% effective (PJCCBI Aug 15, 2011).
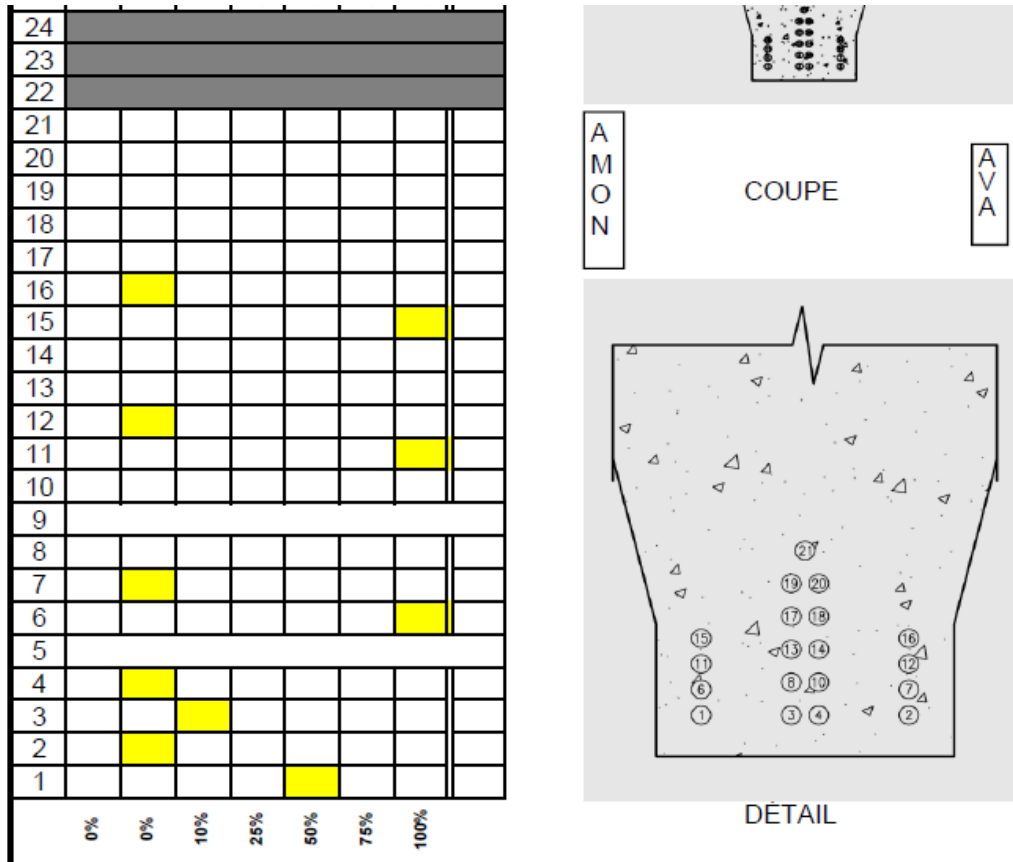
Fig. 11.3: Inspection of tendons in girder P7 of span 10E-11E (Axor-Genivar, Contrôle qualité - Câbles de post-tension des poutres du pont Champlain - Section 7B, 15-09-2011).

It is assumed in the MasterData Table that all 4 of these strands were ineffective (see Fig. 11.4 for tendon locations).
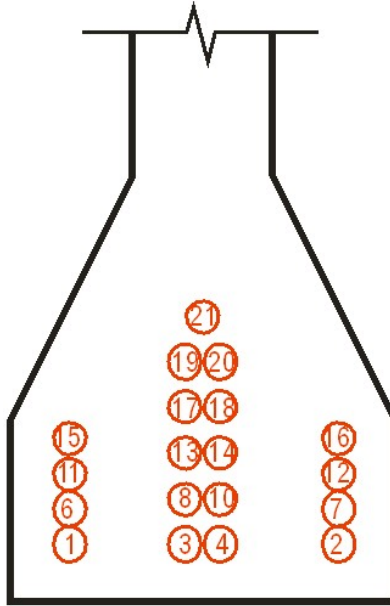
Fig. 11.4: Tendons 1, 6, 11 and 15 assumed ineffective in P7 of span 10E-11E

Figure 11.5 shows the removal of the concrete in the bottom flange of girder P7 and the condition of the GTM prestressing strands. A considerable amount of concrete was removed on both sides and the bottom of the bottom flange during the inspection process in order to report on the condition of tendons 1, 6, 11, 15, 3, 4, 2, 7, 12 and 16 as can be seen in Fig. 11.5.

Fig. 11.5: Concrete removal and condition of GTM strands during repair of bottom flange of Girder P7 in span 10E-11E in August 2011.

11.3.2   Non-Linear Modelling of Girder P7 in Span 10E-11E

Unlike the other spans in Section 7B, Span 10E-11E was not strengthened with QP2.1. The girders in Section 7B have 5 interior diaphragms in the span compared with 2 interior diaphragms in Sections 5 and 7A. It has been reported that girders P1 and P7 in span 10E-11E had 2 and 4 tendons lost out of the original 19 tendons, respectively, as indicated in the November 10, 2015 MasterData Table. This resulted in a loss of tendons of 21% in the midspan region in girder P7. It was assumed that outside of this midspan region the post-tensioned tendons and the stirrups had a uniform loss due to corrosion of 20% of their areas. Figure 11.6

shows the finite element model used for analysis, the loading due to the truck loading causing maximum moment at midspan and the loading due to the added PTE combined with the secondary effects from the loss of tendons. The tendons in the midspan region were reduced by 21% to account for corrosion, while a 20% reduction was assumed for the tendons and stirrups in the remainder of the girder. The PTE applied to the model was 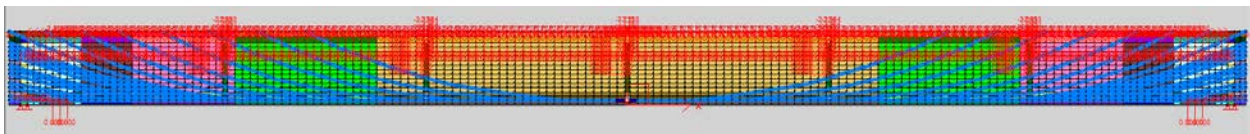reduced by 10% to account for prestress losses, resulting in applied forces of 2359 kN and 586 kN in girders P1 and P7, respectively. The analysis was carried out without the additional PTE2 post-tensioning that was added after major alerts were recorded from the instrumentation on this span.
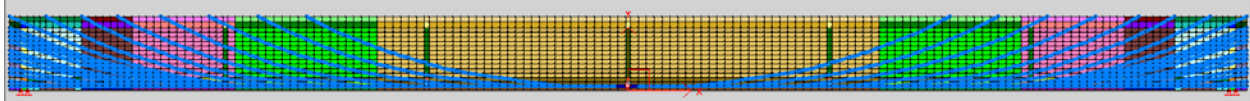
(a) 2D model
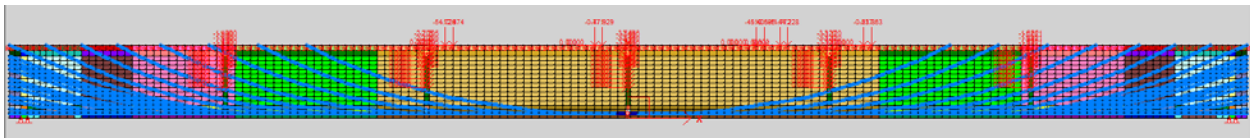
(b) Truck Loading for maximum moment

(c) Loading on P7 for PTE effects

Fig. 11.6: 2-D nonlinear model of girder P7 in span 10E-11E

11.3.3 Predicted Cracking under Service Loading in P7 of Span 10E-11E

Girder P7 is predicted to experience flexural cracking in the midspan region at 1.5 and 1.1 times the service live load for short-term and long-term properties, respectively. It is noted that this analysis does not consider the history of the rehabilitation and the fact that the repair concrete would have considerably higher shrinkage in the bottom flange.

11.3.4   Predicted Ultimate Strength of Girder P7 of Span 10E-11E

After applying the load factors on the dead loads, the live loading was increased until failure was predicted. Flexural failure is predicted to occur by in the midspan region as shown in Fig. 11.7 at an applied load of 2.53 times the live load. The predicted D/C ratio is 0.84.
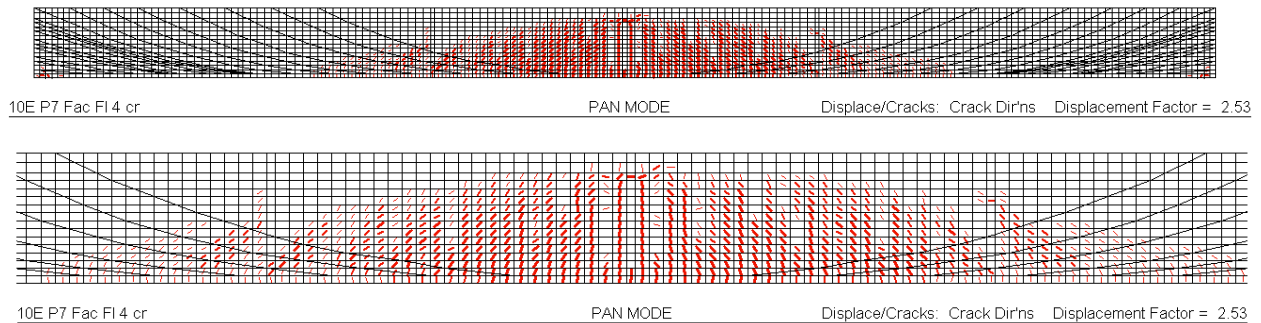

Fig. 11.7: Cracking of girder P7 in span 10E-11E at flexural ultimate.

11.3.5   Evaluation of 10E-11E During Rehabilitation

Additional analyses were carried out to evaluate the conditions of girder P7 of span 10E-11E during the rehabilitation of the bottom flange in August 2011. At this time only the PTE was present and the PTE2 was added later. The photograph shown in Fig. 11.2 shows the condition of the bottom flange prior to the removal of concrete. It is clear that the concrete surrounding the outer tendons was virtually ineffective in carrying tensile stresses and in providing corrosion protection. It was assumed that 4 tendons were lost due to corrosion (November 10, 2015 MasterData Table).

A sectional analysis was carried out to simulate the loss of 4 tendons and to simulate the concrete removed during the rehabilitation process. Figure 11.8 shows the reduced section and the 15 remaining strands and the input parameters for the sectional analysis program Response 2000. The moment at midspan was estimated to be 15758 kNm corresponding to the dead load, service live load, redistribution due to tendon loss and the effects of PTE. Figure 11.9 shows that 0.04 mm cracks are predicted to occur in the bottom flange under these conditions. The cracking is predicted to extend a distance of 113 mm from the bottom face.
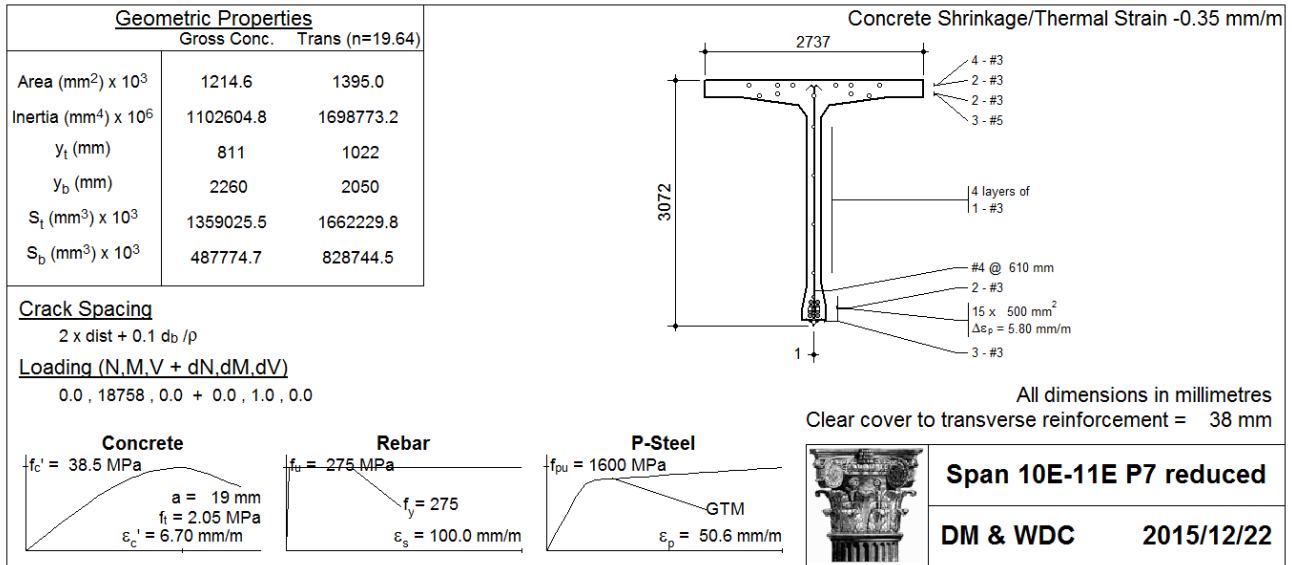
Fig. 11.8: Cross-sectional details of Girder P7 with reduced bottom flange dimensions due to concrete removal and the loss of 4 strands due to corrosion
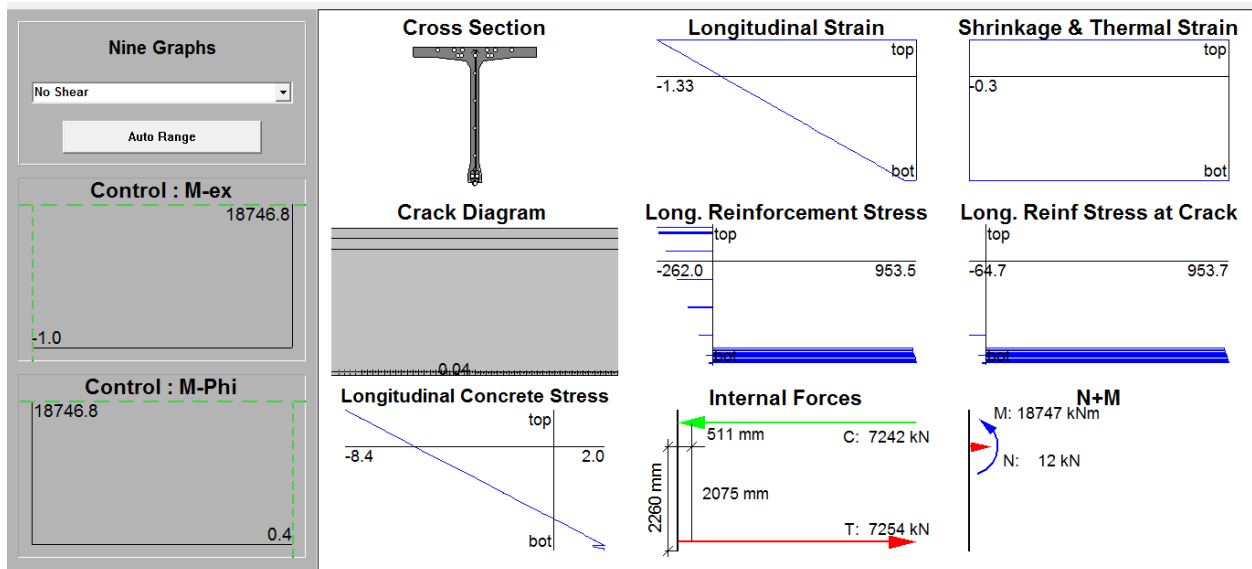
Fig. 11.9: Predicted cracking of Girder P7 with reduced flange dimensions and loss of 4 tendons.

An additional analysis was carried out with the additional repair concrete added to the reduced section. The shrinkage was increased in the bottom flange region to account for the additional shrinkage of the repair concrete. Concrete cracking is predicted to occur in the midspan region

with a maximum crack width of 0.10 under service live load. The cracks are predicted to extend a distance of 283 mm from the bottom face, that is, into the tapered flange region.
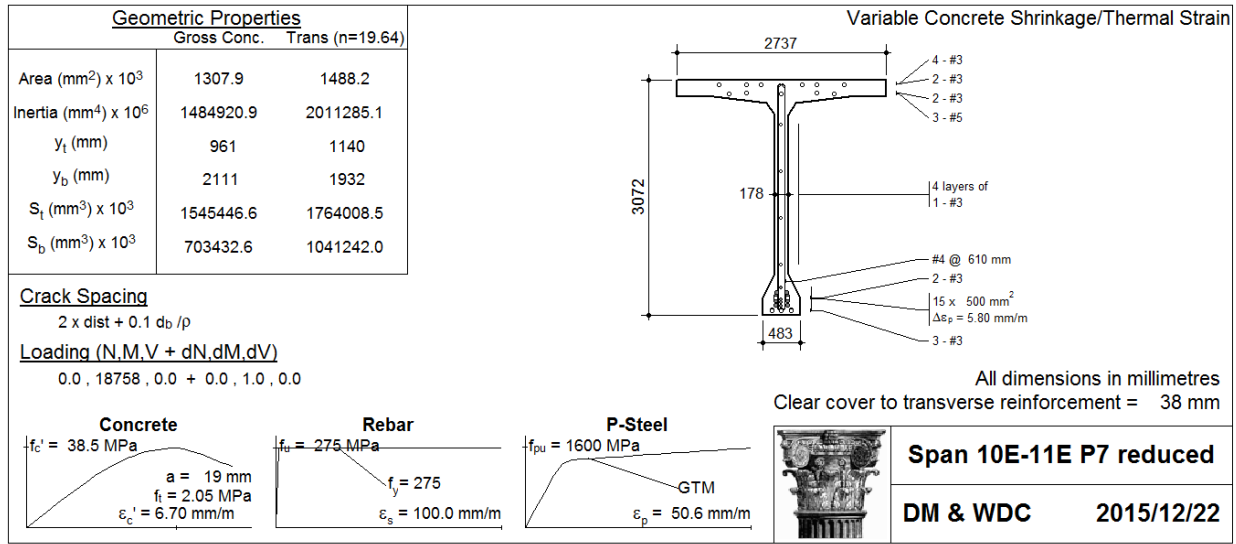
Fig. 11.10: Cross-sectional details of Girder P7 with repair concrete, additional shrinkage and the loss of 4 strands due to corrosion
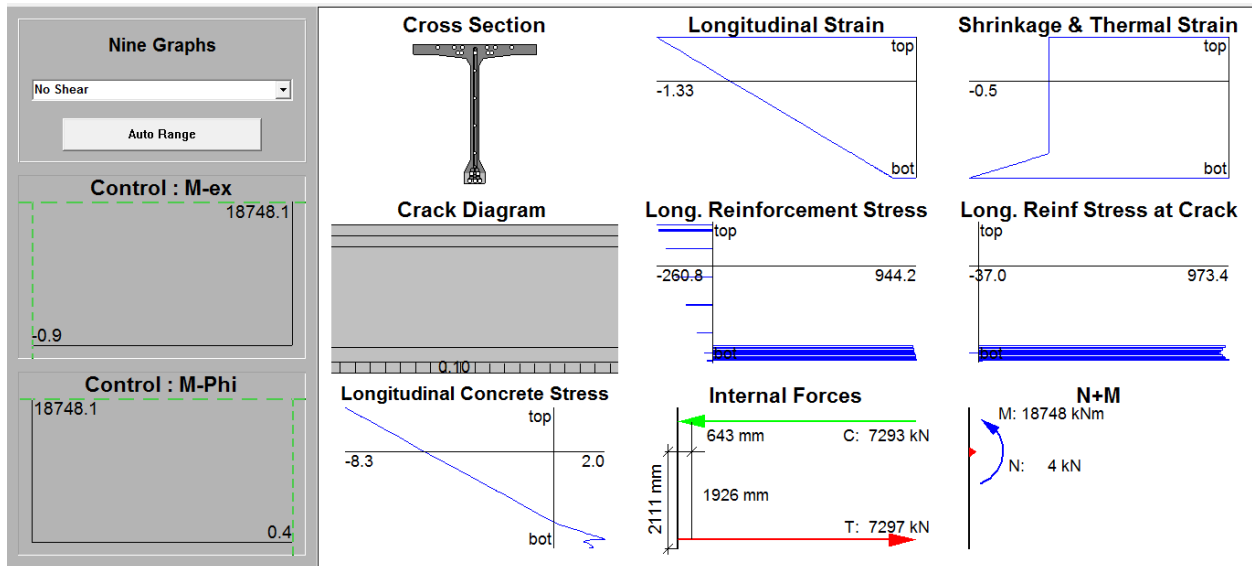
Fig. 11.11: Predicted cracking of Girder P7 with repair concrete and loss of 4 tendons.

Figure 11.12 shows the cracks from the inspection of girder P7 that was carried out in September 2015 after the additional PTE2 was applied to girders in this span. The crack widths are 0.05 mm, with a few cracks extending a short distance into the web.
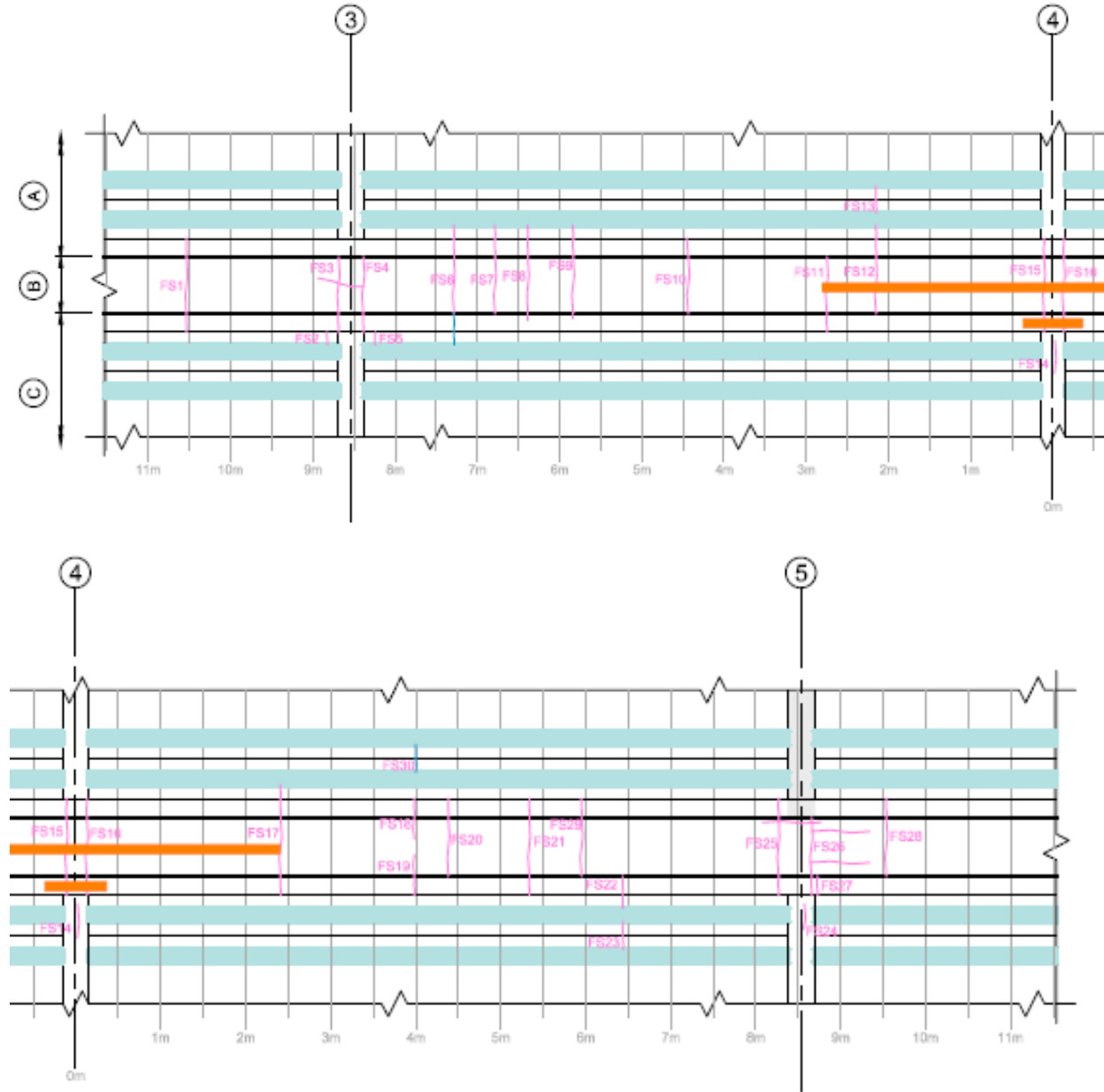
Fig. 11.12: Measured cracks in bottom flange of P7 of span 10E-11E (DESSAU │CIMA+ Rapport d'Inspection de Suivi CT 62057 24 sept, 2015)

11.4 Span 11E-12E with PTE and QP2.1

Girders P1 and P7 of this span has 1 tendon lost and 4 tendons lost, respectively due to corrosion. This resulted in a loss of tendons of 18% in the midspan region in girder P7. It was assumed that outside of this midspan region the post-tensioned tendons and the stirrups had a uniform loss due to corrosion of 17% of their areas. The applied PTE was 2491 kN on P1 and 2485 kN on P7. In addition QP2.1 forces of 1296 kN and 1456 kN were applied to Girders P1 and P7. This span is 168'- 0" center-to-center of bearings and contained 22 tendons. For the 2D non-linear analyses the PTE forces were reduced by 10% giving 2242 kN and 2237 kN in P1 and P7, respectively. The QP2.1 forces were also reduced by 10% and an average QP2.1 force of 1238 kN was assumed for P1 and for P7. Figure 11.13 shows the 2D non-linear model of span 11E-12E with 22 post-tensioned tendons.
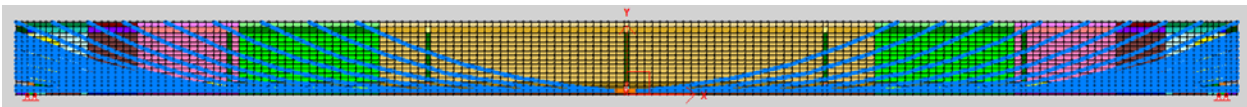
Fig. 11.13: 2D non-linear model of span 11E-12E with 22 tendons.

11.4.1 Results for Critical Loading at Midspan under Service Loading for Combined Case of QP2.1 and PTE - Girder P7

Flexural cracking is predicted to occur at a load corresponding to 2.6 and 2.2 times the live loading for short term and long-term predictions, respectively.

11.4.2 Results for Critical Loading at Midspan under Factored Loading for Combined Case of QP2 and PTE - Girder P7

Figure 11.14 shows the cracking at the predicted maximum load carrying capacity of Girder P7. Failure is predicted to occur under factored dead load plus 3.99 times the live load. The girder is predicted to fail by flexural yielding in the midspan region. At this maximum load inclined shear cracks are also predicted to occur. The predicted D/C ratio is 0.63.

Fig. 11.14: Predicted failure of girder P7 in span 11E-12E at a live load factor of 3.75 assuming 4 tendons lost at midspan.

11.5 Span 12E-13E with PTE and QP2.1

Girders P1 and P7 of this span have 1 tendon lost and 4 tendons lost, respectively due to corrosion. This resulted in a loss of tendons of 21% in the midspan region in girder P7. It was assumed that outside of this midspan region the post-tensioned tendons and the stirrups had a uniform loss due to corrosion of 20% of their areas. The applied PTE was 949 kN on P1 and 2344 kN on P7. In addition QP2.1 forces of 1664 kN were applied to girder P1 and girder P7. This span is 168'- 0" center-to-center of bearings and contained 19 tendons. For the 2D non-linear analyses the PTE forces were reduced by 10% giving 854 kN and 2110 kN in P1 and P7, respectively. The QP2.1 forces were also reduced by 10% in the analyses giving 1498 kN for P1 and for P7.

11.5.1 Results for Critical Loading at Midspan under Service Loading for Combined Case of QP2.1 and PTE - Girder P7

Flexural cracking is predicted to occur at a load corresponding to 2.0 and 1.7 times the live loading for short term and long-term predictions, respectively.

11.5.2 Results for Critical Loading at Midspan under Factored Loading for Combined Case of QP2 and PTE - Girder P7

Figure 11.15 shows the cracking at the predicted maximum load carrying capacity of Girder P7. Failure is predicted to occur under factored dead load plus 3.10 times the live load. The girder is predicted to fail by flexural yielding in the midspan region. At this maximum load inclined shear cracks are also predicted to occur. The predicted D/C ratio is 0.74.
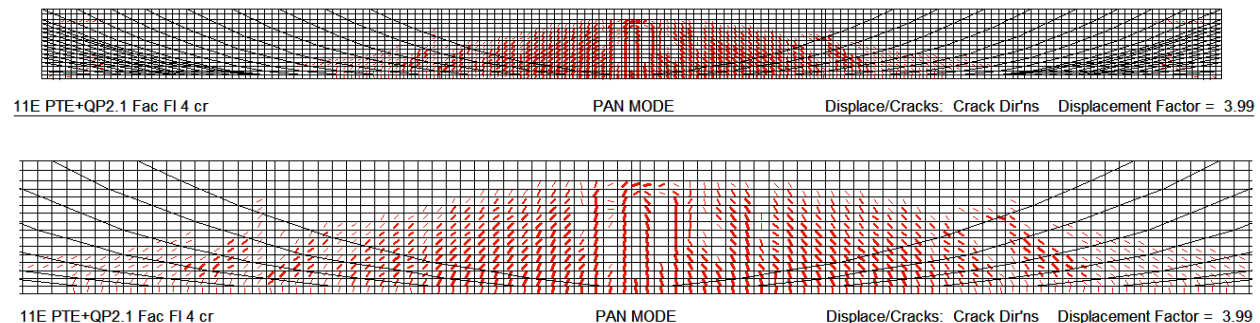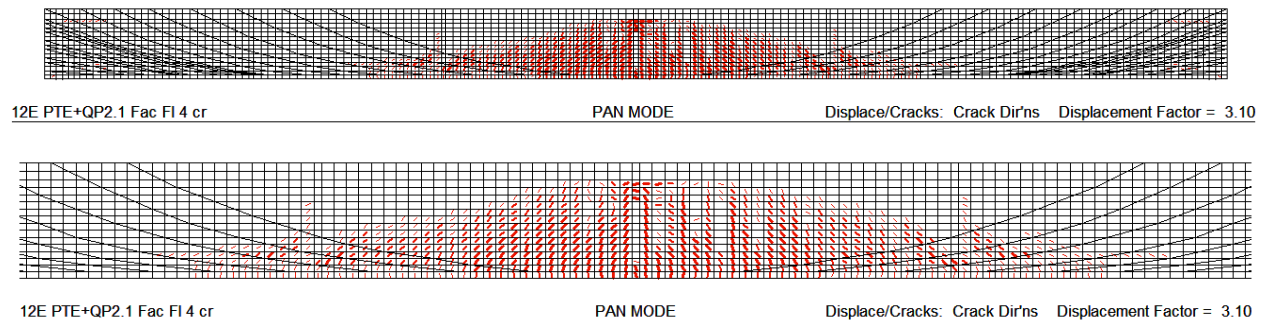

Fig. 11.15: Predicted failure of girder P7 in span 11E-12E at a live load factor of 3.10 assuming 4 tendons lost at midspan.

11.6 Span 13E-14E with PTE and QP2.1

Girders P1 and P7 of this span have zero tendons lost and 5 tendons lost, respectively due to corrosion. This resulted in a loss of tendons of 26% in the midspan region in girder P7. It was

assumed that outside of this midspan region the post-tensioned tendons and the stirrups had a uniform loss due to corrosion of 25% of their areas. The applied PTE was 1879 kN on P1 and 1003 kN on P7. In addition, QP2.1 forces of 1456 kN and 1664 kN were applied to girder P1 and P7, respectively. This span is 168'- 0" center-to-center of bearings and contained 19 tendons. For the 2D non-linear analyses the PTE forces were reduced by 10% giving 1691 kN and 903 kN in P1 and P7, respectively. The QP2.1 forces were also reduced by 10% and an average QP2.1 force of 1404 kN was assumed for P1 and for P7.

11.6.1   Results for Critical Loading at Midspan under Service Loading for Combined Case of QP2.1 and PTE - Girder P7

Flexural cracking is predicted to occur at a load corresponding to 1.6 and 1.2 times the live loading for short term and long-term predictions, respectively.

11.6.2   Results for Critical Loading at Midspan under Factored Loading for Combined Case of QP2 and PTE - Girder P7

Figure 11.16 shows the cracking at the predicted maximum load carrying capacity of Girder P7. Failure is predicted to occur under factored dead load plus 2.61 times the live load. The girder is predicted to fail by flexural yielding in the midspan region. At this maximum load inclined shear cracks are also predicted to occur. The predicted D/C ratio is 0.74.
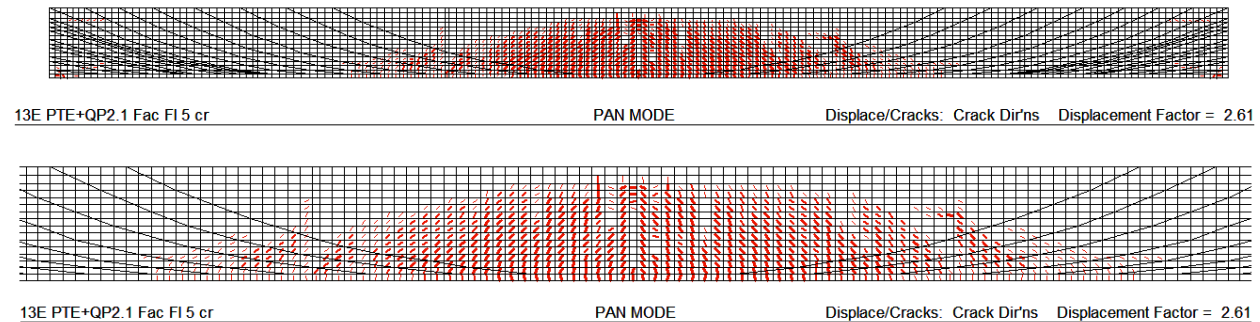

13E PTE+QP2.1 Fac Fl 5 cr   PAN MODE   Displace/Cracks: Crack Dir'ns   Displacement Factor = 2.61

13E PTE+QP2.1 Fac Fl 5 cr   PAN MODE   Displace/Cracks: Crack Dir'ns   Displacement Factor = 2.61

Fig. 11.16: Predicted failure of girder P7 in span 13E-14E at a live load factor of 2.61 assuming 4 tendons lost at midspan.

12 Prioritization of Section 7 Spans

Figure 12.1 shows the factor, X, applied to the service live load that results in predicted flexural cracking. The 4 spans containing in Section 7B are shown in dark green and the 6 spans in Section 7A are shown in light green (on the right in Fig. 12.1). These factors are all above 1.5 for the spans considered.
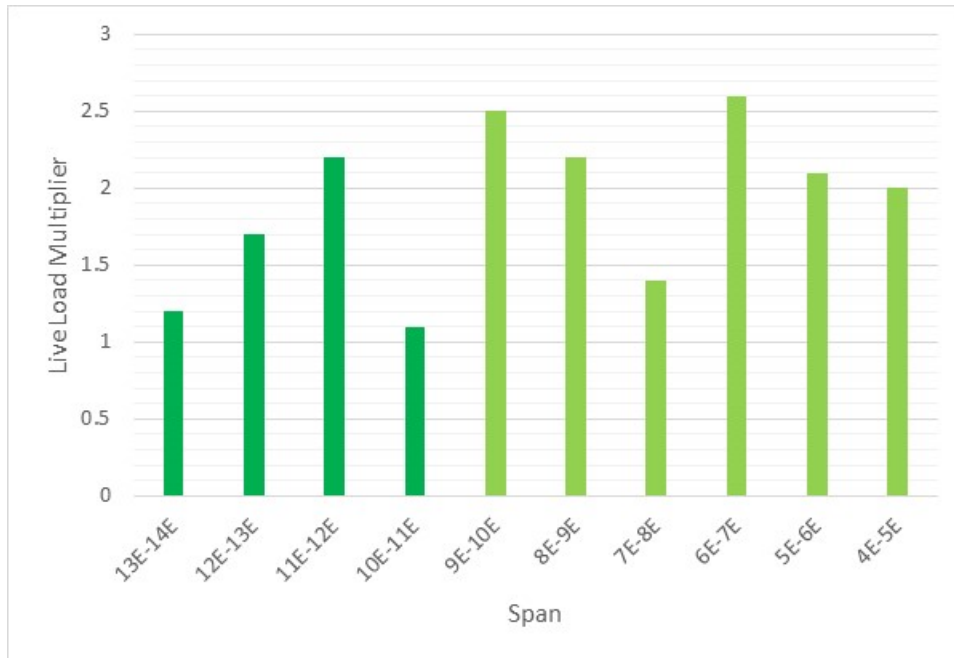
Fig. 12.1: Factor, X, on service live load to cause flexural cracking at midspan.

Figure 12.2 shows the factor, X, applied to the service live load that results in predicted flexural ultimate at midspan. These factors are all above the CSA S6 required live load factor of 1.63.
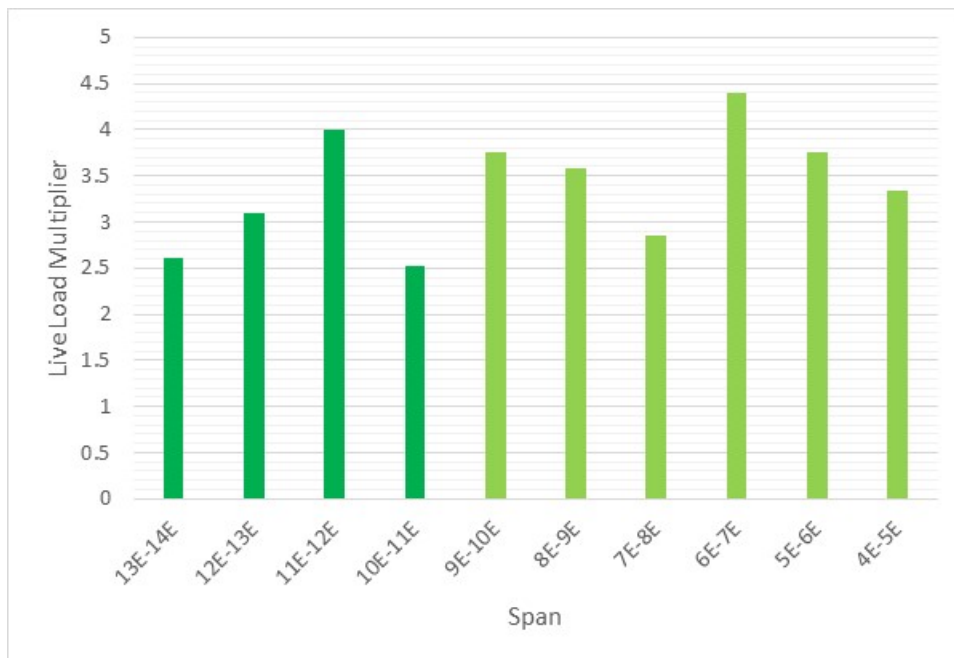
Fig. 12.2: Factor, X, on service live load to cause flexural failure at midspan.

Figure 12.3 shows the variation in the predicted values of demand-to-capacity (D/C) ratios for the spans in Section 7. There are 3 spans having predicted D/C ratios equal to or above 0.70.

Fig. 12.3: Predicted D/C ratios for flexure at midspan.

Table 12.1 shows the key parameters used to judge the priority for strengthening measures for the Section 7 spans. Also indicated are those spans with trusses placed in 2015.

Table 12.1: Determining priority for strengthening with trusses

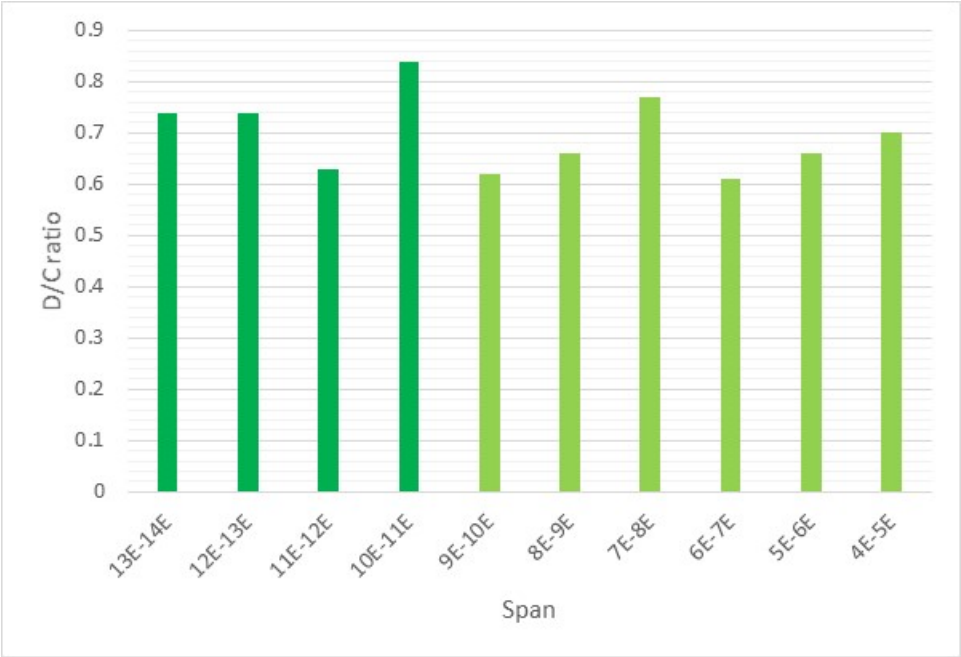| Span	Critical Girder	# tendons Lost/original # (Nov 10, 2015 MDT)		Priority	Comments
Spans in Section 7A					
9E-10E	P1	6/22		9	
8E-9E	P7	7/22		7	
7E-8E	P7	8/24		2	
6E-7E	P7	8/24		10	
5E-6E	P7	5/24		6	
4E-5E*	P1	7/24		5	PTE2 &Truss applied in 2015
Spans in Section 7B					
13E-14E***	P7	5/19		3	Post supports applied in 2015
12E-13E***	P7	4/19		4	Post supports applied in 2015
11E-12E	P7	4/22		8	
10E-11E**	P7	4/19		1	PTE2 & Truss applied in 2015

* before truss applied

** before PTE2 and truss applied

*** before post supports applied

13 Conclusions

The following conclusions are made following the studies reported:

1. Sections 7A and 7B have effective concrete strengths that are somewhat less than the concrete in Section 5.
2. The effects of redistribution from the exterior girders to the interior girders arising from the loss of prestressing tendons was considered in these studies.
3. A re-assessment of span 28W-29W was carried out and the predicted cracking is similar to that observed before the Superbeam was placed.
4. The spans in Section 5 that were reinforced with QP1 or QP2 strengthening measures were analyzed and ranked for possible future strengthening. For all these spans flexural cracking at midspan under service loading was predicted to occur above a load corresponding to 1.5 times the service live load and the D/C ratios were all below 0.80.

5. The spans in Sections 7A and 7B were analyzed and ranked in order of the need for future strengthening. For those spans in Section 7 that were not strengthened with trusses or post supports, flexural cracking at midspan under service loading was predicted to occur at or above 1.4 times the service live load and the D/C ratios were all below 0.80.

6. The combined effects of PTE and PTE2, giving a total force of 3435 +5022 = 8457 kN, together with shear resulted in predicted cracking near the anchorage region for the PTE2 tendons in exterior girder P1 of span 9E-10E. A similar effect was predicted for span 4E-5E. It is recommended that the control of bursting stresses and shear stresses in the web be investigated.

7. An analysis was carried out to examine the effects of the concrete removal and repair of the bottom flange of girder P7 in span 10E-11E, before the PTE2 retrofit and before a truss was added. This study indicated that flexural cracking was predicted to occur during this process after the repair concrete underwent shrinkage. The non-linear finite element analysis indicated that, even without the remedial actions taken, girder P7 was close to flexural cracking at midspan under service load before the PTE2 strengthening measures were taken and before a truss was added.

14 References

Axor-Genivar, Contrôle qualité - Câbles de post-tension des poutres du pont Champlain - Section 7B, 15-09-2011.

DESSAU│CIMA+ Rapport d'Inspection de Suivi CT 62057 24-09- 2015.

AECOM, 2011, « Pont Champlain, Sections 4, 5 and 6, réfection des piles, chevêtres, poutres et joints de tablier (2012-2013) », Contrat no. 61579, dessins 125570.

ASTM, A416/A416M-10, « Standard Specification for Steel Strand, Uncoated Seven-wire for Prestressed Concrete.

ASTM, A722/A722M-12, « Specification for Uncoated High-Strength Steel Bars for Prestressing.

Bentz, E.C. (2015), http://www.ecf.utoronto.ca/~bentz/r2k.htm, Response-2000 webpage last accessed 2015/02/13.

CSA S6-06, 2006, "Canadian Highway Bridge Design Code", Canadian Standards Association, Mississauga, ON.

Les Consultants S.M. Inc., 1999, « Rapport D'Inspection Final – Réparation de huit poutres en béton précontraint », Contrat no. 92-40-8767, mars 1999.

PJCCI, 1998, « Pont Champlain, Sections 5 & 7 Réfection de 8 Poutres de Béton (1998) – Détails de Renforcement des Poutres par Post-Tension », No. Contrat 92-40-8767, No. Dessin 125101-06.

TECHNISOL INC., 2006, « Pont Champlain – Section 5 & 7 - Expertise sur le Béton des Poutres de Béton Précontraint », La Société Les Ponts Jacques Cartier & Champlain Inc., Contrat 60862, Avril 2006.

Vecchio, F.J. (2015), http://www.civ.utoronto.ca/vector, VecTor2 webpage, last accessed 2015/02/13.

Warycha, L. and Skotecky, C., "Construction of Piers and Superstructure - Section 5 and 7A of Champlain Bridge – I Explanatory Note – Calculation and References", Document 0277.